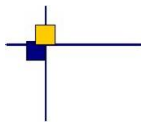


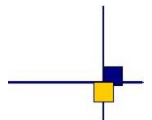


**CalVal Jason-2**



## **Jason-2 validation and cross calibration activities (Annual report 2017)**

**Contract No 160182-14026/00 Lot 1.6.3**



---

**Nomenclature : SALP-RP-MA-EA-23186-CLS**

**Issue : 1 rev 2**

**Date : March 20, 2018**

---

<b>Chronology Issues:</b>		
Issue:	Date:	Reason for change:
1rev0	November 29, 2017	Creation
1rev1	February 08, 2018	Delivery version
1rev2	March 20, 2018	Revision after comments from N. Picot and T. Guinle.

<b>People involved in this issue :</b>				
	<b>AUTHORS</b>	<b>COMPANY</b>	<b>DATE</b>	<b>INITIALS</b>
<b>Written by:</b>	H. Roinard E. Cadier	CLS		
<b>Checked by:</b>				
<b>Approved by:</b>				
<b>Application authorised by:</b>				

<b>Index Sheet :</b>	
Context:	
Keywords:	
Hyperlink:	

<b>Distribution:</b>		
Company	Means of distribution	Names
CLS	electronic copy	V.ROSMORDUC
CNES	electronic copy	thierry.guinle@cnes.fr gerald.dibarboue@cnes.fr nicolas.picot@cnes.fr aqgp_rs@cnes.fr dominique.chermain@cnes.fr delphine.vergnoux@cnes.fr

## List of tables and figures

### List of Tables

1	<i>Planned events</i> . . . . .	10
2	<i>Models and standards adopted for the Jason-2 version “D” products. Adapted from [1]</i> . . . . .	14
3	<i>Missing pass status</i> . . . . .	22
4	<i>Edited measurement status</i> . . . . .	28
5	<i>Editing criteria. Percentage of rejected measurements on each criterion over the whole mission</i> . . . . .	32
6	<i>Seasonal variations of Jason SLA (cm) for years 2008 to 2017</i> . . . . .	73
7	<i>Cycle and sub-cycles for the Jason-2 LRO</i> . . . . .	77
8	<i>17 days, 80 days and 145 days sub-cycles dates for the Jason-2 LRO</i> . . . . .	78

### List of Figures

1	<b>Top:</b> <i>Percentage of missing measurements over ocean and land for Jason-2 and Jason-1. Bottom:</i> <i>Map of percentage of available measurements over land for Jason-2 on cycle 154 (left) and for Jason-1 on cycle 511 (right)</i> . . . . .	23
2	<i>Cycle per cycle percentage of missing measurements over ocean (top left), without anomalies (top right), without anomalies and selecting latitudes lower than 50° and bathymetry area lower than -1000m (bottom).</i> . . . . .	24
3	<i>Cycle per cycle percentage of discarded measurements during selection of ocean/lake measurements.</i> . . . . .	29
4	<i>Percentage of edited measurements by ice flag criterion. Left: Cycle per cycle monitoring. The blue curve shows the trend of edited measurements after adjusting for annual and semi-annual signals. Right: Map over a one year period (cycles 267 to 303 from 2015-10-01 to 2016-10-02). Bottom: Map over interleaved ground-track period from 2016-10-13 to 2017-05-17 (left) and map over LRO period (right), cycles 500 (2017-07-11) to 506 (2017-09-14)</i> . . . . .	30
5	<i>Percentage of edited measurements by altimeter rain flag criterion (all figures computed after iced flagged points remove ). Map over a one year period (cycles 267 to 303). Left: rejected measurements (following method described hereafter ) where rain flag is also activated . Right: valid measurements (following method described hereafter ) where rain flag is activated. Bottom: All points where rain flag is activated.</i> . . . . .	31
6	<i>Cycle per cycle percentage of edited measurements by threshold criteria. The blue curve shows the trend of edited measurements after adjusting for annual and semi-annual signals.</i> . . . . .	33
7	<i>Percentage of edited measurements by 20-Hz measurements number criterion. Left: Cycle per cycle monitoring. The blue curve shows the trend of edited measurements after adjusting for annual and semi-annual signals. Right: Map over a one year period (cycles 267 to 303). Bottom: Map over interleaved with Jason-2 period from 2016-10-13 to 2017-05-17 (left) and map over cycles 500 (2017-07-11) to 506(right)</i> . . . . .	34
8	<i>Percentage of edited measurements by 20-Hz measurements standard deviation criterion. Left: Cycle per cycle monitoring. The blue curve shows the trend of edited measurements after adjusting for annual and semi-annual signals. Right: Map over a one year period (cycles 267 to 303). Bottom: Map over interleaved with Jason-2 period from 2016-10-13 to 2017-05-17 (left) and map over cycles 500 (2017-07-11) to 506(right)</i> . . . . .	35

9	<i>Percentage of edited measurements by SWH criterion. Left: Cycle per cycle monitoring. The blue curve shows the trend of edited measurements after adjusting for annual and semi-annual signals. Right: Map over a one year period (cycles 267 to 303). Bottom: Map over interleaved with Jason-2 period from 2016-10-13 to 2017-05-17 (left) and map over cycles 500 (2017-07-11) to 506(right)</i>	36
10	<i>Percentage of edited measurements by Sigma0 criterion. Left: Cycle per cycle monitoring. The blue curve shows the trend of edited measurements after adjusting for annual and semi-annual signals. Right: Map over a one year period (cycles 267 to 303). Bottom: Map over interleaved with Jason-2 period from 2016-10-13 to 2017-05-17 (left) and map over cycles 500 (2017-07-11) to 506(right)</i>	37
11	<i>Percentage of edited measurements by 20 Hz Sigma0 standard deviation criterion. Left: Cycle per cycle monitoring. The blue curve shows the trend of edited measurements after adjusting for annual and semi-annual signals. Right: Map over a one year period (cycles 267 to 303). Bottom: Map over interleaved with Jason-2 period from 2016-10-13 to 2017-05-17 (left) and map over cycles 500 (2017-07-11) to 506(right)</i>	38
12	<i>Percentage of edited measurements by radiometer wet troposphere criterion. Left: Cycle per cycle monitoring. The blue curve shows the trend of edited measurements after adjusting for annual and semi-annual signals. Right: Map over a one year period (cycles 267 to 303). Bottom: Map over interleaved with Jason-2 period from 2016-10-13 to 2017-05-17 (left) and map over cycles 500 (2017-07-11) to 506(right)</i>	40
13	<i>Percentage of edited measurements by dual frequency ionosphere criterion. Left: Cycle per cycle monitoring. The blue curve shows the trend of edited measurements after adjusting for annual and semi-annual signals. Right: Map over a one year period (cycles 267 to 303). Bottom: Map over interleaved with Jason-2 period from 2016-10-13 to 2017-05-17 (left) and map over cycles 500 (2017-07-11) to 506(right)</i>	41
14	<i>Percentage of edited measurements by square off-nadir angle criterion. Left: Cycle per cycle monitoring. The blue curve shows the trend of edited measurements after adjusting for annual and semi-annual signals. Right: Map over a one year period (cycles 267 to 303). Bottom: Map over interleaved with Jason-2 period from 2016-10-13 to 2017-05-17 (left) and map over cycles 500 (2017-07-11) to 506(right)</i>	42
15	<i>Cycle per cycle percentage of edited measurements by sea state bias criterion (left). The blue curve shows the trend of edited measurements after adjusting for annual and semi-annual signals. Right: Map of percentage of edited measurements by sea state bias criterion over a one year period (cycles 267 to 303). Bottom: Map over interleaved with Jason-2 period from 2016-10-13 to 2017-05-17 (left) and map over cycles 500 (2017-07-11) to 506(right)</i>	43
16	<i>Percentage of edited measurements by altimeter wind speed criterion. Left: Cycle per cycle monitoring. The blue curve shows the trend of edited measurements after adjusting for annual and semi-annual signals. Right: Map over a one year period (cycles 267 to 303). Bottom: Map over interleaved with Jason-2 period from 2016-10-13 to 2017-05-17 (left) and map over cycles 500 (2017-07-11) to 506(right)</i>	44
17	<i>Percentage of edited measurements by ocean tide criterion. Left: Cycle per cycle monitoring. The blue curve shows the trend of edited measurements after adjusting for annual and semi-annual signals. Right: Map over a one year period (cycles 267 to 303). Bottom: Map over interleaved with Jason-2 period from 2016-10-13 to 2017-05-17 (left) and map over cycles 500 (2017-07-11) to 506(right)</i>	45

18	<i>Percentage of edited measurements by sea surface height criterion. Left: Cycle per cycle monitoring. The blue curve shows the trend of edited measurements after adjusting for annual and semi-annual signals. Right: Map over a one year period (cycles 267 to 303). Bottom: Map over interleaved with Jason-2 period from 2016-10-13 to 2017-05-17 (left) and map over cycles 500 (2017-07-11) to 506 (right)</i>	46
19	<i>Percentage of edited measurements by sea level anomaly criterion. Left: Cycle per cycle monitoring. The blue curve shows the trend of edited measurements after adjusting for annual and semi-annual signals. Right: Map over a one year period (cycles 267 to 303). Bottom: Map over interleaved with Jason-2 period from 2016-10-13 to 2017-05-17 (left) and map over cycles 500 (2017-07-11) to 506(right)</i>	47
20	<i>Cyclic monitoring of number of elementary 20 Hz range measurements for Jason-1 and Jason-2 for Ku-band (left) and C-band (right).</i>	49
21	<i>Cyclic monitoring of rms of elementary 20 Hz range measurements for Jason-1 and Jason-2 for Ku-band (left) and C-band (right).</i>	50
22	<i>Square of the off-nadir angle deduced from waveforms (<math>deg^2</math>) for Jason-1 and Jason-2: Daily monitoring (left), histograms for Jason-2 cycle 157 (Jason-1 cycle 513/514).</i>	51
23	<i>Histograms of Jason-2 mispointing after retracking with different antenna beamwidth (from [88]): 1.26° (blue), 1.28° (light blue), 1.30° (dark blue).</i>	51
24	<i>Cyclic monitoring of Sigma0 for Jason-1 and Jason-2 for Ku-band (left) and C-band (right). Daily monitoring of Jason-1 - Jason-2 differences (bottom), a 10 day filter is applied.</i>	52
25	<i>Cyclic monitoring of SWH for Jason-1 and Jason-2 for Ku-band (left) and C-band (right). Daily monitoring of Jason-1 - Jason-2 differences (bottom), a 10 day filter is applied.</i>	53
26	<i>Diagram of dispersion of Jason-1 (GDR-E) - Jason-2 versus Jason-2 dual-frequency ionosphere correction for Jason-2 cycle 15. Left: non-filtered, right: filtered.</i>	54
27	<i>Cyclic monitoring of dual-frequency ionosphere for Jason-1 and Jason-2 (right). Daily monitoring of Jason-1 - Jason-2 differences (left), a 10 day filter is applied.</i>	55
28	<i>Cycle per cycle monitoring of filtered altimeter ionosphere correction minus GIM ionosphere correction for Jason-1 and Jason-2. Left: Mean, right: standard deviation.</i>	55
29	<i>Cycle per cycle monitoring of filtered altimeter ionosphere minus GIM correction computed per local hour time intervals. Mean on left and standard deviation on the right. A one-year smooth is applied.</i>	56
30	<i>Cycle per cycle monitoring of mean (left) and standard deviation (right) of radiometer minus ECMWF model wet troposphere correction over 2017 (until cycle 506) for Jason-2 I/GDR.</i>	57
31	<i>Left: Daily monitoring of radiometer and ECMWF model wet troposphere correction differences for Jason-1 (blue) and Jason-2 (red). Right: daily monitoring for Jason-2 GDRs (red) and IGDRs (pink). Bottom: Daily monitoring for Jason-2 GDRs (red) for 2016. Vertical gray bands correspond to yaw maneuvers on Jason-2.</i>	58
32	<i>Cycle per cycle monitoring of mean (left) and standard deviation (right) of altimeter wind speed for Jason-2 I/GDR. <b>bottom:</b> mean difference of altimeter wind speed for Jason-2 GDR minus model (ECMWF and ERA interim)</i>	59
33	<i>Cyclic monitoring of mean (left) and standard deviation (right) of Jason-2 and Jason-1 sea state bias, using SSB from Jason-1 GDR-E, Jason-2 GDR-D and updated (2012) SSB for Jason-2.</i>	60

34	<i>Top: Monitoring of mean of SSH crossover differences for Jason-2 and Jason-1 using Jason-2 (red), Jason-1 GDR-E (blue), Jason-2 GDR-D Upd with GOT4.10 + POE-E + Tran2012 SSB (pink). Bottom: Monitoring of mean of SSH crossover differences for different data types of Jason-2: IGDR with DUACS updates (green), GDR (red): over 2017 (left) and over 5 years (right).</i>	62
35	<i>Mean of SSH crossovers differences for Jason-2 against ocean tide solution used to compute SSH.</i>	63
36	<i>Bottom: Map of mean of SSH crossovers differences for Jason-2 cycle 1 to 506. note that for cycles 1 to 253, GDR orbit is POE-D. GDR have been available with orbit POE-E since cycle 254. Left: Map of mean of SSH crossovers differences for Jason-2 cycle 1 to 303. Right: Map of mean of SSH crossovers differences for Jason-2 cycle 305 to 327 (less than a year)</i>	64
37	<i>Cycle by cycle standard deviation of SSH crossover differences for Jason-2 and Jason-1 (left) and Jason-2 GDR versus IGDR (right). Only data with abs(latitude) &lt; 50°, bathymetry &lt; -1000m and low oceanic variability were selected.</i>	65
38	<i>Monitoring of pseudo time-tag bias estimated cycle by cycle from GDR products for Jason-2 and Jason-1</i>	65
39	<i>Cycle by cycle monitoring of SSH bias between Jason-1 and Jason-2 before and after Jason-1 ground-track change (black curve and dots) and SSH bias without applying corrections in SSH calculation for both missions only during the tandem phase (gray curve).</i>	67
40	<b>Top left:</b> Maps of SLA (orbit (POE-E) - range - geophysical corrections - MSS 2011 (ref20)) mean differences between Jason-1 and Jason-2 during tandem phase (cycles 1 to 20), using Jason-2 updated GDR-D and Jason-1 GDR-E (the map is centered around the mean of 0.2 cm). <b>Top right:</b> without applying geophysical corrections. <b>Bottom:</b> using GSFC09 orbits without applying geophysical corrections	68
41	<i>Cycle by cycle monitoring of SLA standard deviation for Jason-1 and Jason-2 (using different MSS solutions)</i>	69
42	<i>MSL evolution calculated from Jason-2 data. GIA (-0.3 mm/yr [77]) is applied.</i>	75
43	<i>Jason-2 / tide gauge (GLOSS/CLIVAR network) comparisons. Periodic signals are removed and resulting time series are 2-month (thin line) and 6-month (thick line) low-pass filtered. Dotted line represent a linear regression fit of the time series; slope values are indicated in the legend</i>	75
44	<i>Maps of regional MSL slopes for Jason-2 cycles 1 to 303, seasonal signal removed.</i>	76
45	<i>Jason-2 LRO sampling for 3 subsequent periods of 17 days in black, red and blue (from public release)</i>	78
46		79
47	<i>17-days subcycle 006 (top) to 008 (bottom) - after SHM (2017-09-14 to 2017-10-13), red: missing theoretical points, cyan: available measurements</i>	80
48	<i>80-days subcycle 001 and 002, red: missing theoretical points, blue: available measurements before SHM (2017-09-14 to 2017-10-13), cyan available measurements after SHM (2017-09-14 to 2017-10-13)</i>	81
49	<i>145-days subcycle 001, red: missing theoretical points, blue: available measurements before SHM (2017-09-14 to 2017-10-13), cyan available measurements after SHM (2017-09-14 to 2017-10-13)</i>	81

List of items to be defined or to be confirmed

Applicable documents / reference documents

## Contents

<b>1. Introduction</b>	<b>2</b>
<b>2. Data used and processing status</b>	<b>8</b>
2.1. Mission events	8
2.2. New Long Repeat Orbit [LRO]	10
2.3. Models and Standards History	11
2.4. Main processing events summary	15
2.5. Data Used	15
<b>3. Data coverage and edited measurements</b>	<b>16</b>
3.1. Data availability	16
3.1.1. Missing measurements	16
3.1.2. Over land and ocean	22
3.1.3. Over ocean	24
3.2. Edited measurements	25
3.2.1. Editing criteria definition	25
3.2.2. Edited measurements	25
3.2.3. Selection of measurements over ocean and lakes	29
3.2.4. Flagging quality criteria: Ice flag	30
3.2.5. Flagging quality criteria: Rain flag	31
3.2.6. Threshold criteria: Global	32
3.2.7. Threshold criteria: 20-Hz measurements number	34
3.2.8. Threshold criteria: 20-Hz measurements standard deviation	35
3.2.9. Threshold criteria: Significant wave height	36
3.2.10. Backscatter coefficient	37
3.2.11. Backscatter coefficient: 20 Hz standard deviation	38
3.2.12. Radiometer wet troposphere correction	39
3.2.13. Dual frequency ionosphere correction	41
3.2.14. Square off-nadir angle	42
3.2.15. Sea state bias correction	43
3.2.16. Altimeter wind speed	44
3.2.17. Ocean tide correction	45
3.2.18. Sea surface height	46
3.2.19. Sea level anomaly	47
<b>4. Monitoring of altimeter and radiometer parameters</b>	<b>48</b>
4.1. Methodology	48
4.2. 20 Hz Measurements	48
4.2.1. 20 Hz measurements number in Ku-Band and C-Band	49
4.2.2. 20 Hz measurements standard deviation in Ku-Band and C-Band	50
4.3. Off-Nadir Angle from waveforms	51
4.4. Backscatter coefficient	52
4.5. Significant wave height	53
4.6. Dual-frequency ionosphere correction	54
4.7. AMR Wet troposphere correction	56
4.7.1. Overview	56
4.7.2. Comparison with the ECMWF model	57
4.8. Altimeter wind speed	58

.....	
4.9. Sea state bias . . . . .	59
<b>5. SSH crossover analysis</b>	<b>61</b>
5.1. Overview . . . . .	61
5.2. Mean of SSH crossover differences . . . . .	61
5.3. Standard deviation of SSH crossover differences . . . . .	64
5.4. Estimation of pseudo time-tag bias . . . . .	65
<b>6. Sea Level Anomalies (SLA) Along-track analysis</b>	<b>66</b>
6.1. Overview . . . . .	66
6.2. Mean of SLA differences between Jason-2 and Jason-1 . . . . .	66
6.3. Standard deviation of SLA differences between Jason-2 and Jason-1 . . . . .	68
6.4. Sea level seasonal variations . . . . .	69
<b>7. Mean Sea Level (MSL) calculation</b>	<b>74</b>
7.1. Overview . . . . .	74
7.2. Altimeter Mean Sea Level evolution (MSL) . . . . .	74
7.2.1. Calculation of reference time serie . . . . .	74
7.2.2. External data comparisons with tide gauges . . . . .	75
7.3. Regional mean sea level trend for Jason-2 . . . . .	76
<b>8. Investigations</b>	<b>77</b>
8.1. Safe Hold Modes during 2017 . . . . .	77
8.2. Details on new Long Repeat Orbit sub-cycles . . . . .	77
<b>9. Conclusion</b>	<b>82</b>
<b>10. Appendix: Global Jason-2 Data Quality Assessment on the new Long Repeat Orbit</b>	<b>83</b>
<b>11. References</b>	<b>85</b>

## Glossary

- AMR** Advanced Microwave Radiometer
- CLS** Collecte Localisation Satellites
- CNES** Centre National d'Etudes Spatiales
- CNG** Consigne Numerique de Gain (= Automatic Gain Control)
- DEM** Digital Elevation Model
- DIODE** Détermination Immédiate d'Orbite par Doris Embarqué
- ECMWF** European Centre for Medium-range Weather Forecasting
- GDR** Geophysical Data Record
- GIM** Global Ionosphere Maps
- GOT** Global Ocean Tide
- IGDR** Interim Geophysical Data Record
- JPL** Jet Propulsion Laboratory (Nasa)
- MLE** Maximum Likelihood Estimator
- MOE** Medium Orbit Ephemeris
- MQE** Mean Quadratic Error
- MSS** Mean Sea Surface
- PLTM** PayLoad TeleMetry
- POE** Precise Orbit Ephemeris
- OGDR** Operational Geophysical Data Record
- SALP** Service d'Altimétrie et de Localisation Précise
- SSH** Sea Surface Height
- SLA** Sea Level Anomaly
- SLR** Satellite Laser Ranging
- SSB** Sea State Bias
- SWH** Significant Wave Height
- TM** TeleMetry

## 1. Introduction

This document presents the synthesis report concerning validation activities of Jason-2 GDRs under SALP contract (N° 160182-14026/00 Lot 1.6.3) supported by CNES at the CLS Space Oceanography Division. It covers several points: CAL/VAL Jason-2 activities, Jason-2 / Jason-1 cross-calibration (until mid-2013), and specific studies and investigations.

The present report assesses the Jason-2 data quality. After an executive summary, we present a detailed description of the main performance metrics of the mission including:

- data coverage monitoring,
- edited measurements monitoring,
- relevant parameters derived from instrumental measurements and geophysical corrections analysis,
- accuracy and stability of SLA measurements check.

Hereafter, we present the analyzes focusing on Jason-1/Jason-2 cross-calibration. The SLA performances and consistency with Jason-1 are also described :

- During the tandem configuration (4th July 2008 to 26th January 2009) where both satellites were on the same ground track (This allowed to precisely assess parameter discrepancies between both missions in order to detect geographically correlated biases, jumps or drifts.)
- But even during the formation flight phase (after the end of the tandem phase),
- and after Jason-1 moved to its geodetic orbit, comparison were still possible until the end of the Jason-1 mission in June 2013.

Note that main statistics results are presented here, but other analysis including histograms, plots and maps are continuously produced and used in the quality assessment process. Finally, this report also presents the results of specific investigations undertaken this year, either to better characterize mission performance or as a consequence of mission events.

Note that Jason-3 was launched on 2016, January 17th. Cross-calibration analyzes between Jason-2 and Jason-3 are also performed, but shown in annual report of Jason-3 [11].

## 2017 executive summary on Jason-2

By succeeding to TOPEX/Poseidon and Jason-1 on their primary ground track, Jason-2 has extended the high-precision ocean altimetry data record.

**Please note that 2017 annual report is the last provided on CNES side for Jason-2.**

### History

The OSTM/Jason-2 satellite was successfully launched on June, 20th 2008. Since July, 4th, Jason-2 was on its operational orbit.

- Until January 2009, it was flying in tandem with Jason-1, only 55s apart.
- From May 2012 onwards, Jason-1 was on a geodetic orbit until its last measurement on 21st June 2013, after about 11.5 years in orbit. Cross-calibration results with Jason-1 are available in Jason-1 GDR-E reprocessing<sup>1</sup>
- Jason-3 was launched on 2016, January 17th. Cross-calibration analyzes between Jason-2 and Jason-3 are performed and shown in Jason-3 annual report<sup>2</sup>.
- Jason-2 was moved from its original groundtrack to its new interleaved groundtrack on October 2016.
- Jason-2 was moved to a Long Repeat Orbit (LRO) at the beginning of July 2017.

### CalVal activities

Since the beginning of the mission, Jason-2 data have been analyzed and monitored in order to assess the quality of Jason-2 products. During each cycle, missing measurements were monitored, spurious data were edited and relevant parameters derived from instrumental measurements and geophysical corrections were analysed for OGDR, IGDR and GDR. Cycle per cycle reports are available on AVISO webpage<sup>3</sup>.

**The more of 9 years of Jason-2 data show excellent quality.**

---

<sup>1</sup>Roinard H., Philipps S.: Jason-1 GDR-E release. Global assessment over ocean. SALP-RP-MA-EA-22426-CLS. Available at [http://www.aviso.altimetry.fr/fileadmin/documents/calval/validation\\_report/J1/Jason1\\_ReprocessingReport\\_GDR\\_E.pdf](http://www.aviso.altimetry.fr/fileadmin/documents/calval/validation_report/J1/Jason1_ReprocessingReport_GDR_E.pdf)

<sup>2</sup>H. Roinard, E. Cadier. Jason-3 validation and cross calibration activities (Annual report 2017). SALP-RP-MA-EA-23187-CLS. <https://www.aviso.altimetry.fr/en/data/calval/latest-results.html>

<sup>3</sup><http://www.aviso.altimetry.fr/en/data/calval/systematic-calval.html>

## Main processing events summary

End of 2008 Jason-2 data were already available to end users in OGDR (3h data latency) and IGDR (1-2 days data latency).

- They were first released in version T and switched at cycle 015 to version C.
- They stayed in this version till cycle 149 (till 2012/07/31 12:01:59 for OGDR).
- GDR data were released in standard version C during August 2009.
- During 2012 the whole GDR dataset was reprocessed in GDR-D version.
- **A description of the different Jason-2 products is available in the OSTM/Jason-2 Products handbook** <sup>4</sup>

As concerned mission events that impact processing, note that :

- Since 5th of April 2013 (cycle 175), platform moduleB has been used.
- During cycle 226 and 227, the precise orbit ephemeris (orbit in GDR) was based on DORIS and SLR only due to payload GPS unavailability. Since cycle 228, GPS-B (instead of GPS-A) is operational.
- Since cycle 254, POE-E orbit standard has been applied.
- Jason-2 was moved from its original groundtrack to its new interleaved groundtrack on October 2016 (from October 2nd at 11 :53 UTC (end of cycle 303) until 13-10-2016 at 20:00:00 (cycle 305, pass 164)).
- After several Safe Hold Modes in March and May 2017, Jason-2 was moved to a Long Repeat Orbit (LRO) at the beginning of July 2017. In order to improve data quality, mean sea surface solution in products has been modified to CNES/CLS 2015 solution <sup>5</sup> from cycle 500 (first cycle on LRO) onwards.

**New Long Repeat Orbit [LRO]** During the exceptional JSG held on 2017 June 20th, due to the gyro 1 and 2 status that will need more investigations, the global ageing of the spacecraft, and the already existing recommendation from OSTST to move Jason-2 to a new orbit at 1309.5km, it was decided to start the maneuvers to that new orbit. Jason-2 has been moved in early July to a new LRO (Long Repeat Orbit) orbit. The new orbit was reached on July 8th and the onboard instruments have resumed nominal operations on July 11th.

The Jason-2 data products in the LRO phase follow a similar naming convention as was used when Jason-1 was moved to the LRO phase. Specifically, data products are provided in about 10-days cycles, with cycle numbering beginning at cycle number 500 and each cycle containing 254 passes (half orbit revolutions). The product version remain as version “D”.

The Jason-2 Long Repeat Orbit is approximately 27 km below the historical T/P orbit still used by Jason-3. The very long repeat cycle yields a fine grid of approximately 8-km: it is beneficial for marine geodesy (e.g. improvement of bathymetry and mean sea surface models).

The strategy is inherited from Jason-1 EOL with a try to optimize all sub-cycles, shorter ones for sea-state and mesoscale, and longer ones for geodesy (detail about sub cycles in 2017 annual

---

<sup>4</sup>Available at [http://www.avisioceanobs.com/fileadmin/documents/data/tools/hdbk\\_j2.pdf](http://www.avisioceanobs.com/fileadmin/documents/data/tools/hdbk_j2.pdf).

<sup>5</sup>Mean Sea Surface CNES/CLS model <https://www.avisioceanobs.com/en/data/products/auxiliary-products/mss.html>

report). More details can be found in the JA1-GM <sup>6</sup> and JA2-EOL papers <sup>7</sup>.

*Note that Jason-2 first measurements on Long Repeat Orbit is on 11/07/2017 10:32:39 (cycle 500, pass 033).*

## Data availability

Data availability is excellent for Jason-2. Jason-2 presents more than 99% of measurements available over ocean and after removing specific events or big anomalies (see right of figure 1). The main anomalies on red curve of left side of figure 1 are:

- During 2013, Jason-2 entered safe hold mode twice in March (from 25/03/2013 to 29/03/2013 and from 30/03/2013 until 05/04/2013, during cycles 174 and 175) and a third time in September (from 05/09/2013 to 12/09/2013, during cycles 190-191).
- During 2016, data are missing between April, 5<sup>th</sup> at 13:35:10 and April, 6<sup>th</sup> at 12:02:40 as no altimeter measurements have been performed (altimeter in wait mode) during this period to allow the upload of new GPS onboard software.
- Jason-2 was moved from its original groundtrack to its new interleaved groundtrack on October 2016: During move to interleaved ground track, there is no measurement from October 2nd at 11:53 (end of cycle 303) until the end of the orbit change nominal sequence on 13-10-2016 at 20:00:00 (cycle 305, pass 164).
- Several Safe Hold Modes happened in March and May 2017

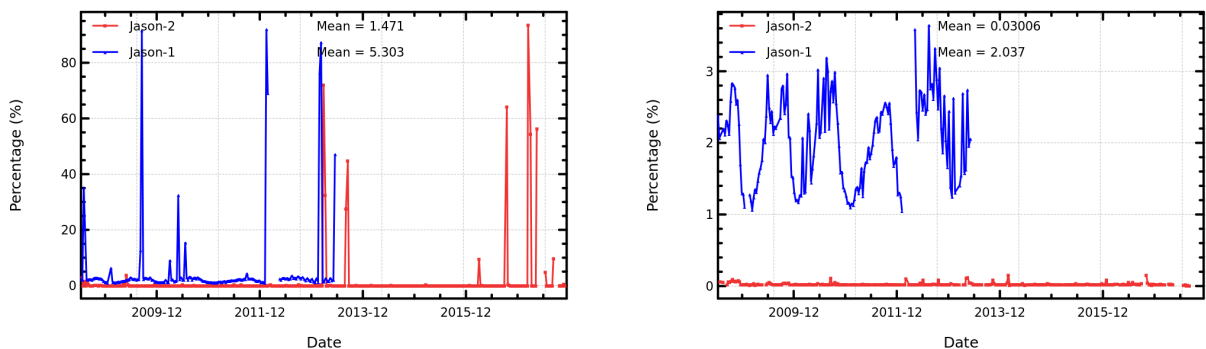


Figure 1 – Jason-2 and Jason-1 GDR data availability over ocean (per cycle). On the right side cycles with missing data due to event or anomaly are excluded.

A selection is done to reject bad points before compute statistics. It leads to a mean of 3.3% of Jason-2 measurements that are rejected on each cycle (after having selected only ocean/lakes measurements, without land and ice flagged points).

<sup>6</sup>JA1-GM <http://dx.doi.org/10.1080/01490419.2012.717854>

<sup>7</sup>JA2-EOL <http://dx.doi.org/10.1175/JTECH-D-16-0015.1>

## Sea Level Anomalies

The monitoring of SLA standard deviation has been computed and plotted in figure 2. Standard deviation of daily SLA average differences is about 10.4 to 10.9 cm against MSS solution that is used.

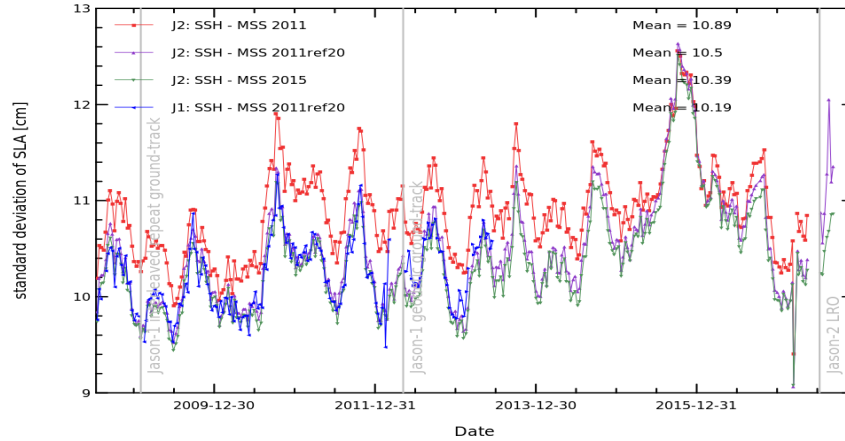


Figure 2 – Cycle by cycle monitoring of SLA standard deviation for Jason-1 and Jason-2 (using different MSS solutions)

## Performances at crossover points

At crossovers Jason-2 shows very good and stable performances for both IGDR and GDR products. The standard deviation of differences at crossover points of 4.9 cm represents a system error of 3.5 cm.

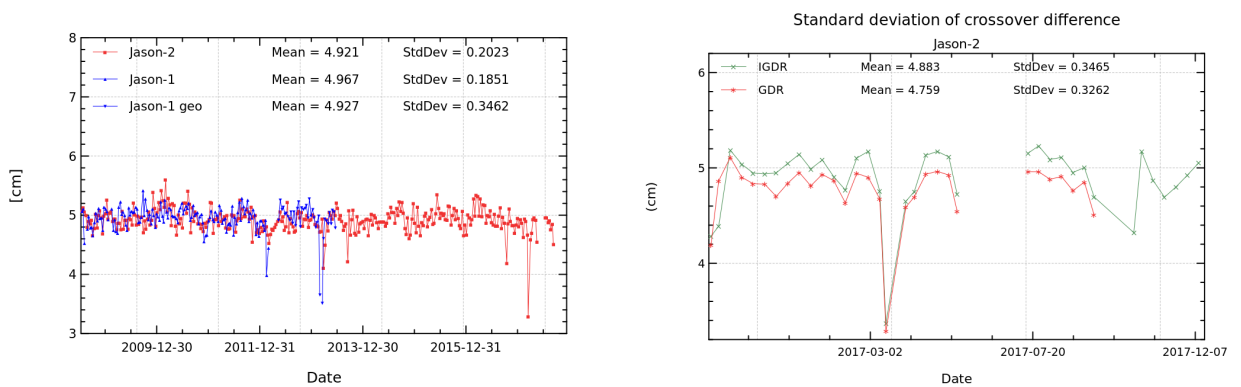


Figure 3 – Cycle by cycle standard deviation of SSH crossover differences for Jason-2 and Jason-1 (left) and Jason-2 GDR versus IGDR (right). Only data with  $abs(latitude) < 50^\circ$ , bathymetry  $< -1000m$  and low oceanic variability were selected.

## Contribution to Global Mean Sea Level

Regional and global biases between missions have to be precisely estimated in order to ensure the quality of the reference GMSL serie. For more precisions, see the dedicated section on AVISO+ website [8] and annual report for this activity<sup>9</sup>.

Jason-2 contributes to the reference GMSL indicator between October 2008 and June 2016. Over this period, its stability is excellent, and no anomalies has been detected as shown on comparison to tide gauges on figure 4. Note that since it has been replaced by Jason-3 data, Jason-2 is no more used to compute the reference serie on historical TOPEX-Poseidon ground track.

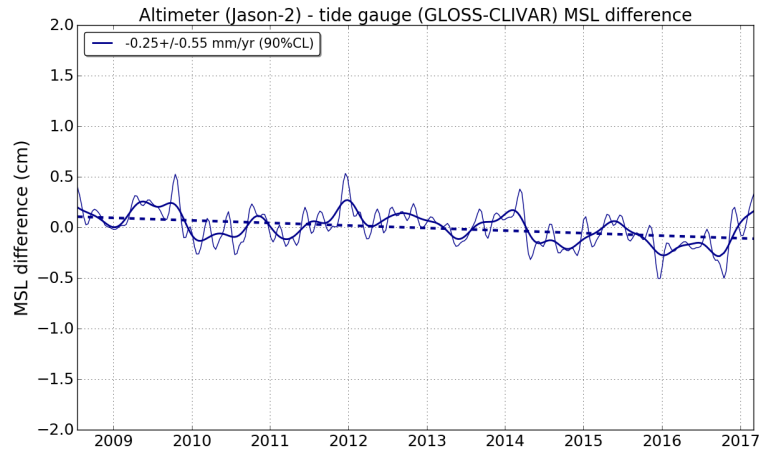


Figure 4 – Jason-2 / tide gauge (GLOSS/CLIVAR network) comparisons. Periodic signals are removed and resulting time series are 2-month (thin line) and 6-month (thick line) low-pass filtered. Dotted line represent a linear regression fit of the time series; slope values are indicated in the legend

<sup>8</sup><https://www.aviso.altimetry.fr/en/data/products/ocean-indicators-products/mean-sea-level.html>

<sup>9</sup>M. Ablain. SALP annual report (2017) of Mean Sea Level Activities (SALP-RP-MA-EA-23189-CLS )

## 2. Data used and processing status

### 2.1. Mission events

The following table shows the major planned events during the Jason-2 mission (calibration events are not mentioned, and non planned events as Safe Hold Modes are detailed in 3).

Dates	Events	Impacts
4 July 2008 5h57	Start of Jason-2 Cycle 0	
4 July 2008 12h15	Start of Poseidon3 altimeter. Tracking mode : autonomous acquisition, median	Start of level2 product generation.
04 July 2008 13:47:52 to 04 July 2008 14:13:36	Poseidon3 altimeter. Tracking mode : Diode acquisition, median	
04 July 2008 14:14:39 to 17 July 2008 15:30:22	Poseidon3 altimeter. Tracking mode : Diode acquisition, SGT	
8 July 2008 4h45 - 5h25	Poseidon3 altimeter. Dedicated period for validation of tracking mode performances	small data gaps on corresponding passes [Cycle 0]
11 July 2008 13h00-13h01 and 13h04-13h12	Poseidon3 altimeter. Tracking mode : Diode-DEM (functional)	Functional test of DIODE-DEM tracking mode while onboard DEM was not correct, leading to wrong waveforms and so impacts on altimeter retracking outputs.
12 July 2008 1h20	Start of Jason-2 Cycle 1	
16 July 2008 7h10-17h08	upload Poseidon-3 - DEM	Data gap on corresponding passes [Cycle 1, Pass 108-144]
17 July 2008 7h29-11h30	upload Poseidon-3 - DEM	Data gap on corresponding passes [Cycle 1, Pass 108-144]
17 July 2008 15:30:22 to 31 July 2008 21:17:08 UTC	Poseidon-3 altimeter. Tracking mode : Diode acquisition, median	
21 July 2008 23h18	Start of Jason-2 Cycle 2	
31 July 2008 21:17:09 to 10 August 2008 19:15:39	Jason-2 Cycle 3: Poseidon3 altimeter. Tracking mode : Diode-DEM	
.../...		

Dates	Events	Impacts
10 August 2008 19:15:40 to 20 August 2008 17:14:10	Jason-2 Cycle 4: Poseidon3 altimeter. Tracking mode : Diode acquisition, median	
20 August 2008 17:14:11 to 30 August 2008 15:12:43	Jason-2 Cycle 5: Poseidon3 altimeter. Tracking mode : Diode-DEM	
30 August 2008 15:12:43 to 9 September 2008 13:11:15	Jason-2 Cycle 6: Poseidon3 altimeter. Tracking mode : Diode acquisition, median	
9 September 2008 13:11:15 to 19 September 2008 11:09:47	Jason-2 Cycle 7: Poseidon3 altimeter. Tracking mode : Diode-DEM	
19 September 2008 11:09:47 to 29 September 2008 09:08:19	Jason-2 Cycle 8: Poseidon3 altimeter. Tracking mode : Diode acquisition, median	
11 Mai 2009 12:09 to 14 Mai 2009 13:09	Upload Poseidon-3 (new DEM)	data gaps (northern hemisphere) for passes 154 to 231
2 February 2009 06:55:11 to 15:58:05	software upload to Poseidon-3	data gap between passes 204 and 213
4 June 2009 06:31:27 to 14 June 2008 04:29:59	Jason-2 Cycle 34: Poseidon3 altimeter. Tracking mode : Diode-DEM	
12 February 2010	Upload of Doris V8.0 flight software	improved OGDR orbit accuracy
16 September 2010	Jason-2 Cycle 81: Upload of DEM patch for Gavdos transponder calibration	data gap for passes 087 and 237
17 February 2011	GPSP OBS revert upload	
12-14 September 2012	DORIS OBS upload (DORIS restart on 19th September)	OGDR data gap (during the DORIS restart)
15 May 2013	update on Usingen receiver was done on 15-May-2013 at 11:05Z in order to solve a problem with the TM receiver	
.../...		

Dates	Events	Impacts
5-15 March 2014	Jason-2 Cycle 209: Tracking mode : Diode-DEM	gain of available measurements on earth
18 March 2014	Update of TRIODE software (for OGDR).	Reduction of 14days signal in OGDR SLA.
22 June-2 July 2014	Jason-2 Cycle 220: Tracking mode : Diode-DEM	gain of available measurements on earth
9 September 2014	cycle 228: switch to GPS-B (instead of GPS-A)	
25 May 2015	cycle 254: orbit standard switches to POE-E from this cycle onwards.	
5-6 April 2016	cycle 285: upload of new GPS On Board software	Data gap: no scientific products have been processed between April, 5 at 13:35:10 and April, 6 at 12:02:40.
2-13 October 2016	from cycle 304 pass 001 to cycle 305 pass 163: move to interleaved ground track	Data gap: Poseidon-3 altimeter is put in WAIT mode.
4-6 October 2016	upload of a new DEM	
05-15 December 2016	Jason-2 Cycle 311: Tracking mode : Diode-DEM	gain of available measurements on earth
July 2017	Move to Long Repeat Orbit	
19 July 2017	TC-GROUP (*2: first one during about 20sec and second one during around 4sec)	
03 November 2017	Upload flight software (6'56")	

Table 1 – Planned events

## 2.2. New Long Repeat Orbit [LRO]

During the exceptional JSG held on 2017 June 20th, due to the gyro 1 and 2 status that will need more investigations, the global ageing of the spacecraft, and the already existing recommendation from OSTST to move Jason-2 to a new orbit at 1309.5km, it was decided to start the maneuvers to that new orbit. Jason-2 has been moved early July to a new LRO (Long Repeat Orbit) orbit. The new orbit was reached on July 8th and the onboard instruments have resumed nominal operations on July 11th.

The Jason-2 data products in the LRO phase follow a similar naming convention as was used when Jason-1 was moved to the LRO phase. Specifically, data products are provided in about 10-days

cycles, with cycle numbering beginning at cycle number 500 and each cycle containing 254 passes (half orbit revolutions). The product version remain as version “D”.

The Jason-2 Long Repeat Orbit is approximately 27 km below the historical T/P orbit still used by Jason-3. The very long repeat cycle yields a fine grid of approximately 8-km: it is beneficial for marine geodesy (e.g. improvement of bathymetry and mean sea surface models).

The strategy is inherited from Jason-1 EOL with a try to optimize all sub-cycles, shorter ones for sea-state and mesoscale, and longer ones for geodesy (detail about sub cycles in part 8.2.). More details can be found in the JA1-GM [100] and JA2-EOL papers [101].

*Note that Jason-2 first measurements on Long Repeat Orbit is on 11/07/2017 10:32:39 (cycle 500, pass 033).*

### 2.3. Models and Standards History

---

Three versions of the Jason-2 Operational Geophysical Data Records (OGDRs) and Interim Geophysical Data Records (IGDRs) have been generated up to now.

- These three versions are identified by the version numbers “T” (for test), “C” and “D” in the product filename. For example,
  - version “T” IGDRs are named “JA2\_IPN\_2PT”,
  - version “C” IGDRs are named “JA2\_IPN\_2Pc”,
  - and version “D” IGDRs are named “JA2\_IPN\_2Pd”.
- All three versions adopt an identical data record format described in Jason-2 User Handbook [1].
- Versions “T” and “C” differ only slightly (names of variables are corrected and 3 variables added).
- Version “T” O/IGDRs were the first version released soon after launch and was disseminated only to OSTST community.
- Version “C” O/IGDRs were first implemented operationally from data segment 141 of cycle 15 for the OGDRs (3rd December 2008) and cycle 15 for the IGDRs.
- Version “C” of Jason-2 data is consistent with version “C” of Jason-1 data.
- Version “D” O/IGDRs were first implemented operationally from data segment 78 of cycle 150 for the OGDRs (31st July 2012) and cycle 150 for the IGDRs.
- GDR data switched to version “D” from cycle 146 onwards, but previous cycles 1 to 145 were reprocessed in version “D” during 2012. Therefore the whole Jason-2 mission is available in GDR version “D”.

The table 2 below summarize the models and standards that are adopted for version “D” of Jason-2 data. Differences with the previous version ( “T” / “C” ) are detailed in [7]). More details on some of these models are provided in Jason-2 User Handbook document [1].

Model	Product version "D"
Orbit	<p>Based on Doris onboard navigator solution for OGDRs.</p> <p>DORIS tracking data for IGDRs (except for cycles 20 to 78 : DORIS + SLR tracking ). Using POE-E standards from 25/05/215 onwards.</p> <p>DORIS+SLR+GPS-A tracking data for GDRs cycles 1 to 225.</p> <p>DORIS + SLR tracking for GDRs for cycles 226 and 227)</p> <p>DORIS+SLR+GPS-B tracking data for GDRs from cycle 228 onwards.</p> <p>Using POE-C standard for GDRs until cycle 254 and POE-E from cycle 254 onwards</p>
Altimeter Retracking	<p>“Ocean MLE4” retracking: MLE4 fit from 2nd order Brown analytical model: MLE4 simultaneously retrieves the 4 parameters that can be inverted from the altimeter waveforms:</p> <ul style="list-style-type: none"> <li>• Epoch (tracker range offset) → altimeter range</li> <li>• Composite Sigma → SWH</li> <li>• Amplitude → Sigma0</li> <li>• Square of mispointing angle (Ku band only, a null value is used in input of the C band retracking algorithm)</li> </ul> <p>“Ocean MLE3” retracking: MLE3 fit from 1st order Brown analytical model: MLE3 simultaneously retrieves the 3 parameters that can be inverted from the altimeter waveforms:</p> <ul style="list-style-type: none"> <li>• Epoch (tracker range offset) → altimeter range</li> <li>• Composite Sigma → SWH</li> <li>• Amplitude → Sigma0</li> </ul> <p>“Ice” retracking: Geometrical analysis of the altimeter waveforms, which retrieves the following parameters:</p> <ul style="list-style-type: none"> <li>• Epoch (tracker range offset) → altimeter range</li> <li>• Amplitude → Sigma0</li> </ul>
.../...	

Model	Product version "D"
Altimeter Instrument Corrections	Two sets: <ul style="list-style-type: none"> <li>• on set consistent with MLE4 retracking</li> <li>• on set consistent with MLE3 retracking</li> </ul>
Jason-2 Advanced Microwave Radiometer (AMR) Parameters	Using calibration parameters derived from long term calibration tool developed and operated by NASA/JPL.
Dry Troposphere Range Correction	From ECMWF atmospheric pressures and model for S1 and S2 atmospheric tides
Wet Troposphere Range Correction from Model	From ECMWF model
Ionosphere correction from model	Based on Global Ionosphere TEC Maps from JPL
Sea State Bias Model	Two empirical models: <ul style="list-style-type: none"> <li>• MLE4 version derived from 1 year of MLE4 Jason-2 altimeter data with version "d" geophysical models</li> <li>• MLE3 version derived from 1 year of MLE3 Jason-2 altimeter data with version "d" geophysical models</li> </ul>
Mean Sea Surface Model	MSS_CNES_CLS11 until cycle 327. MSS_CNES_CLS15 from cycle 500 onwards
Mean Dynamic Topography Model	MDT_CNES-CLS09
Geoid	EGM96
Bathymetry Model	DTM2000.1
Inverse Barometer Correction	Computed from ECMWF atmospheric pressures after removing S1 and S2 atmospheric tides
Non-tidal High-frequency De-aliasing Correction	Mog2D high resolution ocean model on I/GDRs. None on OGDRs. Ocean model forced by ECMWF atmospheric pressures after removing S1 and S2 atmospheric tides.
Tide Solution 1	GOT4.8 + S1 ocean tide. S1 and M4 load tide included.
Tide Solution 2	FES2004 + S1 and M4 ocean tides. S1 and M4 load tides ignored
.../...	

Model	Product version “D”
Equilibrium long-period ocean tide model.	From Cartwright and Taylor tidal potential.
Non-equilibrium long-period ocean tide model.	Mm, Mf, Mtm, and Msqm from FES2004
Solid Earth Tide Model	From Cartwright and Taylor tidal potential.
Pole Tide Model	Equilibrium model
Wind Speed from Model	ECMWF model
Altimeter Wind Speed	Wind speed table derived from Jason-1 data (Collard, [40]). In addition, a calibration bias of 0.32 is applied to JA2 Ku-band sigma0 prior wind speed computation.
Rain flag	Derived from comparisons to thresholds of the radiometer-derived integrated liquid water content and of the difference between the measured and the expected Ku-band backscatter coefficient
Ice flag	Derived from comparison of the model wet tropospheric correction to a dual-frequency wet tropospheric correction retrieved from radiometer brightness temperatures, with a default value issued from a climatology table

Table 2 – Models and standards adopted for the Jason-2 version “D” products. Adapted from [1]

- During 2012, the whole Jason-2 mission was reprocessed in GDR-D standard. For more details, please refer to the reprocessing reports [7] and [6].
- **Note that orbit switched to standard POE-E from GDR cycle 254 onwards.**
- From cycle 170 to 178, the flag “qual\_inst\_corr\_1hz\_sig0\_ku” was wrongly set to one because of an out of thresholds criterion. From cycle 179 onwards, the flag “qual\_inst\_corr\_1hz\_sig0\_ku” won’t constantly be set as the threshold used to set this flag has been adjusted in the processing chain, in order to take into account the natural instrumental drift.
- **Change of MSS GDR standard:** To improve the Sea Surface Height Anomaly (SSHA) data quality in the Jason-2 LRO data products an updated Mean Sea Surface (MSS) model has been adopted. The new MSS model is the latest CNES/CLS MSS 2015 solution [103], which is referenced to the 20-year period spanning 1993-2012. The MSS model provided on the prior data products (version “D” products during the 10-day exact repeat phase) was the 2011 solution, referenced to the 7-year period spanning 1993-1999 and has a lower quality on LRO ground tracks. The global bias between these two MSS models is approximately 2.5 cm, due to their different reference periods. Users are therefore cautioned that the SSHA values provided on the respective version “D” data products from the LRO and 10-day exact repeat mission phases are biased by 2.5 cm. The SSHA provided on the version “D” LRO-phase products is lower by 2.5 cm than on the 10-day exact-repeat-phase products. The same evolution was performed on SARAL one year ago when the spacecraft was moved to its LRO

orbit. Note that this MSS 2015 model is proposed for the future version “E” data products [102].

## 2.4. Main processing events summary

---

End of 2008 Jason-2 data were already available to end users in OGDR (3h data latency) and IGDR (1-2 days data latency).

- They were first released in version T and switched at cycle 015 to version C.
- They stayed in this version till cycle 149 (till 2012/07/31 12:01:59 for OGDR).
- GDR data were released in standard version C during August 2009.
- During 2012 the whole GDR dataset was reprocessed in GDR-D version.
- **A description of the different Jason-2 products is available in the OSTM/Jason-2 Products handbook [1].**

As concerned mission events that impact processing, note that :

- Since 5th of April 2013 (cycle 175), platform moduleB has been used.
- During cycle 226 and 227, the precise orbit ephemeris (orbit in GDR) was based on DORIS and SLR only due to payload GPS unavailability. Since cycle 228, GPS-B (instead of GPS-A) is operational.
- Since cycle 254, POE-E orbit standard has been applied.
- Jason-2 was moved from its original groundtrack to its new interleaved groundtrack on October 2016 (from October 2nd at 11 :53 UTC (end of cycle 303) until 13-10-2016 at 20:00:00 (cycle 305, pass 164)).
- After several Safe Hold Modes in March and May 2017, Jason-2 was moved to a Long Repeat Orbit (LRO) at the beginning of July 2017. In order to improve data quality, mean sea surface solution in products has been modified to CNES/CLS 2015 solution from cycle 500 (first cycle on LRO) onwards.

## 2.5. Data Used

---

**In this report, Jason-2 data used are GDR-D from cycle 1 to 506 (until 14/09/2017) and IGDR until cycle 515 (15/12/2017).** Note that in order to improve their product quality (and also to use as much as possible same corrections for multimission products), DUACS system applies some updates to IGDR data (see [104]). If no precision is done, IGDR results that are presented in this document contains DUACS updates (also called here IGDR-L2P).

As Jason-1 data were reprocessed recently, the new GDR-E version of Jason-1 data are used and presented in this report (for more information about Jason-1 GDR-E data, see [4])

### 3. Data coverage and edited measurements

In this report, data used are GDR-D from cycle 1 to 506 (until 14/09/2017) and IGDR until cycle 515 (15/12/2017).

#### 3.1. Data availability

##### 3.1.1. Missing measurements

This section presents a summary of major satellite or ground segment events that occurred from cycle 0 to 506. Table 3 gives a status about the number of missing passes (or partly missing) for GDRs, as well as the associated events for each cycle.

During 2017, cycles 305 to 327 and 500 to 506 were analyzed (note that there is a gap in cycle numbering between 328 and 499). Jason-2 turned into a first safe hold mode between 2017-03-15 (cycle 321) and 2013-03-30 (cycle 322) so that no Jason-2 measurement is available from 15-03-2017 18:33:17 to 30-03-2017 08:47:31 - and into a second safe hold mode on 2017-05-17 (cycle 327). After this second turn into SHM, it was decided to move Jason-2 on its end-of-life drifting orbit, so that the last measurement on the interleaved repetitive ground track was on 17-05-2017 at 22:08:10. After move to new orbit at -27 km (final orbit transfer activities were completed on 10 July 2017), at 09:16 UTC on Tuesday, 11 July, CNES control centre successfully commanded the restart of the core Jason-2 payload instruments. Note that as it was the case with Jason-1, science cycle numbering for the new LRO mission phase on Jason-2 began at cycle 500.

The following table gives an overview over missing data and why it is missing.

Jason-2 Cycles/Pass	Dates	Events
000/222-224	10/07/2008 - 18:28:02 to 20:25:04	Missing telemetry (Usingen station pb)
000/232	11/07/2008 - 03:57:08 to 04:30:30	Partly missing due to altimeter calibration (long LPF)
000/235	11/07/2008 - 07:01:28 to 07:27:41	Partly missing due to altimeter calibration (CNG step)
001/44-46	13/07/2008 - 17:40:00 to 19:37:30	Missing telemetry (Usingen station pb)
001/48-50	13/07/2008 - 21:37:02 to 23:30:00	Missing telemetry (NOAA station pb)
001/108-144		several passes partly missing due to upload of new DEM (planned unavailability)
.../...		

Jason-2 Cycles/Pass	Dates	Events
003/032-035	02/08/2008 - 02:23:45 to 05:46:30	Passes 32 and 35 are partly missing, passes 33 and 34 are completely missing due to missing telemetry (Usingen)
005/236-241	29/08/2008 - 21:44:56 to 30/08/2008 02:52:07	Missing telemetry (Usingen station pb): passes 237 to 240 completely missing, passes 236 and 241 partly missing
006/232	08/09/2008 - 15:48:00 to 16:21:22	pass 232 partially missing due to altimeter calibration (long LPF)
006/235	08/09/2008 - 18:53:00 to 19:19:10	pass 235 partially missing due to altimeter calibration (CNG step)
016/73	10/12/2008 - 15:11:19 to 15:13:27	pass 73 partially missing due to 1) upload of correction for low signal tracking anomaly and 2) memory dumps (planned unavailability)
026/33	18/03/2009 - 05:09:15 to 05:10:44	pass 33 has approximately 90 seconds of missing ocean measurements in gulf of guinea (probably due to missing telemetry)
029/209-210	23/04/2009 - 20:18:36 to 20:35:11	data gap over land (on transition between passes 209 and 210) due to missing telemetry
031/154-231	11/05/2009 12:09 to 14/05/2009 13:09	Upload of new DEM leading to missing portions (northern hemisphere) for passes 154 to 231
033/204-213	02/06/2009 - 06:55:11 to 15:58:05	Passes 205 to 212 are completely missing. Passes 204 and 213 are partly missing with respectively 100% and 96% of missing measurements over ocean. This is due to software upload to Poseidon-3.
034/232	13/06/2009 - 07:07:03 to 07:40:23	Due to long calibration, pass 232 is partly missing with 65% of missing measurements over ocean.
034/235	13/06/2009 - 10:11:41 to 10:37:50	Due to calibration CNG step, pass 235 is partly missing with 8% of missing measurements over ocean.
037/54	06/07/2009 - 02:33:12 to 02:34:33	pass 054 has a small data gap due to missing PLTM
053/57	11/12/2009 - 20:38:19 to 21:29:43	passes 57 and 58 have a data gap due to Gyro calibration
053/232	18/12/2009 - 16:39 to 17:12	pass 232 has a data gap due to CAL2 calibration
053/235	18/12/2009 - 19:43	pass 235 has a 26 minutes data gap due to CNG calibration (mostly over land)
.../...		

Jason-2 Cycles/Pass	Dates	Events
072/199	23/06/2010 - 19:15:37 to 19:16:59	pass 199 has small data gap due to missing telemetry
073/232	05/07/2010 - 00:09:33 to 00:42:54	pass 232 has a data gap due to CAL2 calibration
073/235	05/07/2010 - 03:14:11 to 03:40:20	pass 235 has a data gap due to CNG calibration (mostly over land)
081/087	16/09/2010 - 16:40:22 to 16:52:48	pass 087 has a data gap due to upload of DEM update (for GAVDOS transponder calibration)
081/237	22/09/2010 - 13:07:27 to 13:18:12	pass 237 has a data gap due to upload of DEM update (for GAVDOS transponder calibration)
084/031	14/10/2010 - 06:02 to 06:11:15	Calibration (I2 and Q2)
084/031-032	14/10/2010 - 06:12 to 06:21:15	Calibration (I and Q)
084/043	14/10/2010 - 17:00:57 to 17:02:39	pass 043 has a small data gap due to missing PLTM
094/231	29/01/2011 - 04:50 to 04:55	Calibration CAL1 (14% of missing ocean data)
094/232	29/01/2011 - 05:38 to 06:11	Calibration CAL2 (65% of missing ocean data)
094/235	29/01/2011 - 08:37 to 09:03	Calibration CNG (mostly over land, 9% of missing ocean data)
101/133-135	04/04/2011 - 18:49:08 to 21:03:48	Telemetry outage at Usingen, passes 133 to 135 have respectively 23%, 100%, and 91% of missing ocean data
110/158-159	04/07/2011 - 00:27:29 to 01:27:29	Gyro calibration. Passes 158 and 159 have respectively 18% and 88% of missing ocean data
115/232	25/08/2011 - 11:07:35 to 11:40:56	Calibration CAL2: 65% of missing ocean data
115/235	25/08/2011 - 14:12 to 14:38	Calibration CNG: mostly over land, 8% of missing ocean data
132/232	10/02/2012 - 00:42:26 to 01:14:03	Calibration CAL2: 65% of missing ocean data
132/235	10/02/2012 - 03:47:11 to 04:13:20	Calibration CNG: mostly over land, 8% of missing ocean data
.../...		

Jason-2 Cycles/Pass	Dates	Events
135/105	05/03/2012 - 19:54:49 to 20:26:14	technical problem and operator error: 25% of missing ocean data
136/191	19/03/2012 - 02:15:18 to 02:50:11	problem of ACK: 56% of missing ocean data
145/143	14/06/2012 - 11:41:15 to 11:42:58	pass 143 has a small data gap due to missing telemetry
145/248	18/06/2012 - 13:20:10 to 13:21:29	pass 248 has a small data gap
147/022	29/06/2012 - 13:45:30 to 13:49:46	pass 022 has a small data gap due to missing telemetry (8% of missing ocean data)
147/134	03/07/2012 - 22:41:25 to 22:43:58	pass 134 has a small data gap due to operator error (5% of missing ocean data)
154/210	14/09/2012 - 07:45:08 to 07:46:07	pass 210 has a small portion of missing data in central Pacific
156/232	05/10/2012 - 00:07:08 to 00:40:30	Calibration CAL2: 66% of missing ocean data
156/235	05/10/2012 - 03:11:47 to 03:37:57	Calibration CNG: mostly over land, 9% of missing ocean data
168/158-159	29/01/2013 - 03:08:20 to 04:02:37	Gyro calibration. Passes 158 and 159 have respectively 14% and 100% of missing ocean data
172/96-97	07/03/2013 - 08:18:37 to 09:30:49	Operator error. Passes 96 and 97 have respectively 72% and 52% of missing ocean data
174/43-161	25/03/2013 - 02:42 to 29/03/2013 17:53	First Safe Hold Mode. Pass 43 has 63% of missing ocean data and passes 44 to 161 are entirely missing
174-191/175-83	30/03/2013 - 21:57 to 05/04/2013 14:49	Second Safe Hold Mode. About cycle 174, pass 191 has 9% of missing ocean data and passes 192 to 254 are entirely missing. About cycle 175, passes 1 to 82 are entirely missing and pass 83 has 90% of missing measurements over ocean.
178/234		Due to a problem with TM receiver, pass 234 is partly missing (north of pacific) and has 10% of missing measurements over ocean
179/ 38		Due to a problem with TM receiver, pass 38 has 6.8% of missing measurements over ocean
.../...		

Jason-2 Cycles/Pass	Dates	Events
182/235	19/06/2013 from 22 :33 :29 to 22 :59 :37	pass 235 has a data gap due to CNG calibration (mostly over land)
190/185 - 191/116	05/09/2013 at 07 :44 :17 to 12/09/2013 at 12 :25 :52	Third Safe Hold Mode. Concerning cycle 190, pass 185 has 10.2% of missing measurements over sea and passes 186 to 254 are entirely missing. Concerning cycle 191, passes 1 to 115 are missing.
197/035	07/11/2013 - 20:45	Pass 35 has a small data gap.
198/235	25/11/2013 - 14:04:02 to 14:37:35	Calibration (I and Q) with 8% of missing ocean data
207/178	20/02/2014 - 14:30:33 to 14:43:50	24.6% of global missing data and 11.8% missing data over ocean due to DEM upload
208/027	24/02/2014 - 14:38:26 to 14:52:07	40.7% missing data over ocean due to recurring network problems between Fairbanks and SOCC
218/235	11/06/2014 - 21:34:36 to 22:13:13	Poseidon3/Jason2 special calibration. 9% missing data over ocean
222/114	16/07/2014 - between 20:05:19 and 20:10:34 and between 20:23:21 and 20:34:51	Gyro calibration. Pass 114 has 73% of missing ocean data
226/235	07/12/2014 - 09:13:54 TU (26 minutes and 10 seconds)	Poseidon3/Jason2 special calibration. Only 8.3% of missing measurements over ocean (most of the missing measurements are over land.)
247/227-228		Passes 227 and 228 are partly missing due to telemetry dropouts during pass and ack sent by mistake at ground station. 13.91% of pass 228 is missing (over land only). 80.37% of pass 227 is missing (76.69% over sea).
256/235	23/06/2015 16:44:28 TU (26 minutes and 10 seconds)	Poseidon3/Jason2 special calibration. Only 8.3% of missing measurements over ocean (most of the missing measurements are over land.)
275/235	29/12/2015 02:16:30 TU (26 minutes and 10 seconds)	Poseidon3/Jason2 special calibration. Only 8.3% of missing measurements over ocean (most of the missing measurements are over land.)
285/217-241	05/04/2016 13:35:10 to 06/04/2016 12:02:40	Upload of new GPS On Board software.
287/024	17/04/2016 20:15:50 to 20:39:41	Data dropout at Fairbanks (pass 024 is partly missing)
.../...		

Jason-2 Cycles/Pass	Dates	Events
294/211	03/07/2016 13:26:00 TU (26 minutes and 10 seconds)	Poseidon3/Jason2 special calibration.
295	12/07/2016	AMR cold sky calibration
297/123	29/07/2016	cycle 297 pass 123 has dotted line of missing measurements : 66 points over ocean
301	05/09/2016	AMR cold sky calibration
304/001-305/164	02/10/2016 11:53:32 to 13/10/2016 20:00:00	move to interleaved ground track. Data gap: Poseidon-3 altimeter is put in WAIT mode.
305/164 to 307/094	13/10/2016 to 30/10/2016	missing parts of passes due to calibrations badly located over ocean
307	07/11/2016	AMR cold sky calibration
308/071	08/11/2016 from 23:11:19 to 23:13:48	pass 071 has 5.09% of missing measurements over sea due to telemetry loss
310		there are some non continuous missing points on pass 146 (2.4% over ocean) on 01-12-2016 around 17:32 to 17:35.
312	CAL CNG on 2016-12-25 00:26:00 (26 minutes and 10 seconds)	part of pass 235 is missing due to Poseidon3/Jason2 special calibration. Only 5.0% of missing measurements over ocean (most of the missing measurements are over land.)
314	10/01/2017	AMR cold sky calibration
317		Pass 70 has 3.2% of ocean data missing due to missing TM. There are several discontinuous gaps on a section of the track
318	26/02/2017	AMR cold sky calibration
321/18 + 19 to 254 322/001 to 136 + 137		Abnormal gyros status triggered a SAFE HOLD MODE starting at 2017-03-15 19:19:58 (on cycle 321) and ending on cycle 322 at 2017-03-30 08:47:30.
322/170 + 171	Gyrometers calibration on 31/03/2017 from 15:29:59 UTC to 16:10:27 UTC	Due to gyro calibration, passes 170 and 171 are partially missing with respectvely 54.83% and 35.45% of missing data (70.86% and 41.20% over sea).
.../...		

Jason-2 Cycles/Pass	Dates	Events
323	CNG Calibration on 13/04/2017 from 02:10:00 to 02:36:10 mainly on land	due to the CNG calibration, 5% of missing data on ocean on pass 235 (north of the Red Sea).
324		10 consecutive points are missing on track 97.
324	26/04/2017	AMR cold sky calibration
327/111 + 112 to 254		Abnormal gyros status triggered a SAFE HOLD MODE starting at 2017-05-17 at 22:26:57. Passes 112 to 254 are missing, and pass 111 has 31.49% of missing data (7.74% over ocean).
500		New numbering after move to LRO. 222 passes only in that cycle: passes 1 to 32 are missing (restart after SHM and move of orbit).
500/038	11/07/2017 from 15:40:41 to 15:47:02	part of pass 038 is missing in Indian Ocean(related to slew before AMR Calibration)
500	CNG Calibration on 11/07/2017 at 13:17:00	(26mn 10s mostly over land)
500	11/07/2017	AMR cold sky calibration
503	13/08/2017	AMR cold sky calibration
506 (part of 178 + 179 to 254), + 507, +508, 509 (1 to 161 + part of 162)	from 14/09/2017 06:12:04 to 13/10/2017 05:59:12	SAFE HOLD MODE
511	01/11/2017	AMR cold sky calibration

Table 3 – Missing pass status

### 3.1.2. Over land and ocean

Determination of missing measurements relative to the theoretically expected orbit ground pattern is an essential tool to detect missing telemetry or satellite events for instance. Applying the same procedure for Jason-1 and Jason-2, the comparison of the percentage of missing measurements has been performed. Jason-2 can use several onboard tracking modes: Split Gate Tracker (ie the Jason-1 tracking mode, used for cycle 0 and half of cycle 1), Diode/DEM (used for cycles 3, 5, 7,

34, 209, 220 and 311) and median tracker (used for the other cycles). These different tracking modes are described by [45]. Thanks to the new modes of onboard tracking (median tracker and Diode/DEM), the data coverage over land surface was dramatically increased in comparison with Jason-1 depending on the tracker mode and the period. Top of figure 1 shows the percentage of missing measurements for Jason-2 and Jason-1 (all surfaces) computed with respect to a theoretical possible number of measurements. Due to differences between altimeter tracking algorithms, the number of available data is greater for Jason-2 than for Jason-1. Differences appear on land surfaces as shown in bottom of figure 1. The missing data are highly correlated with the mountains location. The monitoring shows a slight annual signal. During 2013, Jason-2 entered in safe hold mode twice in March (from 25/03/2013 to 29/03/2013 and from 30/03/2013 until 05/04/2013, during cycles 174 and 175) and a third time in September (from 05/09/2013 to 12/09/2013, during cycles 190-191). During 2016, data are missing between April, 5 at 13:35:10 and April, 6 at 12:02:40 as no altimeter measurements have been performed (altimeter in wait mode) during this period to allow the upload of new GPS onboard software. Jason-2 was moved from its original groundtrack to its new interleaved groundtrack on October 2016: October 2nd at 11 :53 UTC (end of cycle 303) the Poseidon-3 altimeter is put in WAIT mode and there is no more measurement until the end of the move to interleaved ground track (13-10-2016 at 20:00:00 (cycle 305, pass 164)). After several Safe Hold Modes in March and May 2017, Jason-2 was moved to a Long Repeat Orbit (LRO) at the beginning of July 2017.

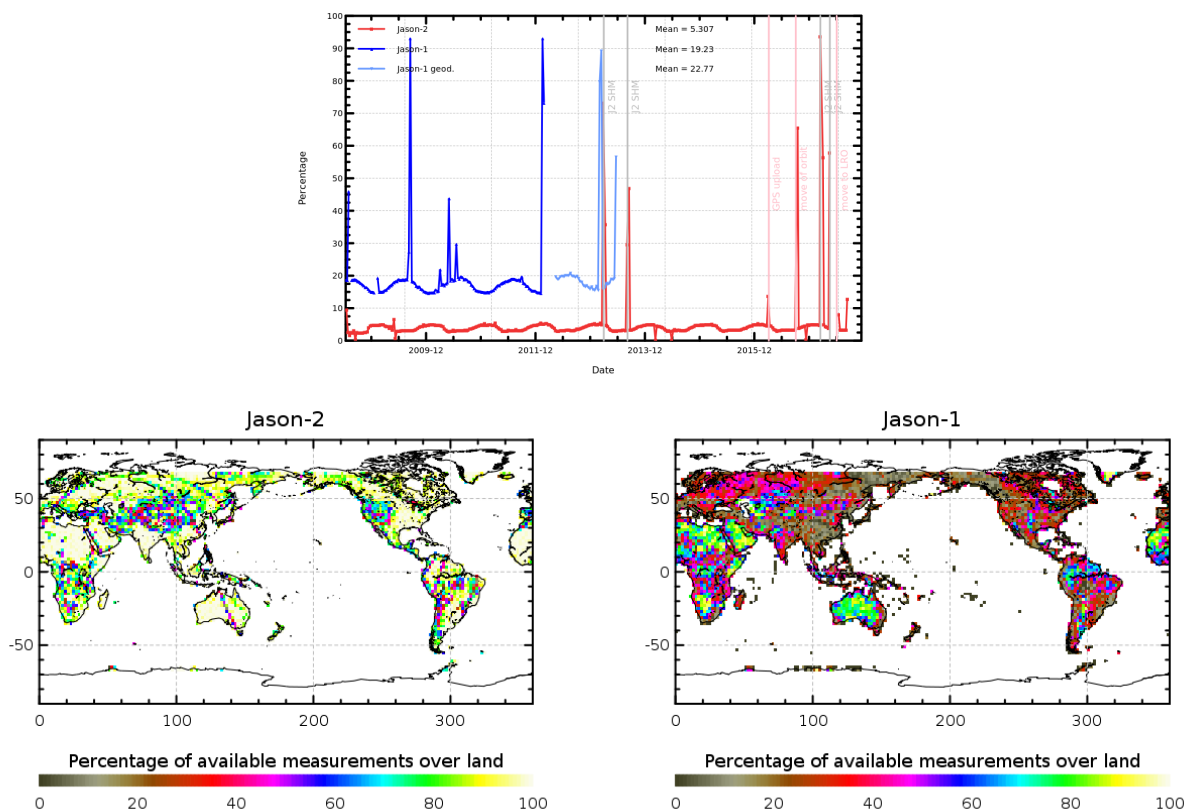


Figure 1 – **Top:** Percentage of missing measurements over ocean and land for Jason-2 and Jason-1. **Bottom:** Map of percentage of available measurements over land for Jason-2 on cycle 154 (left) and for Jason-1 on cycle 511 (right)

### 3.1.3. Over ocean

When considering ocean surface, the same analysis method leads also to an improvement of Jason-2 data coverage compared to Jason-1, as plotted on the top left figure 2. It represents the percentage of missing measurements relative to the full coverage, when limited to ocean surfaces. Note that when Jason-1 was on a geodetic ground-track, it was roughly once per month during about 2 h in INIT mode (no science data), due to Jason-2 overflight. The mean value is about 1.5% for Jason-2, 5.3% for Jason-1. Even if already very low, this figure of missing measurements is not significant due to events on the payload during which the measurements are missing. All these events are described on table 3.

On figure 2 on the top right, the percentage of missing measurements is plotted without taking into account the cycles where instrumental events or other big anomalies occurred. The mean value of missing measurements lowers down to 0.03% for Jason-2 and 2.0% for Jason-1.

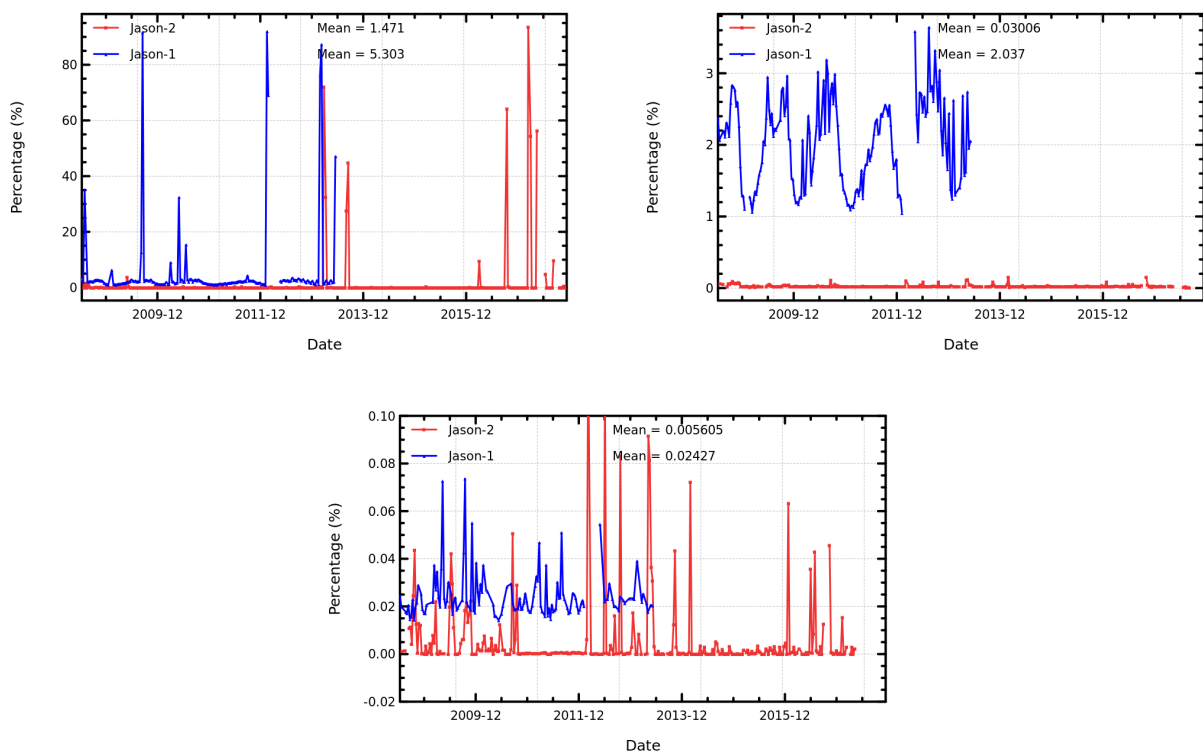


Figure 2 – Cycle per cycle percentage of missing measurements over ocean (top left), without anomalies (top right), without anomalies and selecting latitudes lower than  $50^\circ$  and bathymetry area lower than  $-1000\text{m}$  (bottom).

Indeed, selecting latitudes lower than  $50^\circ$  and bathymetry area lower than  $-1000\text{m}$  (see bottom of figure 2), the Jason-1 percentage becomes very weak (close to 0.02%) which represents less than 100 missing measurements per cycle over open ocean. For Jason-2, the same statistic is smaller with around 0.006% of missing measurements over open ocean. This weak percentage of missing measurements is mainly explained by the rain cells and sigma0 blooms, as these sea states can disturb significantly the Ku band waveform shape leading to an altimeter lost of tracking.

## 3.2. Edited measurements

---

### 3.2.1. Editing criteria definition

Editing criteria are used to select valid measurements over ocean. The editing process is divided into 4 parts.

- First, only measurements over ocean and lakes are kept (see section 3.2.3.) as the editing performed here are dedicated to ocean applications.
- Second, some flags are used as described in section 3.2.4.. Note that though the altimeter rain flag is now available in the current release of GDR (D), it is not used hereafter in the editing procedure. But measurements corrupted by rain are well detected by other altimeter parameter criteria.
- Then, threshold criteria are applied on altimeter, radiometer and geophysical parameters and are described in the table 5. Except for the dual frequency ionosphere correction, only Ku-band measurements are used in this editing procedure, as they mainly represent the end user dataset.
- Moreover, a spline criterion is applied to remove the remaining spurious data.
- For each criterion, the cycle per cycle percentage of edited measurements has been monitored. This allows detection of anomalies in the number of removed data, which could come from instrumental, geophysical or algorithmic changes.

### 3.2.2. Edited measurements

Table 4 indicates particular high editing periods (see section 3.2.1.). Most of the occurrences correspond to radiometer wet troposphere correction at default value (due to AMR unavailability) or altimeter low signal tracking anomaly (AGC anomaly), though the latter concerns only few measurements and was corrected during cycle 16.

Jason-2 Cycles/Passes	Date	Comments
000/89	05/07/08 - 14:22:07 to 14:23:38	Partly edited by several parameters out of threshold (AGC anomaly)
000/134	07/07/08 - 08:06:37 to 08:28:57	Partly edited by several parameters out of threshold (AGC anomaly)
000/156	08/07/08 - 04:35:12 to 05:31:01	rain flag is set (dotted), probably related to start/stop sequence (from 04:45 to 05:24)
.../...		

Jason-2 Cycles/Passes	Date	Comments
000/234	11/07/08 - 05:45:12 to 05:49:03	Partly edited by several parameters out of threshold (AGC anomaly)
000/241	11/07/08 - 13:04:27 to 13:09:11	Partly edited by ice flag (number of elementary Ku-band measurements at 0, AGC=16.88) due to test of altimeter DEM mode
001/		several passes partly edited by several parameters out of threshold (AGC anomaly)
002/		several passes partly edited by several parameters out of threshold (AGC anomaly)
004/		several passes partly edited by several parameters out of threshold (AGC anomaly)
006/		several passes partly edited by several parameters out of threshold (AGC anomaly)
008/		several passes partly edited by several parameters out of threshold (AGC anomaly)
009/		several passes partly edited by several parameters out of threshold (AGC anomaly)
010/		several passes partly edited by several parameters out of threshold (AGC anomaly)
011/		several passes partly edited by several parameters out of threshold (AGC anomaly)
012/		several passes partly edited by several parameters out of threshold (AGC anomaly)
013/		several passes partly edited by several parameters out of threshold (AGC anomaly)
014/		several passes partly edited by several parameters out of threshold (AGC anomaly)
015/		several passes partly edited by several parameters out of threshold (AGC anomaly)
019/024-042	07/01/ 11:00:35 to 08/01/2009 03:23:34	radiometer wet troposphere correction at default value due to AMR unavailability
019/119-161	11/01/ 03:56:38 to 12/01/2009 19:26:14	radiometer wet troposphere correction at default value due to AMR unavailability
.../...		

Jason-2 Cycles/Passes	Date	Comments
110/047	29/09/2011 16:14 to 16:20	a portion of pass 47 is edited by radiometer wet troposphere correction out of threshold or at default values (radio-frequency interference from a ground based source)
168/141-144	28/01/2013 10:50 to 13:22	radiometer wet troposphere correction at default value due to AMR unavailability
169/176-181	08/02/2013 17:37 to 22:44	radiometer wet troposphere correction at default value due to AMR unavailability
174/162-163	29/03/2013 17:53 to 29/03/2013 19:36	radiometer wet troposphere correction at default value after first Safe Hold Mode
175/83-85	05/04/2013 14:18 to 16:27	radiometer wet troposphere correction at default value after second Safe Hold Mode
191/116-125	12/09/2013 12:25:52 to 21:56:39	radiometer wet troposphere correction at default value after third Safe Hold Mode
194/227	16/10/2013 15:02:08 to 15:04:17	a part of pass 227 is rejected near Kamchatka Peninsula because of ice flag (linked to high radiometer minus model wet troposphere difference, and probably related to typhoon WIPHA that happened in the region between the 15th and 17th October 2013)
238/020-043	18/12/2014 19:18:48 to 19/12/2014 17:47:57	AMR unavailability: No AMR data. Passes 21 to 42 are completely edited. Passes 20 and 43 are partly edited with respectively 33.73%, and 20.28% of edited measurements.
269/111-115	25/10/2015 from 18:18 to 22:25	Anomaly on AMR-H leading to radiometer unavailability: Passes 112,113,114 are fully edited; Passes 111 and 115 are partially edited with respectively 15% and 93% of ocean data due to radiometer wet tropospheric correction at default values.
277/35-37	10/01/2016 02:45:05 to 05:03:03	Anomaly on AMR: passes 35, 36 and 37 have respectively 44%, 100% and 81% of rejected measurements
279/17-20	19/01/2016 05:58:31 to 08:21	Due to AMR reset, missing radiometer data for part of passes 17 and 20 and whole passes 18 and 19
285/85-87	31/03/2016 09:30:52 to 11:39:11	Due to AMR anomaly, missing radiometer data for part of passes 85 and 87 and whole pass 86
308/249	15/11/2016 from 21:57:59 to 21:58:25	radiometer parameters have 26 measurements set to default value
.../...		

Jason-2 Cycles/Passes	Date	Comments
313	31/12/2017 23:59:59	Leap second: discontinuities are visible on datation, orbit and range at 23:59:43 and 23:59:59 on 31-12-2017  a jump of about 3.3m on Orbit minus range is visible (2 points) on 2016-12-31 at 23:59:43 due to leap second management on GPS and Doris. These points are rejected thanks to editing procedure.
325		Non continuous points have radiometer parameters set to default values on passes 126 and 217 to 230 due to AMR anomaly.
326/11-15	04/05/2017 from 02:34:19 to 06:31:45	Due to radiometer parameters set to default value, part of pass 11 and whole passes 12, 13, 14, 15 are rejected on wet tropospheric correction thresholds
326	10/05/2017	pass 173 has 62 measurements with radiometer parameters set to default value
325 - 326	from 2017/05/03 02:18:55 to 2017/05/04 02:35:47	The 02/05/2017 AMR reset (at 17:14:48 UTC) did not clear the AMR error : AMR data still degraded from 2017/05/03 02:18:55 UTC (Cycle325) to 2017/05/04 02:35:47 UTC (Cycle326) : POWER CYCLE and AMR-H unit reset were performed on 2017/05/04 from 06:29:57 UTC to 06:30:03 UTC
500		pass 033 (first pass) rejected due to radiometer data set to default values (just after TM restart)

Table 4 – Edited measurement status

### 3.2.3. Selection of measurements over ocean and lakes

In order to remove data over land, a land-water mask is used. Only measurements over ocean or lakes are kept. This allows to keep data near the coasts and so to detect potential anomalies in these areas. Figure 3 shows the cycle per cycle percentage of measurements eliminated by this selection. The signal shows mainly a seasonal cycle, due to changing properties of land reflection. But it also reveals the impact of the different altimeter tracking modes: SGT (split gate tracking), Median and DIODE/DEM (digital elevation model).

- SGT mode, the nominal mode for Jason-1, was used for Jason-2 during cycle 0 and half of cycle 1. This mode does not perform very well over land (as also depicted on right side of figure 1), therefore a comparable small percentage of measurements are edited over land for cycle 1 (approximately 24%).
- Most of Jason-2 cycles (cycles 2, 4, 6, 8 to 33, 35 to 208, 210 to 219, 221 to 310 and from cycle 312 onwards) were operated in Median mode (also used by Envisat). This mode is more adapted for tracking over land than SGT and provides therefore more measurements over land (as also seen on left side of figure 1) and so more measurements are edited (between 25.5% and 27% depending on season) due to the ocean/land criteria.
- A new tracking mode, DEM, was used during cycles 3, 5, 7, 34, 209, 220 and 311. It has been designed to provide more data over inland water surfaces and coastal areas. Therefore during these cycles, almost 29% of measurements are removed by the selection.

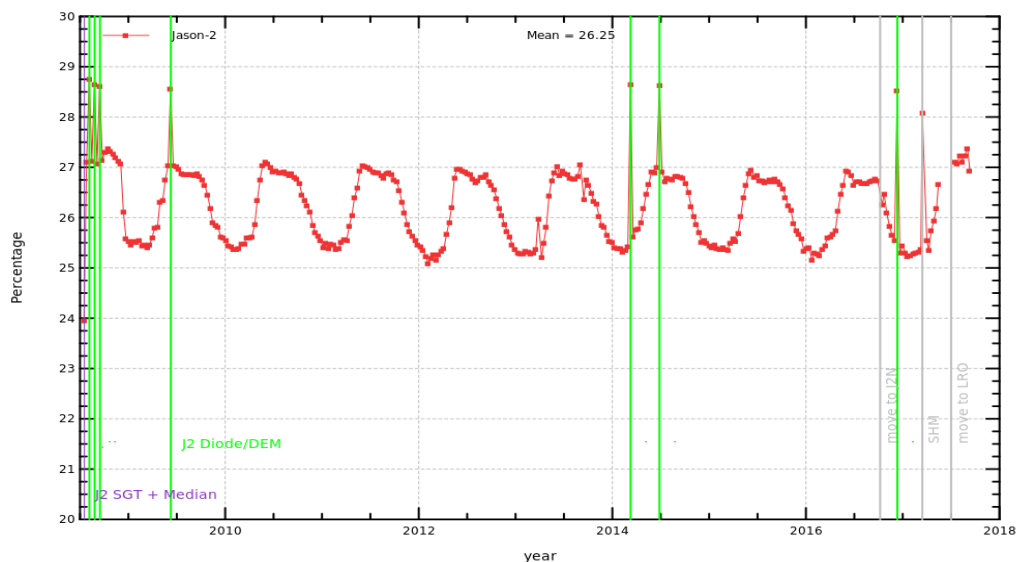


Figure 3 – Cycle per cycle percentage of discarded measurements during selection of ocean/lake measurements.

### 3.2.4. Flagging quality criteria: Ice flag

The ice flag (from GDR product ice\_flag) is used to remove the sea ice data. Figure 4 shows the cycle per cycle percentage of measurements edited by this criterion. Over the shown period, no anomalous trend is detected (figure 4 left) but the nominal annual cycle is visible. Indeed, the maximum number of points over ice is reached during the southern winter (i.e. July - September). As Jason-2 acquires measurements between 66° north and south, it does not detect thawing of sea ice (due to global warming), which takes place especially in northern hemisphere over 66°N. A slight decrease is visible over the last two years: it is also visible with SARAL/AltiKa data [13]. The percentage of measurements edited by ice flag is plotted in the right of figure 4 for a period of 1 year (the last year on initial ground track), and over interleaved with Jason-3 phase (13/10/2016 to 17/05/2017) and LRO phase (11/07 to 14/09/2017) at bottom side of figure 4. On bottom right, summer in northern hemisphere, figure shows no ice at high latitude.

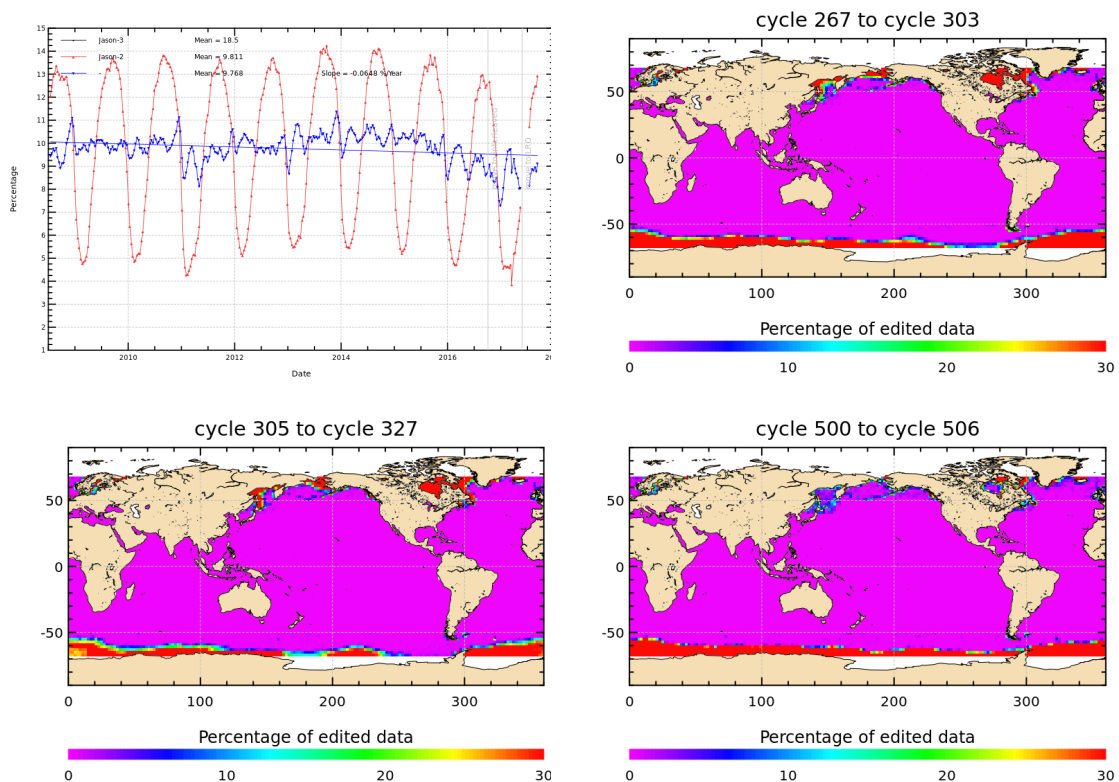


Figure 4 – Percentage of edited measurements by ice flag criterion. Left: Cycle per cycle monitoring. The blue curve shows the trend of edited measurements after adjusting for annual and semi-annual signals. Right: Map over a one year period (cycles 267 to 303 from 2015-10-01 to 2016-10-02). Bottom: Map over interleaved ground-track period from 2016-10-13 to 2017-05-17 (left) and map over LRO period (right), cycles 500 (2017-07-11) to 506 (2017-09-14)

### 3.2.5. Flagging quality criteria: Rain flag

Though the altimeter rain flag is now present in GDR-D release, it is not used hereafter during the editing procedure. The percentage of measurements where rain flag is set to 1 is plotted in figure 5 over cycles 267 to 303 (covering 12 months). It shows that measurements are especially edited near coasts, but also in the equatorial zone and open ocean. The altimeter rain flag would lead to edit 6.8% to 6.9% of additional measurements (for location see right part of figure 5).

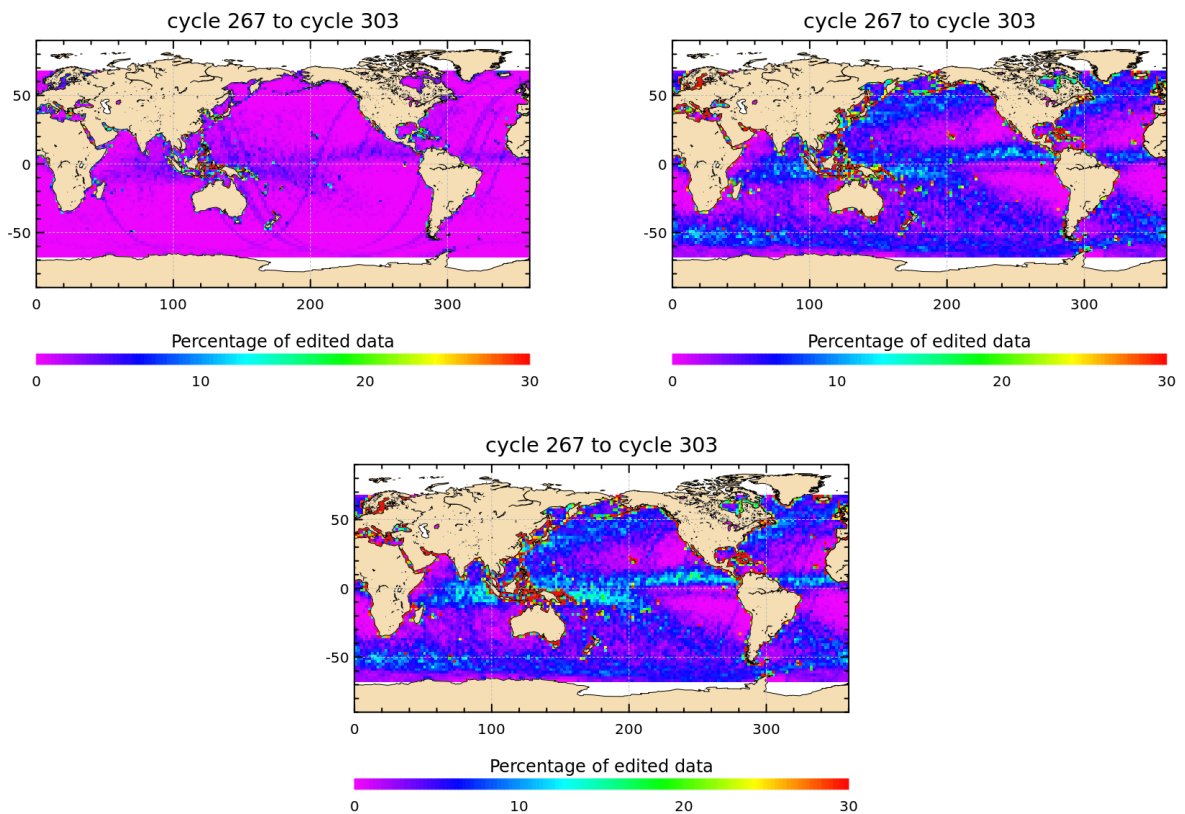


Figure 5 – Percentage of edited measurements by altimeter rain flag criterion (all figures computed after iced flagged points remove ). Map over a one year period (cycles 267 to 303). Left: rejected measurements (following method described hereafter ) where rain flag is also activated . Right: valid measurements (following method described hereafter ) where rain flag is activated. Bottom: All points where rain flag is activated.

### 3.2.6. Threshold criteria: Global

Instrumental parameters have also been analyzed from comparison with thresholds, after having selected only ocean/lakes measurements and applied flagging quality criteria (ice flag). Therefore measurements appear not as edited by thresholds, when they were already edited by land or sea ice flag. Thresholds used are summarized in table 5, along with the average percentage of edited data for each parameter. Note that one measurement can be edited by several different thresholds, so the sum of individual criterion percentages does not equal the all thresholds combined percentage.

Parameter	Min thresholds	Max thresholds	mean edited
Sea surface height	-130 m	100 m	0.77%
Sea level anomaly	-10 m	10.0 m	1.04%
Number measurements of range	10	<i>Not applicable</i>	1.04%
Standard deviation of range	0	0.2 m	1.40%
Squared off-nadir angle	-0.2 deg <sup>2</sup>	0.64 deg <sup>2</sup>	0.58%
Dry troposphere correction	-2.5 m	-1.9 m	0.00%
Inverted barometer correction	-2.0 m	2.0 m	0.00%
AMR wet troposphere correction	-0.5m	-0.001 m	0.23%
Ionosphere correction	-0.4 m	0.04 m	1.18%
Significant wave height	0.0 m	11.0 m	0.65%
Sea State Bias	-0.5 m	0.0 m	0.62%
Number measurements of Ku-band Sigma0	10	<i>Not applicable</i>	1.03%
Standard deviation of Ku-band Sigma0	0	1.0 dB	1.94%
Ku-band Sigma0 <sup>1</sup>	7.0 dB	30.0 dB	0.60%
Ocean tide	-5.0 m	5.0 m	0.01%
Equilibrium tide	-0.5 m	0.5 m	0.00%
Earth tide	-1.0 m	1.0 m	0.00%
Pole tide	-15.0 m	15.0 m	0.00%
Altimeter wind speed	0 m.s <sup>-1</sup>	30.0 m.s <sup>-1</sup>	1.02%
All together	-	-	3.27%

Table 5 – Editing criteria. Percentage of rejected measurements on each criterion over the whole mission

.....

Note that no measurement is edited by the following corrections:

- dry troposphere correction,
  - inverted barometer correction (including DAC),
  - equilibrium tide,
  - earth tide,
  - pole tide.
- Indeed these parameters are only checked in order to detect data at default values, which might happen during a processing anomaly.

The percentage of edited measurements using all criteria is monitored on a cycle per cycle basis (figure 6). The mean percentage of edited measurements is about 3.3%. A small annual cycle is visible (related to 20 Hz standard deviation for range 3.2.8. and backscatter coefficient 3.2.11.). The high percentage of edited measurements of cycles 019, 168, 169, 238, 269 and 326 are explained by an AMR anomaly, which resulted in defaulted radiometer values during several passes. Concerning cycles 174 and 191, it is explained by the time lag between the altimeter restart and the radiometer restart after safe hold modes.

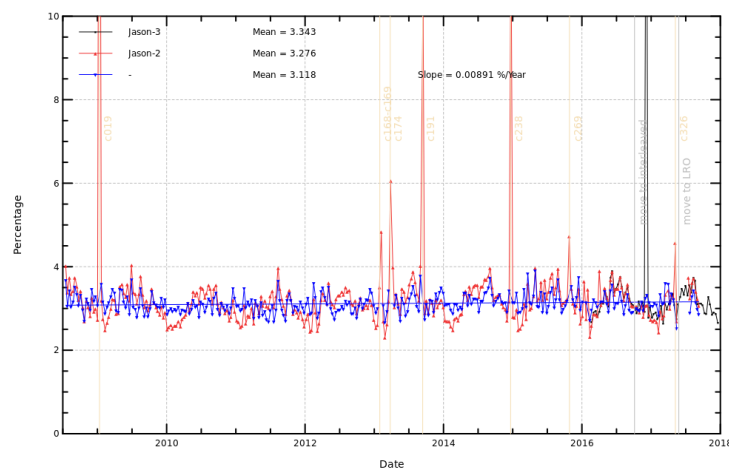


Figure 6 – Cycle per cycle percentage of edited measurements by threshold criteria. The blue curve shows the trend of edited measurements after adjusting for annual and semi-annual signals.

<sup>1</sup>The thresholds used for the Ku-band Sigma0 are the same than for Jason-1 and T/P, but the same sigma0 bias as between Jason-1 and T/P (about 2.4 dB) is applied.

**3.2.7. Threshold criteria: 20-Hz measurements number**

The percentage of edited measurements because of a too low number of 20-Hz measurements is represented on left side of figure 7. No trend neither any anomaly has been detected. The map of measurements edited by 20-Hz measurements number criterion is plotted on right side of figure 7 and shows correlation with heavy rain and wet areas (in general regions with disturbed sea state). Indeed waveforms are distorted by rain cells, which makes them often meaningless for SSH calculation. As a consequence, edited measurements due to several altimetric criteria are often correlated with wet areas.

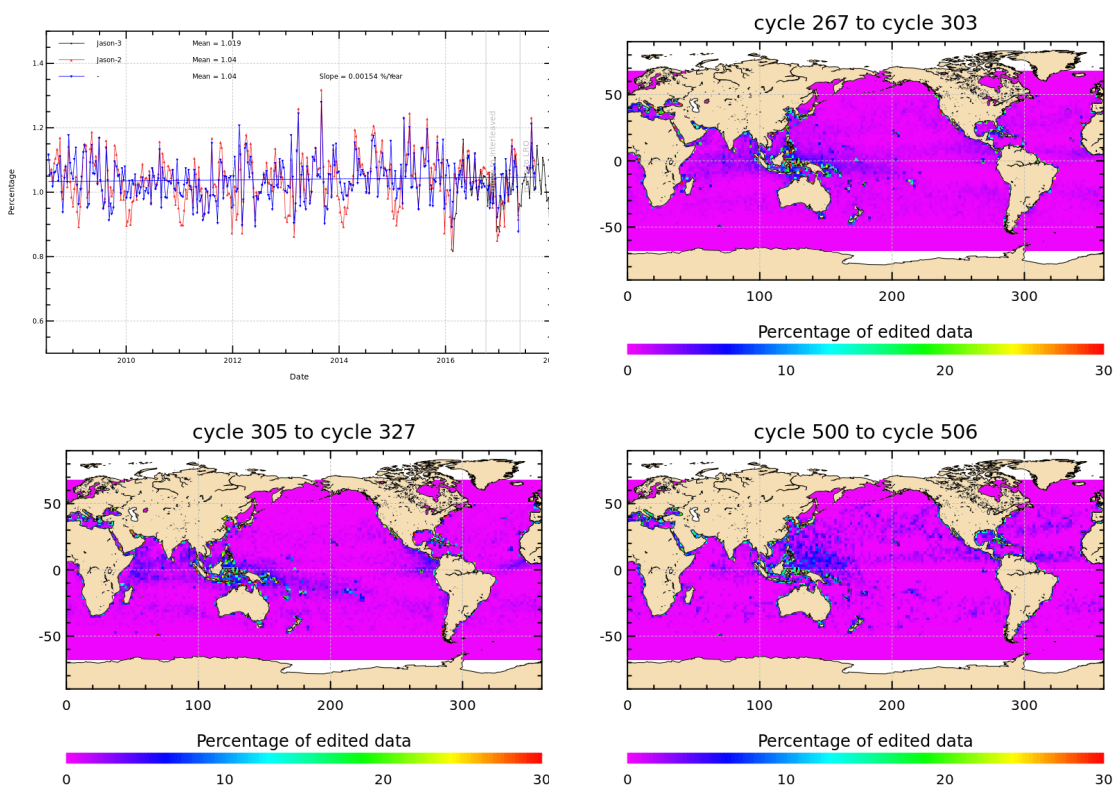


Figure 7 – Percentage of edited measurements by 20-Hz measurements number criterion. Left: Cycle per cycle monitoring. The blue curve shows the trend of edited measurements after adjusting for annual and semi-annual signals. Right: Map over a one year period (cycles 267 to 303). Bottom: Map over interleaved with Jason-2 period from 2016-10-13 to 2017-05-17 (left) and map over cycles 500 (2017-07-11) to 506(right)

### 3.2.8. Threshold criteria: 20-Hz measurements standard deviation

The percentage of edited measurements due to 20-Hz measurements standard deviation criterion is shown in figure 8 (left). This criterion reveals points whose quality can be degraded due to bloom or rain cells). During cycle 1, slightly more measurements are edited by 20-Hz measurements standard deviation criterion than during other cycles. This is likely due to low signal tracking anomaly which impacted especially this cycle. The right side of figure 8 shows a map of measurements edited by the 20-Hz measurements standard deviation criterion. As in section 3.2.7., edited measurements are correlated with wet areas, but also in regions where ice flag probably missed detection of sea ice (near Antarctic). This also very likely explains the annual signal in left side of the figure.

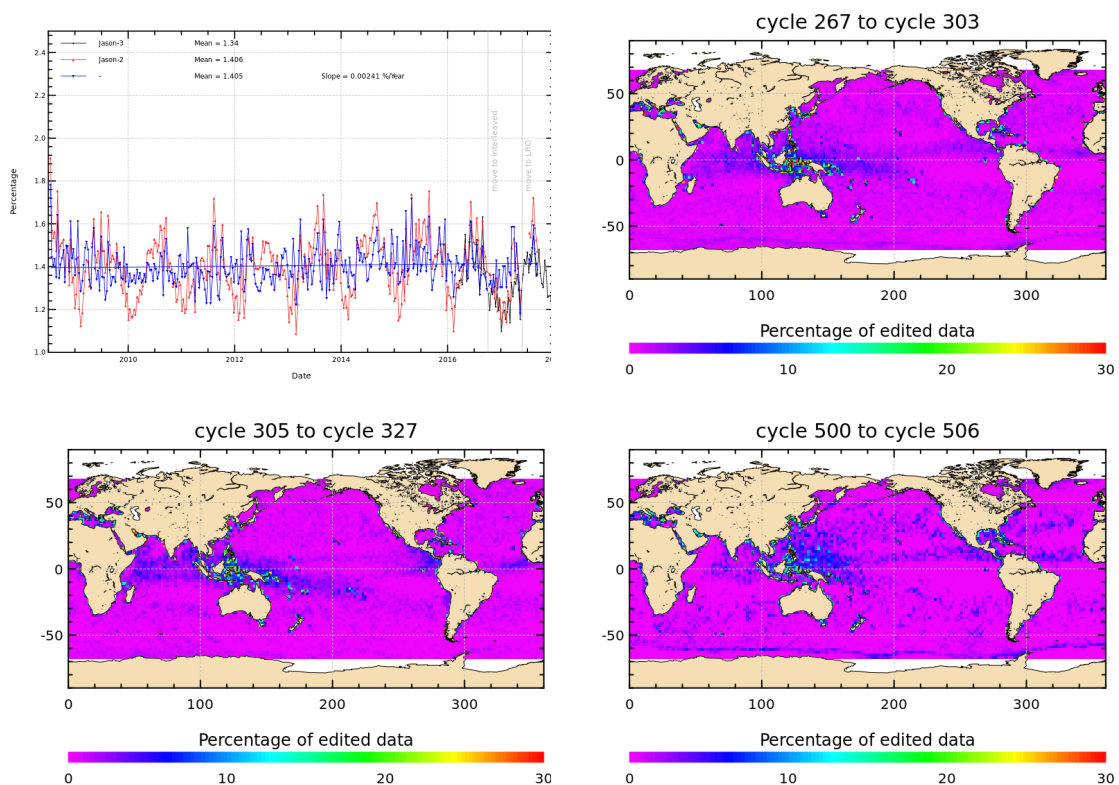


Figure 8 – Percentage of edited measurements by 20-Hz measurements standard deviation criterion. Left: Cycle per cycle monitoring. The blue curve shows the trend of edited measurements after adjusting for annual and semi-annual signals. Right: Map over a one year period (cycles 267 to 303). Bottom: Map over interleaved with Jason-2 period from 2016-10-13 to 2017-05-17 (left) and map over cycles 500 (2017-07-11) to 506(right)

### 3.2.9. Threshold criteria: Significant wave height

The percentage of edited measurements due to significant wave height criterion is represented in figure 9. It is about 0.65%. In the beginning of the mission, the curve of measurements edited by SWH threshold criterion is quite irregular, as low signal tracking anomalies occurred during SGT and Median tracking modes, whereas there are no low signal tracking anomalies during DEM tracking modes (cycles 3, 5, and 7). Indeed during periods of low signal tracking anomaly, parameters like significant wave height, backscatter coefficient and squared off-nadir angle from waveforms are out of thresholds and therefore edited. Figure 9 (right part) shows that measurements edited by SWH criterion are especially found near coasts in the equatorial regions and in the Mediterranean Sea.

It seems there are few more data rejected on this criterion since Long Repeat Orbit (under investigation).

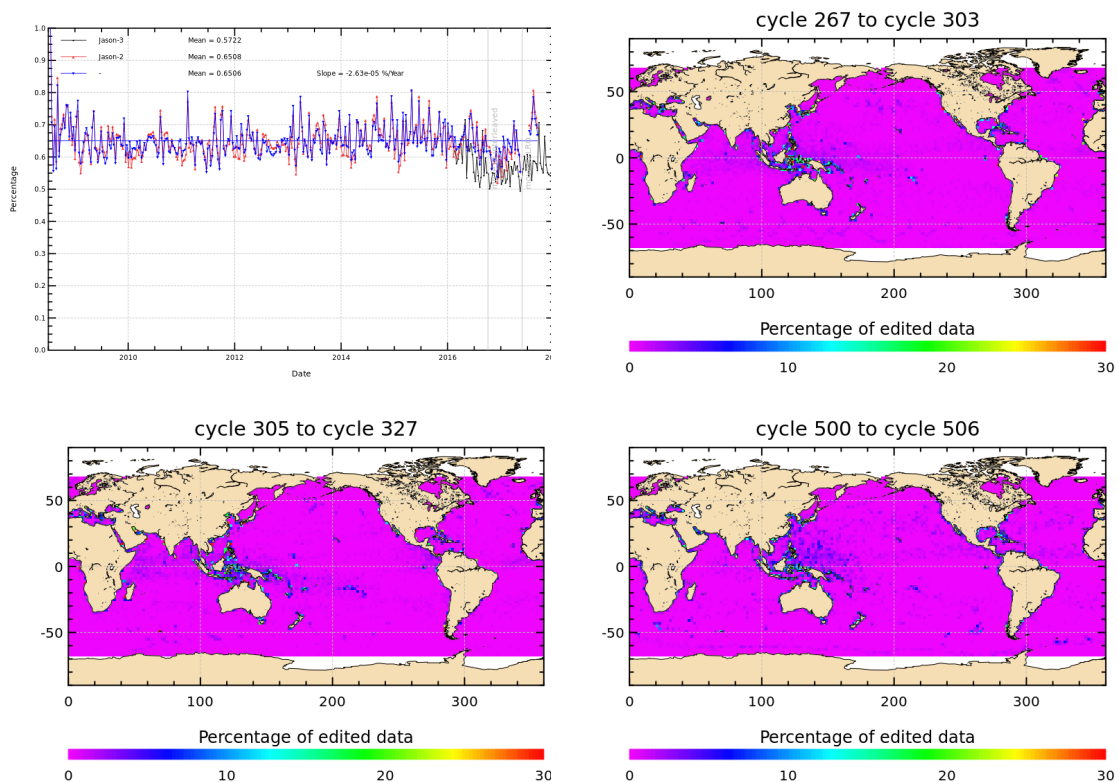


Figure 9 – Percentage of edited measurements by SWH criterion. Left: Cycle per cycle monitoring. The blue curve shows the trend of edited measurements after adjusting for annual and semi-annual signals. Right: Map over a one year period (cycles 267 to 303). Bottom: Map over interleaved with Jason-2 period from 2016-10-13 to 2017-05-17 (left) and map over cycles 500 (2017-07-11) to 506(right)

**3.2.10. Backscatter coefficient**

The percentage of edited measurements due to backscatter coefficient criterion is represented in figure 10. It is about 0.61%. It is also impacted by low signal tracking anomalies until cycle 16 (and especially during cycle 1). The right part of figure 10 shows that measurements edited by backscatter coefficient criterion are especially found near coasts in the equatorial regions and enclosed sea.

As for SWH, it seems there are few more data rejected on this criterion since Long Repeat Orbit (under investigation).

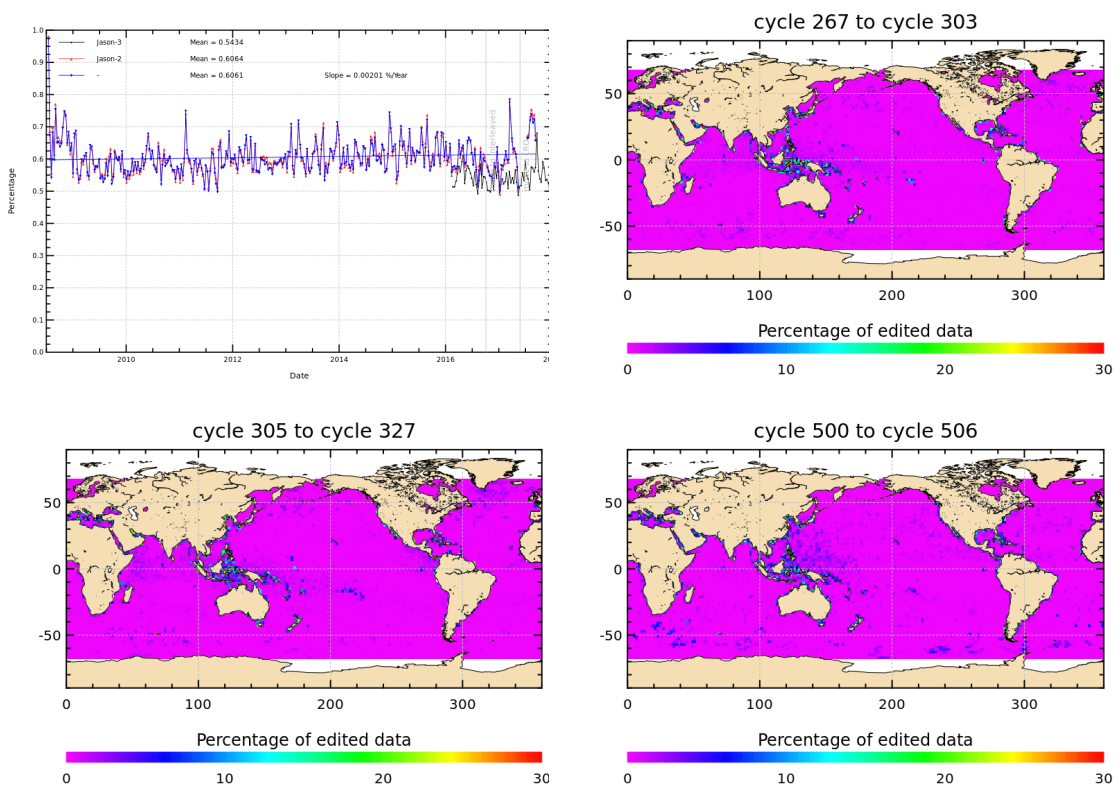


Figure 10 – Percentage of edited measurements by Sigma0 criterion. Left: Cycle per cycle monitoring. The blue curve shows the trend of edited measurements after adjusting for annual and semi-annual signals. Right: Map over a one year period (cycles 267 to 303). Bottom: Map over interleaved with Jason-2 period from 2016-10-13 to 2017-05-17 (left) and map over cycles 500 (2017-07-11) to 506(right)

**3.2.11. Backscatter coefficient: 20 Hz standard deviation**

The percentage of edited measurements due to 20 Hz backscatter coefficient standard deviation criterion is represented in figure 11. It is about 1.94%. The right part of figure 10 shows that measurements edited by 20 Hz backscatter coefficient standard deviation criterion are especially found in regions with disturbed waveforms.

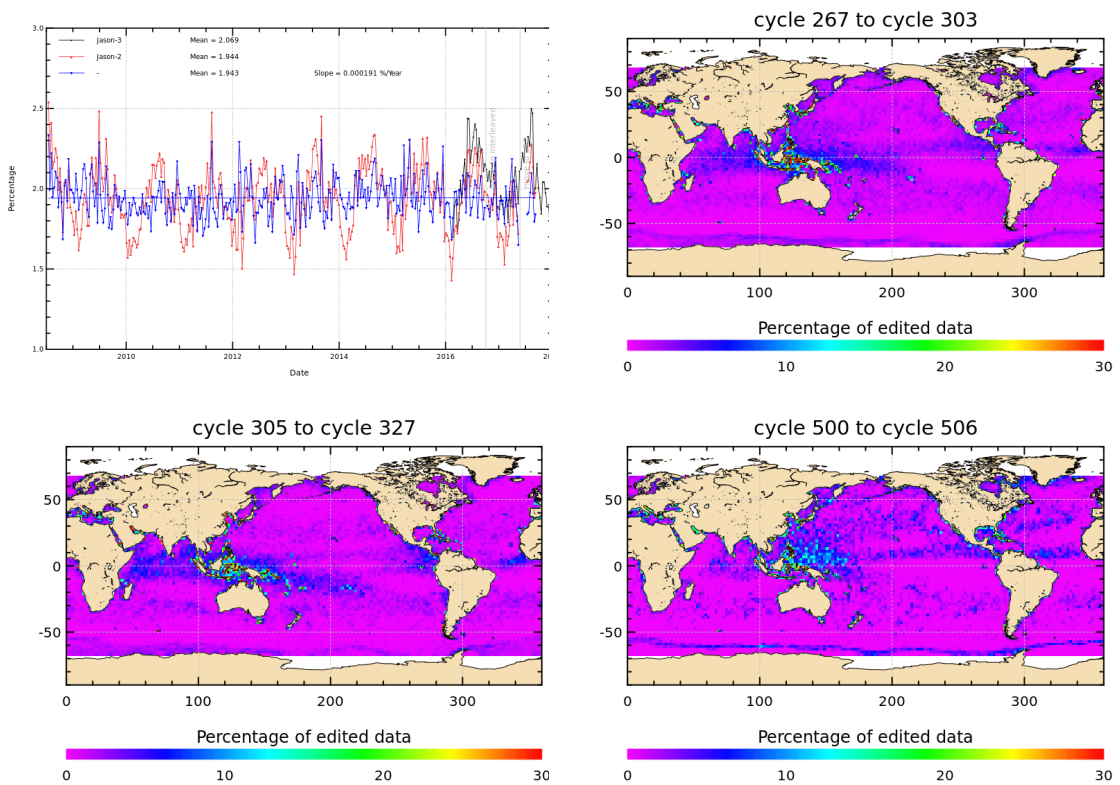


Figure 11 – Percentage of edited measurements by 20 Hz Sigma0 standard deviation criterion. Left: Cycle per cycle monitoring. The blue curve shows the trend of edited measurements after adjusting for annual and semi-annual signals. Right: Map over a one year period (cycles 267 to 303). Bottom: Map over interleaved with Jason-2 period from 2016-10-13 to 2017-05-17 (left) and map over cycles 500 (2017-07-11) to 506(right)

### 3.2.12. Radiometer wet troposphere correction

The percentage of edited measurements due to radiometer wet troposphere correction criterion is represented in figure 12. It is about 0.23%. When removing cycles which experienced problems, percentage of edited measurements drops to less than 0.1%. For some cycles the percentage of edited measurements is higher than usual. This is linked to radiometer wet troposphere correction at default value due to AMR unavailability in case of cycle 19, 238, 269 and 326, AMR reset in case of cycles 168 and 169, and time lag between altimeter restart and radiometer restart after safe hold modes in case of cycles 174, 175, 191 and 500.

On the top right part of figure 12 (computed over a one year complete period), the following unavailability periods are visible:

- there were no AMR data on 25/10/2015 from 18h18 to 22h25 (cycle 269 passes 111 to 115),
- on 10/01/2016 from 02:45:05 to 05:03:03 (impacting cycle 277 passes 035 to 037)
- on 19/01/2016 from 05:58:31 to 08:21 (cycle 279 passes 017 to 020).
- and on 31/03/2016 from 09:30:52 to 11:39:11 (cycle 285 passes 085 to 087).

During cycle 325 and 326 of its interleaved flight phase, Jason-2 radiometer anomalies occurred. It led to radiometer parameters set to default value, so that part of pass 11 and whole passes 12, 13, 14, 15 are rejected on wet tropospheric correction thresholds (bottom left of figure 12).

On bottom right of figure 12, one pass is underlined as just after restart on cycle 500, radiometer data are set to default value.

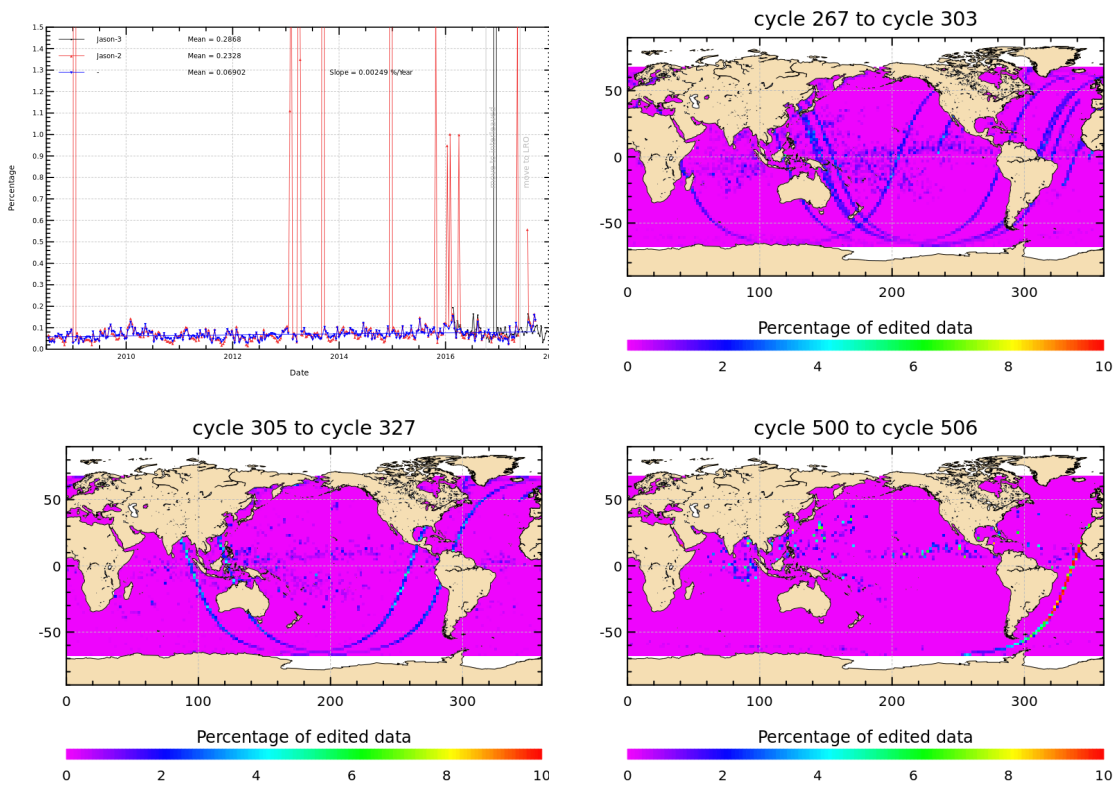


Figure 12 – Percentage of edited measurements by radiometer wet troposphere criterion. Left: Cycle per cycle monitoring. The blue curve shows the trend of edited measurements after adjusting for annual and semi-annual signals. Right: Map over a one year period (cycles 267 to 303). Bottom: Map over interleaved with Jason-2 period from 2016-10-13 to 2017-05-17 (left) and map over cycles 500 (2017-07-11) to 506(right)

### 3.2.13. Dual frequency ionosphere correction

The percentage of edited measurements due to dual frequency ionosphere correction criterion is represented in figure 13. It is about 1.2% and shows no drift. The map 13 shows that measurements edited by dual frequency ionosphere correction are mostly found in equatorial regions, but also near sea ice.

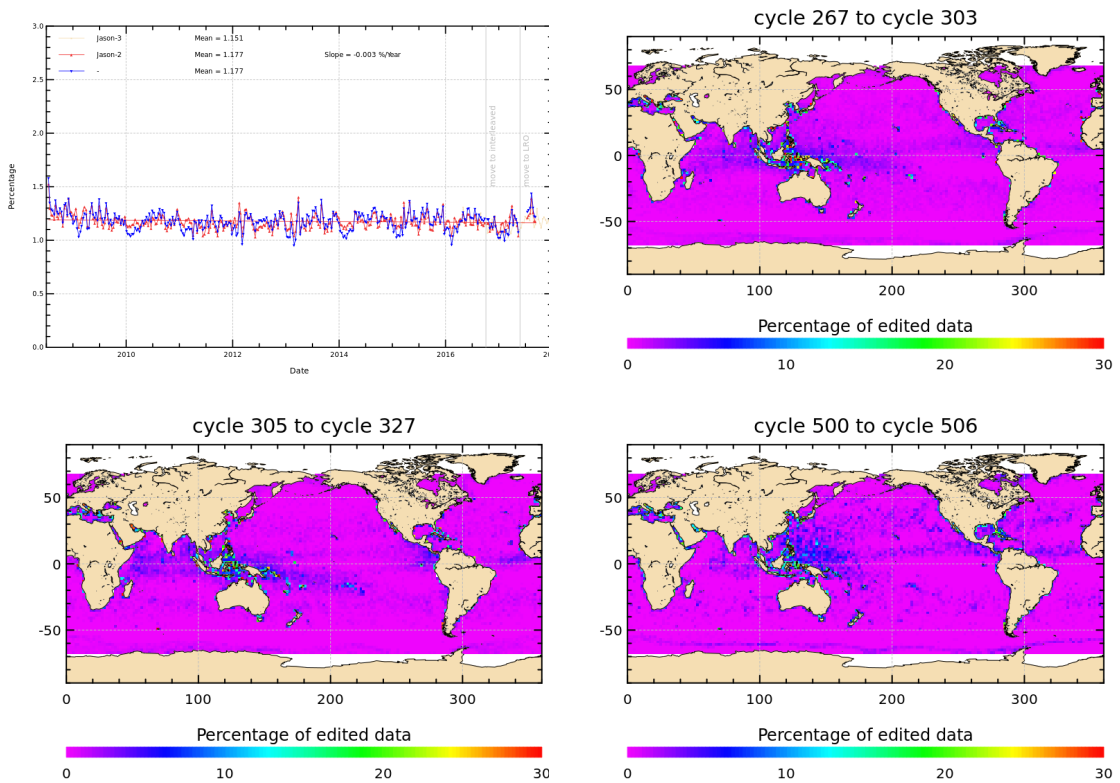


Figure 13 – Percentage of edited measurements by dual frequency ionosphere criterion. Left: Cycle per cycle monitoring. The blue curve shows the trend of edited measurements after adjusting for annual and semi-annual signals. Right: Map over a one year period (cycles 267 to 303). Bottom: Map over interleaved with Jason-2 period from 2016-10-13 to 2017-05-17 (left) and map over cycles 500 (2017-07-11) to 506(right)

### 3.2.14. Square off-nadir angle

The percentage of edited measurements due to square off-nadir angle criterion is represented in figure 14. It is about 0.6%. As for other parameters, impact of low signal tracking anomalies is visible in general for the first 16 cycles and especially for cycle 1. It seems there are few more data rejected on this criterion since Long Repeat Orbit (under investigation). The map 14 shows that edited measurements are mostly found in coastal regions and regions with disturbed waveforms.

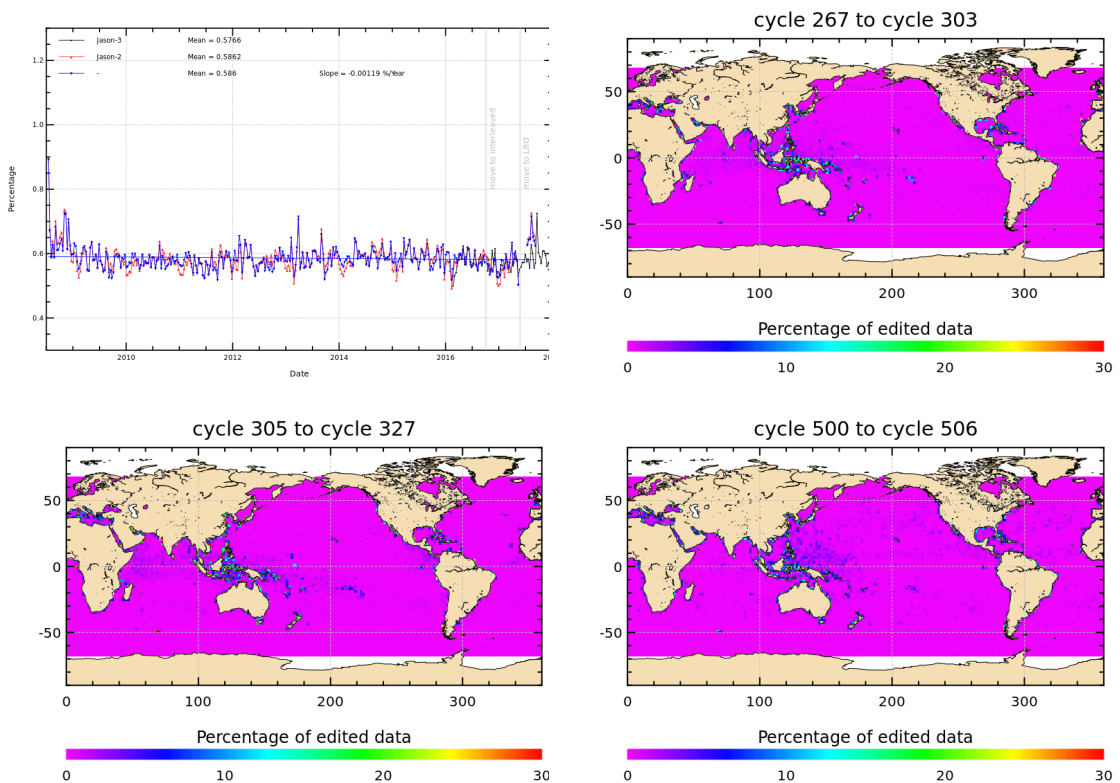


Figure 14 – Percentage of edited measurements by square off-nadir angle criterion. Left: Cycle per cycle monitoring. The blue curve shows the trend of edited measurements after adjusting for annual and semi-annual signals. Right: Map over a one year period (cycles 267 to 303). Bottom: Map over interleaved with Jason-2 period from 2016-10-13 to 2017-05-17 (left) and map over cycles 500 (2017-07-11) to 506(right)

### 3.2.15. Sea state bias correction

The percentage of edited measurements due to sea state bias correction criterion is represented in figure 15. The percentage of edited measurements is about 0.6% and shows no drift. The map 15 shows that edited measurements are mostly found in equatorial regions near coasts. As for SWH or SIG0, it seems there are few more data rejected on this criterion since Long Repeat Orbit (under investigation).

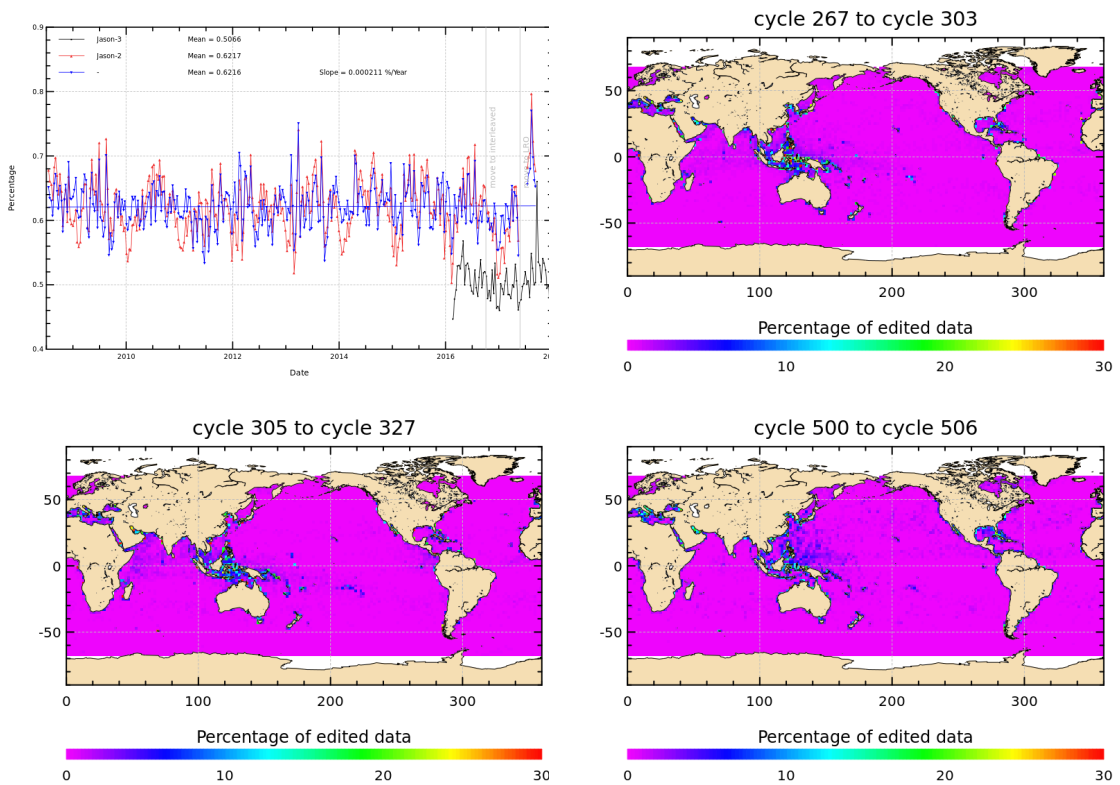


Figure 15 – Cycle per cycle percentage of edited measurements by sea state bias criterion (left). The blue curve shows the trend of edited measurements after adjusting for annual and semi-annual signals. Right: Map of percentage of edited measurements by sea state bias criterion over a one year period (cycles 267 to 303). Bottom: Map over interleaved with Jason-2 period from 2016-10-13 to 2017-05-17 (left) and map over cycles 500 (2017-07-11) to 506(right)

### 3.2.16. Altimeter wind speed

The percentage of edited measurements due to altimeter wind speed criterion is represented in figure 16. It is about 1.0%. The measurements are edited because they have default values. This is the case when sigma0 itself is at default value, or when it shows very high values (higher than 25 dB), which occur during sigma bloom and also over sea ice. Indeed, the wind speed algorithm (which uses backscatter coefficient and significant wave height) can not retrieve values for sigma0 higher than 25 dB.

Wind speed is also edited, when it has negative values, which can occur in GDR products. Nevertheless, sea state bias is available even for negative wind speed values. Therefore, the percentage of edited altimeter wind speed is higher than that of edited sea state bias.

The map 16 showing percentage of measurements edited by altimeter wind speed criterion is correlated with maps 15 and 9.

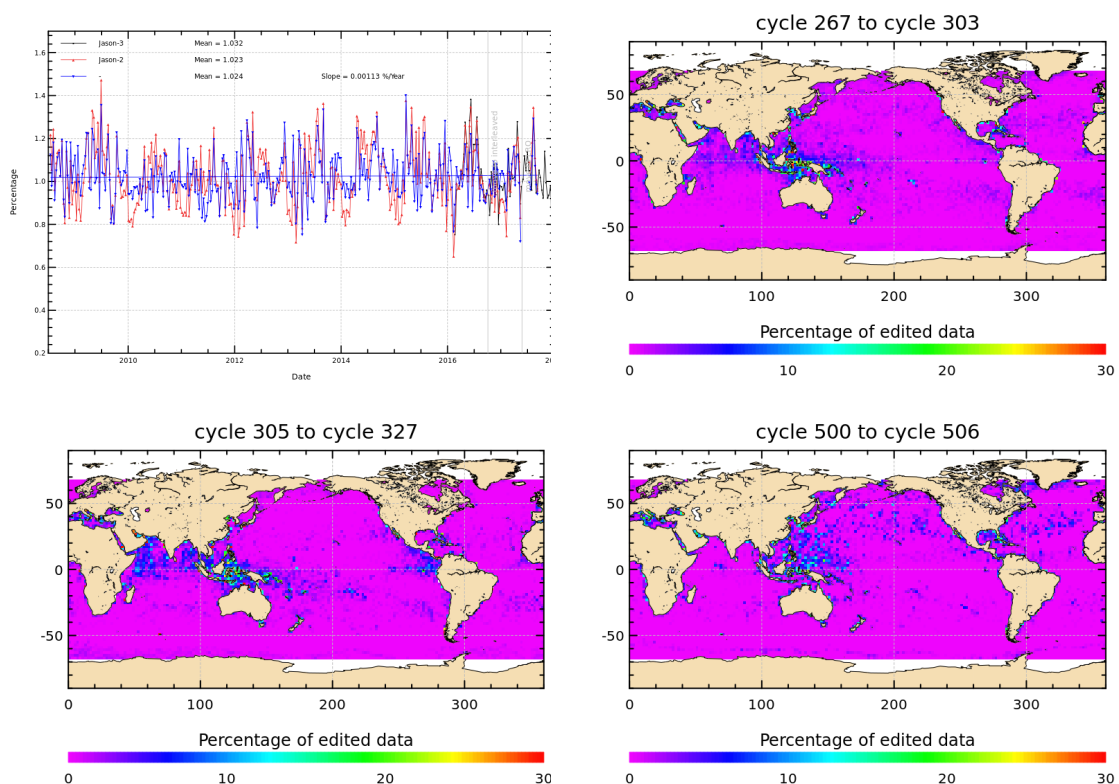


Figure 16 – Percentage of edited measurements by altimeter wind speed criterion. Left: Cycle per cycle monitoring. The blue curve shows the trend of edited measurements after adjusting for annual and semi-annual signals. Right: Map over a one year period (cycles 267 to 303). Bottom: Map over interleaved with Jason-2 period from 2016-10-13 to 2017-05-17 (left) and map over cycles 500 (2017-07-11) to 506(right)

### 3.2.17. Ocean tide correction

The percentage of edited measurements due to ocean tide correction criterion is represented in figure 17. It is less than 0.01%. The ocean tide correction is a model output, there should therefore be no edited measurements. Indeed there are no measurements edited in open ocean areas, but only very few near coasts (Alaska, Kamchatka, Labrador). These measurements are mostly at default values. The percentage of measurement increases for cycle 174 and 175 (2013 safe hold mode). The level of edited measurements decreased when move to interleaved orbit, and increased with move to Long Repeat Orbit. This is related to the different ground tracks, which do not overflow the same areas.

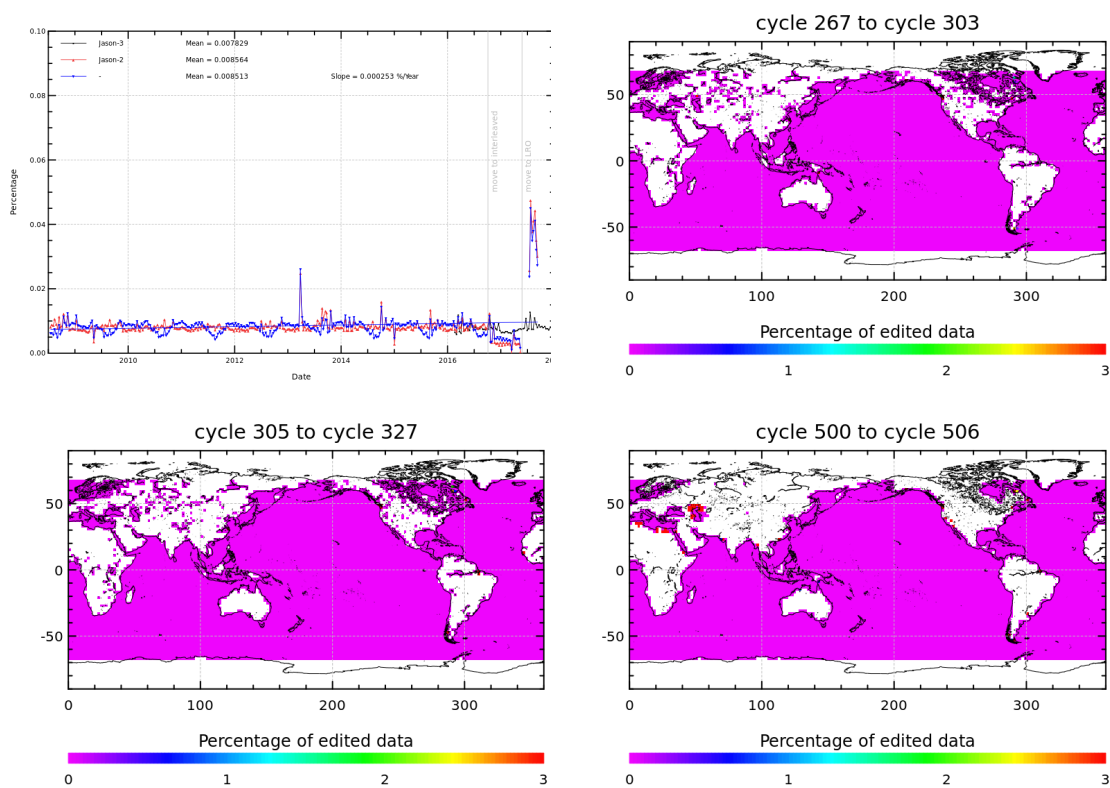


Figure 17 – Percentage of edited measurements by ocean tide criterion. Left: Cycle per cycle monitoring. The blue curve shows the trend of edited measurements after adjusting for annual and semi-annual signals. Right: Map over a one year period (cycles 267 to 303). Bottom: Map over interleaved with Jason-2 period from 2016-10-13 to 2017-05-17 (left) and map over cycles 500 (2017-07-11) to 506(right)

### 3.2.18. Sea surface height

The percentage of edited measurements due to sea surface height (orbit - ku-band range) criterion is represented in figure 18. It is about 0.77% and shows no drift. The measurements edited by sea surface height criterion are mostly found near coasts in equatorial regions (see map 18). The majority of the edited measurements has defaulted range values. There are few more data rejected on this criterion since Long Repeat Orbit.

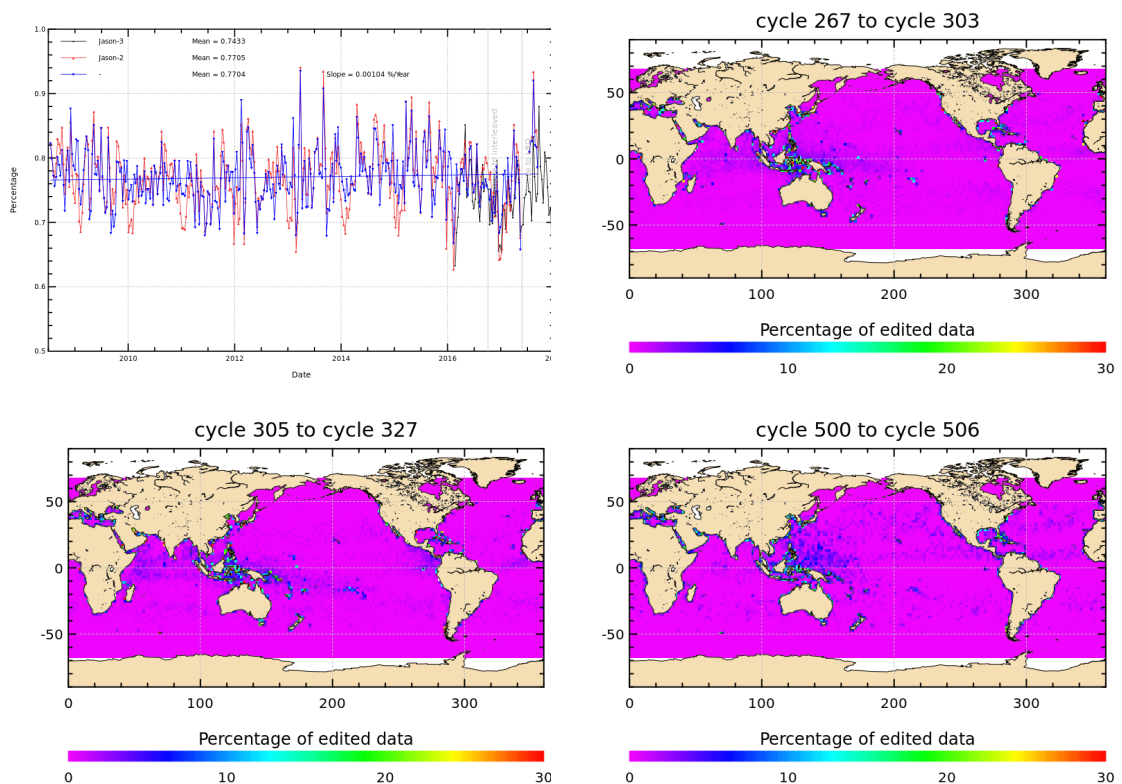


Figure 18 – Percentage of edited measurements by sea surface height criterion. Left: Cycle per cycle monitoring. The blue curve shows the trend of edited measurements after adjusting for annual and semi-annual signals. Right: Map over a one year period (cycles 267 to 303). Bottom: Map over interleaved with Jason-2 period from 2016-10-13 to 2017-05-17 (left) and map over cycles 500 (2017-07-11) to 506 (right)

### 3.2.19. Sea level anomaly

The percentage of edited measurements due to sea level anomaly criterion is represented in figure 19. It is about 1.05% (0.9% without cycles 19,168,169,174,175,191,238 and 269) and shows no drift. The peaks are related to AMR unavailabilities (see figure 12 showing the percentage of measurements edited by AMR), as the SLA clip contains, among other parameters, the radiometer wet troposphere correction.

The map in figure 19 allows us to plot the measurements edited due to sea level anomaly out of thresholds (after applying all other threshold criteria). There are only very few measurements, principally located in Caspian Sea.

As for some criteria detailed before, it seems there are few more data rejected on this criterion since Long Repeat Orbit.

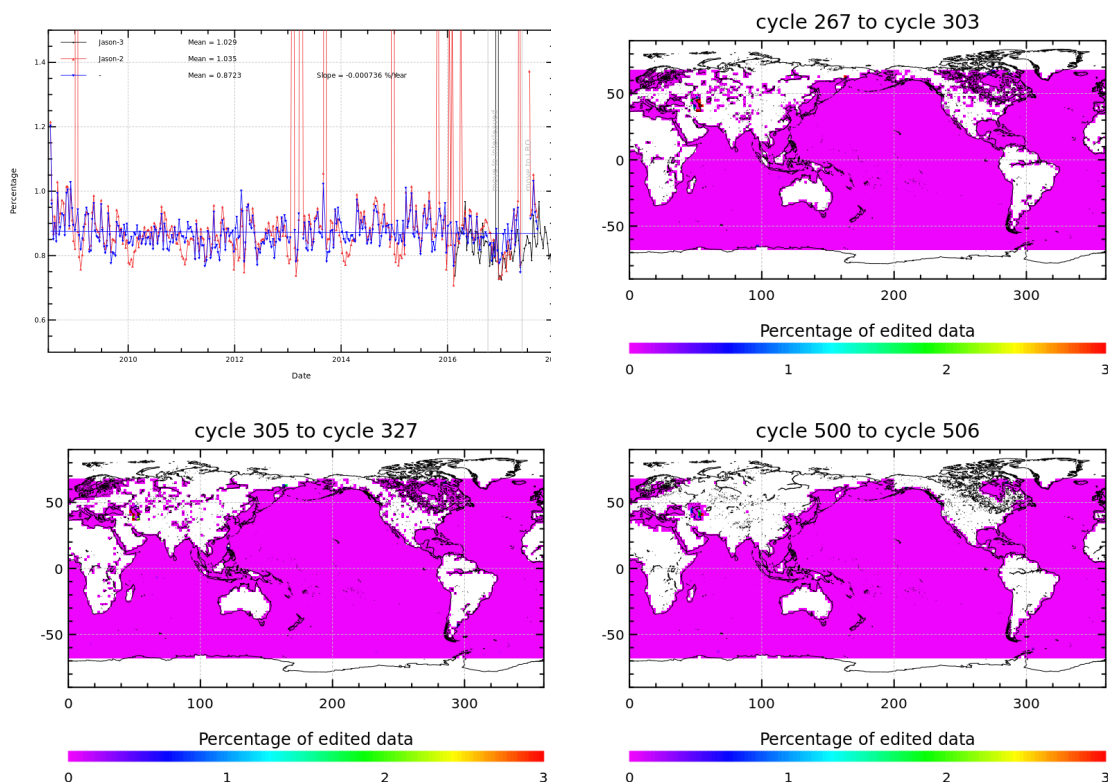


Figure 19 – Percentage of edited measurements by sea level anomaly criterion. Left: Cycle per cycle monitoring. The blue curve shows the trend of edited measurements after adjusting for annual and semi-annual signals. Right: Map over a one year period (cycles 267 to 303). Bottom: Map over interleaved with Jason-2 period from 2016-10-13 to 2017-05-17 (left) and map over cycles 500 (2017-07-11) to 506(right)

## 4. Monitoring of altimeter and radiometer parameters

### 4.1. Methodology

Both mean and standard deviation of the main parameters of Jason-2 (GDR-D) have been monitored since the beginning of the mission. Moreover, a comparison with Jason-1 (GDR-E) parameters has been performed: it allows us to monitor the bias between the parameters of the 2 missions. Two different methods have been used to compute the bias:

- Till Jason-2 cycle 20, Jason-2 and Jason-1 are on the same ground track and are spaced out about 1 minute apart (tandem phase). The mean of the Jason-1 - Jason-2 differences can be computed using a point by point repeat track analysis. Results with this method are detailed in [9].
- From Jason-2 cycle 21 (Jason-1 cycle 260), a maneuver sequence was conducted (from 26th of January to 14th of February 2009) to move Jason-1 to the new formation flight mission orbit. Jason-1 has a repeat ground-track which is interleaved with Jason-2. It is the same ground-track as already used by Topex/Poseidon during its formation flight phase with Jason-1, but there is a time shift of 5 days. Geographical variations are then too strong to directly compare Jason-2 and Jason-1 parameters on a point by point basis. Therefore day per day global differences have been carried out to monitor differences between the two missions. A filter over 11 days was applied. Nevertheless the differences are still quite noisy, especially for corrections which vary rapidly in time and space. Therefore occasional small jumps might be covered by the noise of the differences. Nevertheless it should be possible to detect drifts and permanent jumps. Jason-2 and Jason-1 were in this formation flight phase from Jason-2 cycles 22 to 135 (Jason-1 cycles 262 to 374).

In February and March of 2012, Jason-1 experienced several safe holds (anomaly on gyro3, double EDAC error in RAM memory). It was decided to move Jason-1 to a geodetic orbit (more about the Jason-1 geodetic mission can be found in [19]). Science data on the geodetic orbit are available from 7th of May 2012 onwards. Note that the first cycle on the geodetic orbit starts with cycle 500 (this corresponds to end of Jason-2 cycle 141). The last (incomplete) cycle of Jason-1 on the repeat ground-track was cycle 374. As during the formation flight phase, day per day global differences of the parameters have been carried out to monitor differences between the two missions. Finally, after loss of telemetry on 21 June 2013 (during cycle 537), Jason-1 was passivated and decommissioned on 01 July 2013, with the last command sent at 16:37:40 UTC. Note that differences are done over Jason-2 cycles 1 to 183, corresponding to Jason-1 cycles 240 to 537.

### 4.2. 20 Hz Measurements

The monitoring of the number and standard deviation of 20 Hz elementary range measurements used to derive 1 Hz data is presented here. These two parameters are computed during the altimeter ground processing. For both Jason-1 and Jason-2, before performing a regression to derive the 1 Hz range from 20 Hz data, a MQE (mean quadratic error) criterion is used to select valid 20 Hz measurements. This first step of selection consists in verifying that the 20 Hz waveforms can be approximated by a Brown echo model (Brown, 1977 [33]) (Thibaut et al. 2002 [86]). Then, through an iterative regression process, elementary ranges too far from the regression line are discarded until convergence is reached. Thus, monitoring the number of 20 Hz range measurements and the

standard deviation computed among them is likely to reveal changes at instrumental level. The Jason-1 MQE threshold are not applicable to Jason-2, using those thresholds would edit more measurements than necessary. Therefore, for the first GDR release of Jason-2 (GDR-T), the MQE threshold had been set to default, leading to no editing based on MQE values. Note that for Jason-2 data in version GDR-D, specific Jason-2 MQE thresholds were computed and are applied. Detailed comparisons over Jason-2/Jason-1 tandem phase are presented in [9].

#### 4.2.1. 20 Hz measurements number in Ku-Band and C-Band

GDR-D Jason-2 number of elementary 20 Hz range measurements is very similar to Jason-1's (especially for C-band) with an average of 19.61 for Ku-band and 19.25 for C-band as shown on figure 20. For both satellites a slight annual signal is visible (especially for C-band). Number of 20 Hz Ku-band range measurements is slightly higher for Jason-2 than for Jason-1. The regions where Jason-1 has less elementary Ku-band range measurements are especially located around Indonesia (shown in [9]). Indeed in regions of sigma bloom or rain, using a MQE criterion during the regression to derive 1Hz from 20Hz data, discards 20 Hz measurements and therefore reduces the value of number of the 20 Hz measurements used for the 1 Hz data. It is possible that differences in the tuning of the MQE criterion for Jason-1 and Jason-2 Ku-band explain what is observed.

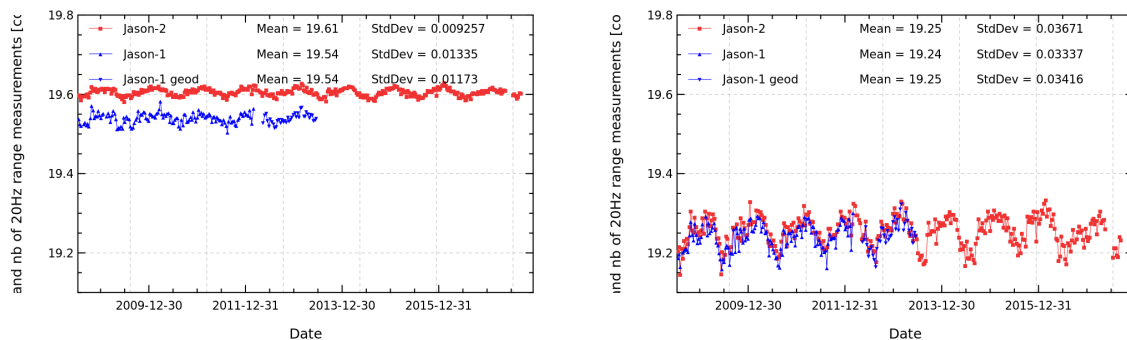


Figure 20 – Cyclic monitoring of number of elementary 20 Hz range measurements for Jason-1 and Jason-2 for Ku-band (left) and C-band (right).

**4.2.2. 20 Hz measurements standard deviation in Ku-Band and C-Band**

Jason-2 standard deviation of the 20 Hz measurements is 8.0 cm for Ku-Band and 17.4 cm for C-Band (figure 21). It is very similar to Jason-1 data. Detailed comparisons over Jason-2/Jason-1 tandem phase are presented in [9].

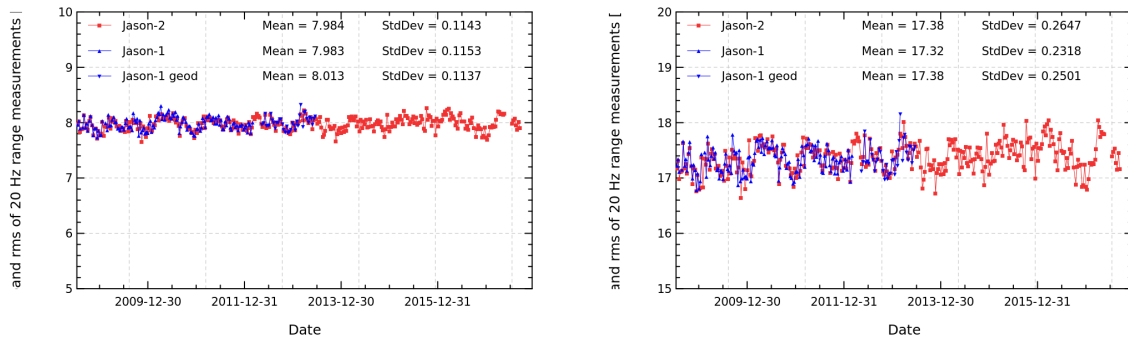


Figure 21 – Cyclic monitoring of rms of elementary 20 Hz range measurements for Jason-1 and Jason-2 for Ku-band (left) and C-band (right).

### 4.3. Off-Nadir Angle from waveforms

The off-nadir angle is estimated from the waveform shape during the altimeter processing. The square of the off-nadir angle, averaged on a daily basis, has been plotted for Jason-1 and Jason-2 on the left side of figure 22, whereas the right side shows the histograms over one cycle. For GDR-D Jason-2 the mispointing is very stable and very close to zero (though very slightly negative). Whereas Jason-1 may show higher values (related to the reduced tracking performance of both star trackers, especially during fixed-yaw). Jason-1 experienced especially during 2010 very high mispointing values, for more information see Jason-1 validation report [2]. Jason-1 mispointing situation has been highly improved since end of 2010.

Jason-2 GDR-T mispointing was slightly positive (see also reprocessing report ([7])), which was related to the antenna aperture values used for data processing ( $1.26^\circ$  for GDR-T,  $1.29^\circ$  for GDR-D). Indeed [88] shows, that retracking with different values of antenna aperture, changes the mean value of Jason-2 mispointing (see figure 23). Note that for Jason-1  $1.28^\circ$  is used for the antenna aperture.

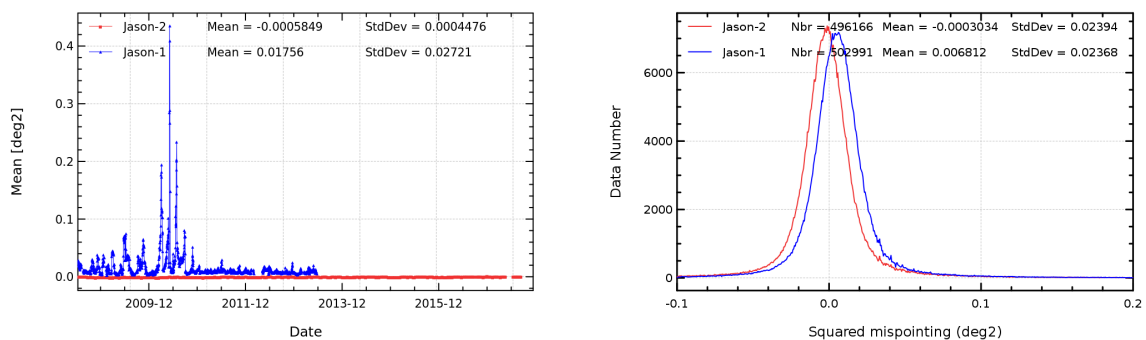


Figure 22 – Square of the off-nadir angle deduced from waveforms ( $\text{deg}^2$ ) for Jason-1 and Jason-2: Daily monitoring (left), histograms for Jason-2 cycle 157 (Jason-1 cycle 513/514).

Mispointing distribution computed with PISTACH rtk MLE4 algo for varying antenna beamwidth and 21520sm filter

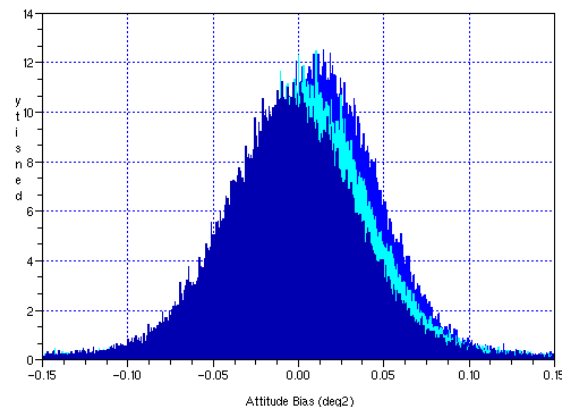


Figure 23 – Histograms of Jason-2 mispointing after retracking with different antenna beamwidth (from [88]):  $1.26^\circ$  (blue),  $1.28^\circ$  (light blue),  $1.30^\circ$  (dark blue).

#### 4.4. Backscatter coefficient

The Jason-2 Ku-band and C-band backscatter coefficient shows good agreement with Jason-1 as visible on cyclic monitoring in figure 24 (top left and right). Note that backscatter coefficients include instrumental corrections, which also include radiometer atmospheric attenuation. Therefore differences between backscatter coefficients can also be partly due to differences between the atmospheric attenuation algorithms of Jason-1 and Jason-2. The main reasons for the differences (between Jason-1 and Jason-2 backscatter coefficients) are related to the antenna calibrations and to the internal calibrations of the altimeters (steps of numerical gain control).

Detailed comparisons over Jason-2/Jason-1 tandem phase are presented in [9].

Mean differences show a bias close to 0.29 dB (see bottom of figure 24). After the last safe hold mode of Jason-1 (March 2013), a small jump is visible in the Jason-1 minus Jason-2 Sigma0 difference.

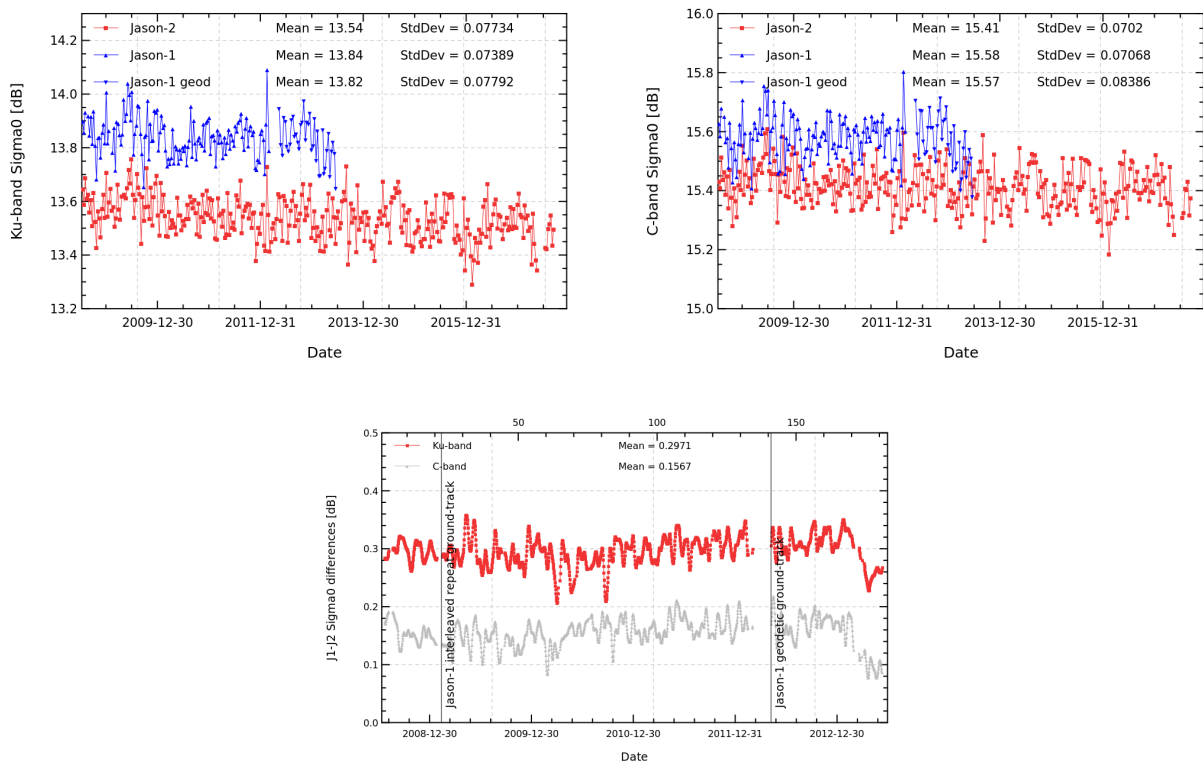


Figure 24 – Cyclic monitoring of Sigma0 for Jason-1 and Jason-2 for Ku-band (left) and C-band (right). Daily monitoring of Jason-1 - Jason-2 differences (bottom), a 10 day filter is applied.

#### 4.5. Significant wave height

As for Sigma0 parameter, a very good consistency between both significant wave height is shown (see figure 25). A small bias close to around -1.3 cm is calculated over the tandem phase, it is close to -1.7 cm in C-band (details in [9]). As previously, extending the monitoring of SWH bias during the formation flight phase (bottom of figure 25) highlights larger variations since both satellites do not measure the same SWH.

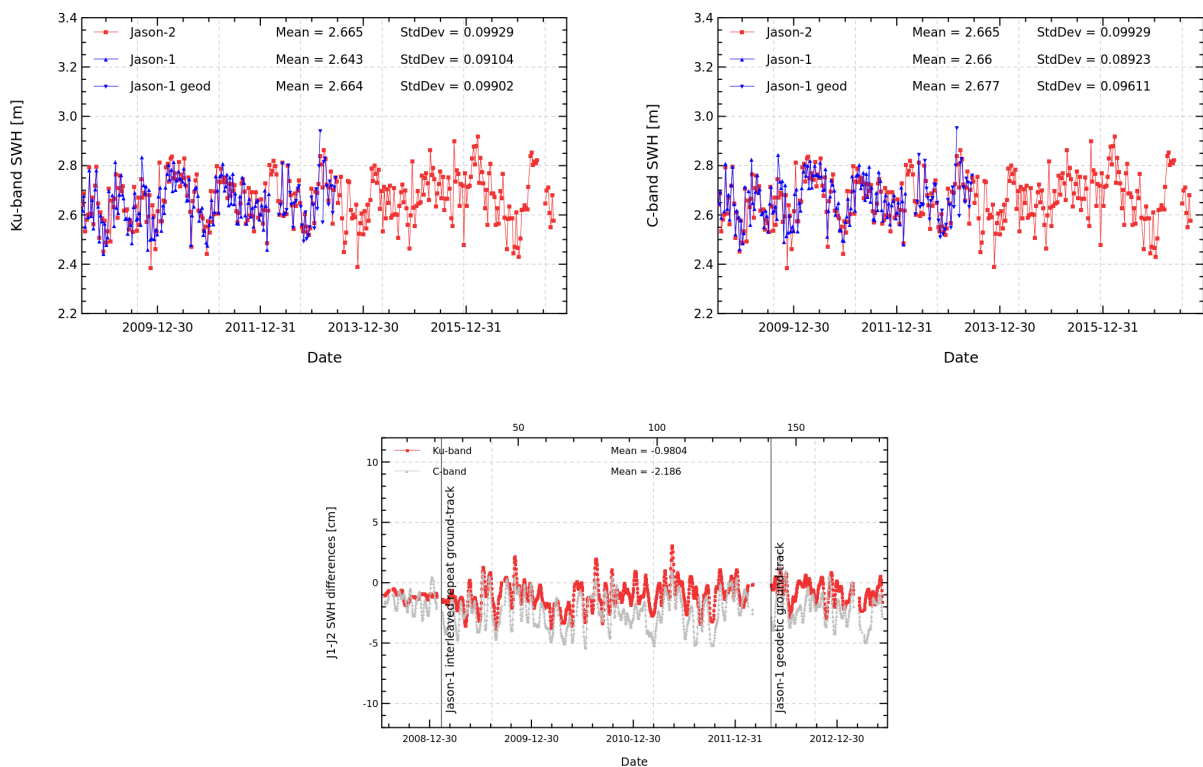


Figure 25 – Cyclic monitoring of SWH for Jason-1 and Jason-2 for Ku-band (left) and C-band (right). Daily monitoring of Jason-1 - Jason-2 differences (bottom), a 10 day filter is applied.

### 4.6. Dual-frequency ionosphere correction

Detailed comparisons over Jason-2/Jason-1 tandem phase are presented in [9].

Notice that, as for TOPEX and Jason-1 (Le Traon et al. 1994 [63], Imel 1994 [58], Zlotnicky 1994 [93]), it is recommended to filter the Jason-2 dual frequency ionosphere correction before using it as a SSH geophysical correction (Chambers et al. 2002 [39]). A low-pass filter has thus been used to remove the noise of the correction in all SSH results presented in the following sections. Plotting difference of non-filtered ionospheric correction between Jason-1 and Jason-2 versus Jason-2 ionospheric correction shows an apparent scale error, which disappears when using filtered data (see figure 26). As in the beginning of the Jason-2 mission, ionosphere correction was very low, the ionosphere noise is of the same order of magnitude as the ionosphere correction itself. Therefore plotting the difference of non-filtered dual-frequency ionospheric correction versus dual-frequency ionospheric correction induces an apparent scale error.

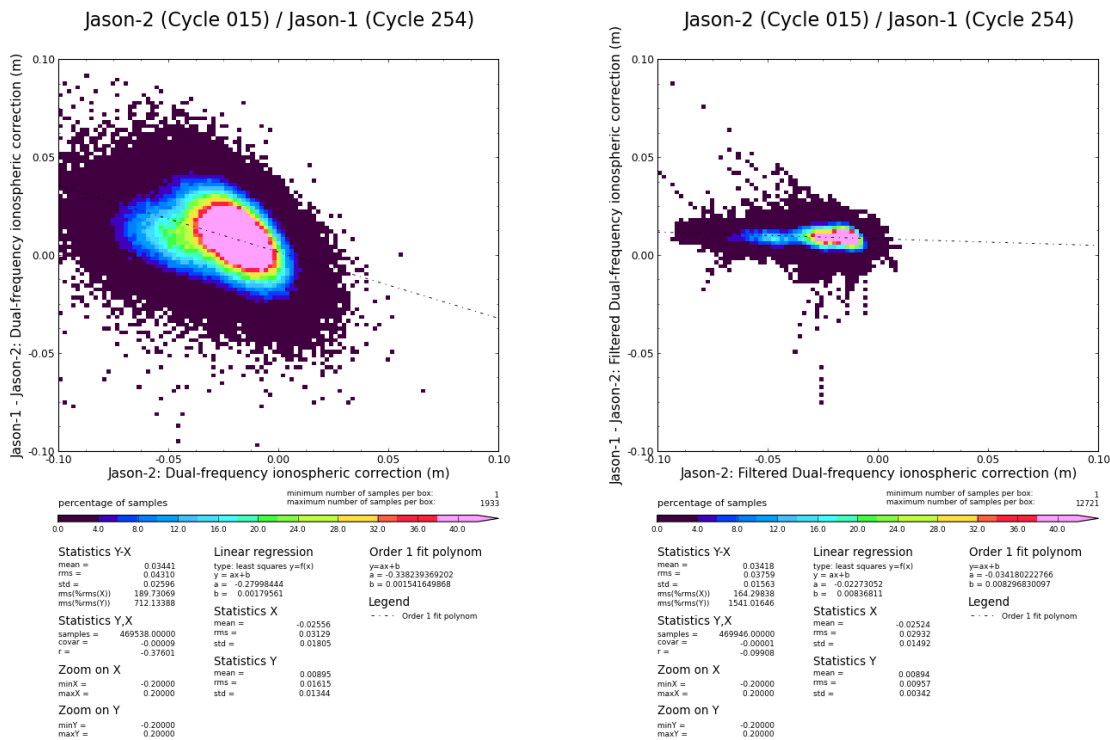


Figure 26 – Diagram of dispersion of Jason-1 (GDR-E) - Jason-2 versus Jason-2 dual-frequency ionosphere correction for Jason-2 cycle 15. Left: non-filtered, right: filtered.

During 2011, as at the end of 2013 and the beginning of 2014 solar activity has increased and therefore also the absolute value of ionosphere correction (right part of figure 27).

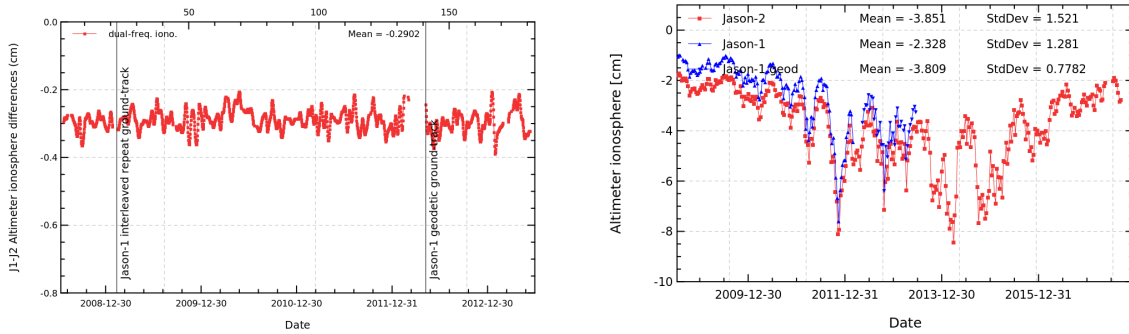


Figure 27 – Cyclic monitoring of dual-frequency ionosphere for Jason-1 and Jason-2 (right). Daily monitoring of Jason-1 - Jason-2 differences (left), a 10 day filter is applied.

When comparing altimeter ionosphere correction to GIM correction (figure 28), mean as well as standard deviation of this difference increases between 2011 and 2015. This concerns both Jason missions (for 2011) and is due to the higher solar activity during which the GIM model is less accurate than the correction measured by the altimeter.

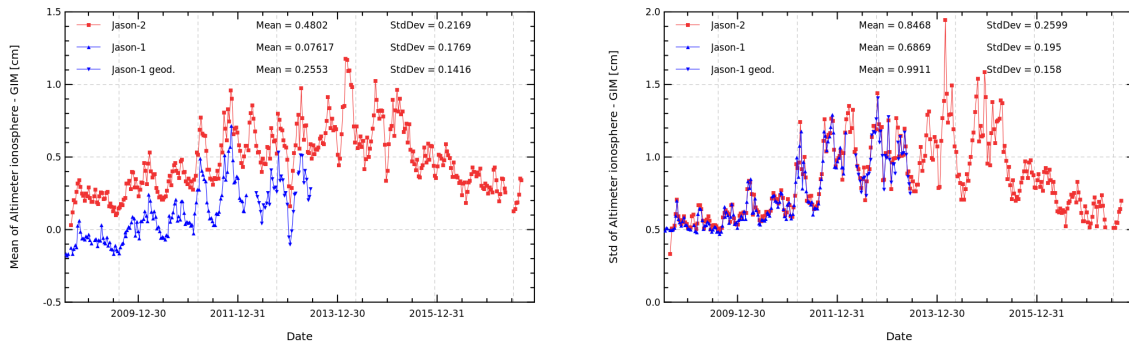


Figure 28 – Cycle per cycle monitoring of filtered altimeter ionosphere correction minus GIM ionosphere correction for Jason-1 and Jason-2. Left: Mean, right: standard deviation.

Figure 29 shows the mean difference between altimeter ionosphere and GIM correction after a one-year smooth for slots of local hours. Ionosphere differences between altimeter and GIM are higher for day time measurements than for night time measurements.

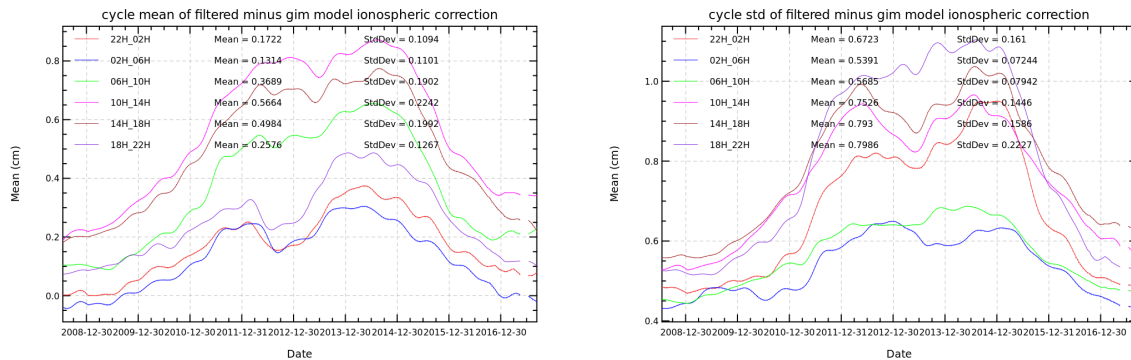


Figure 29 – Cycle per cycle monitoring of filtered altimeter ionosphere minus GIM correction computed per local hour time intervals. Mean on left and standard deviation on the right. A one-year smooth is applied.

## 4.7. AMR Wet troposphere correction

### 4.7.1. Overview

The Jason-2 radiometer wet troposphere correction available contains an improved retrieval algorithm near coasts ([36]). Note that the product AMR radiometer wet troposphere correction has (according to S. Brown) several level of calibration:

- Cycles 1-113 - Climate data record quality calibration Cycles
- 114-140 - Intermediate quality calibration ( somewhere between climate quality and operational(ARCS) quality)
- Cycle 141 onward - Operational(ARCS) quality calibration

Note that since 12 July 2016 (cycle 295), Jason-2 AMR have been recalibrated with cold sky calibration (as for Jason-3). Until end of year 2017, AMR cold sky calibrations have occurred on:

- 12 July 2016 (Cycle 295 )
- 05 September 2016 (Cycle 301 )
- 07 November 2016 (Cycle 307 )
- 10 January 2017 (Cycle 314 )
- 26 February 2017 (Cycle 318 )
- 26 April 2017 (Cycle 324 )
- 11 July 2017 (Cycle 500 )
- 13 August 2017 (Cycle 503 )
- 01 November 2017 (Cycle 511 )

Detailed comparisons over Jason-2/Jason-1 tandem phase are presented in [9].

#### 4.7.2. Comparison with the ECMWF model

The ECMWF wet troposphere correction has been used to check the radiometer correction. Daily differences are calculated and plotted in figure 31. It clearly appears (on left side of figure 31) that Jason-2 radiometer correction (AMR) from GDR products is much more stable than for Jason-1 (JMR). Thanks to the ARCS (Autonomous Radiometer Calibration System) (Brown et al. 2009, [35]) calibration system set up for Jason-2, AMR radiometer correction is calibrated at each GDR cycle and the calibration coefficients are modified if necessary. The AMR wet troposphere correction shows jumps and drifts in the IGDRs. The calibrations applied for the GDRs correct most of these anomalies, nevertheless small jumps persist. There can also be small drifts visible within a cycle, as the ARCS corrections apply a constant value over a whole cycle.

Figure 30 shows mean and standard deviation for cycle per cycle differences between Jason-2 radiometer and ECMWF model wet troposphere corrections for several data types. Over year 2017, there were several changes of radiometer calibration coefficients. The radiometer minus ECMWF model wet troposphere differences shows some jumps due to safe hold mode events (in march (cycle 321), in may (cycle 327) and in september (cycle 506)). After the application of new calibration coefficients in GDR, the mean of IGDR and GDR radiometer minus ECMWF model wet troposphere differences are different from cycle 321 to 327. The standard deviation (right part of the figure) is quite stable.

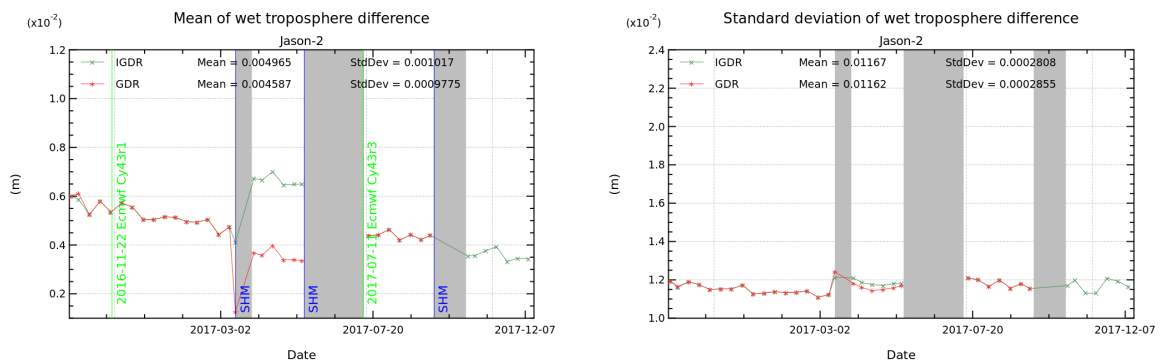


Figure 30 – Cycle per cycle monitoring of mean (left) and standard deviation (right) of radiometer minus ECMWF model wet troposphere correction over 2017 (until cycle 506) for Jason-2 I/GDR.

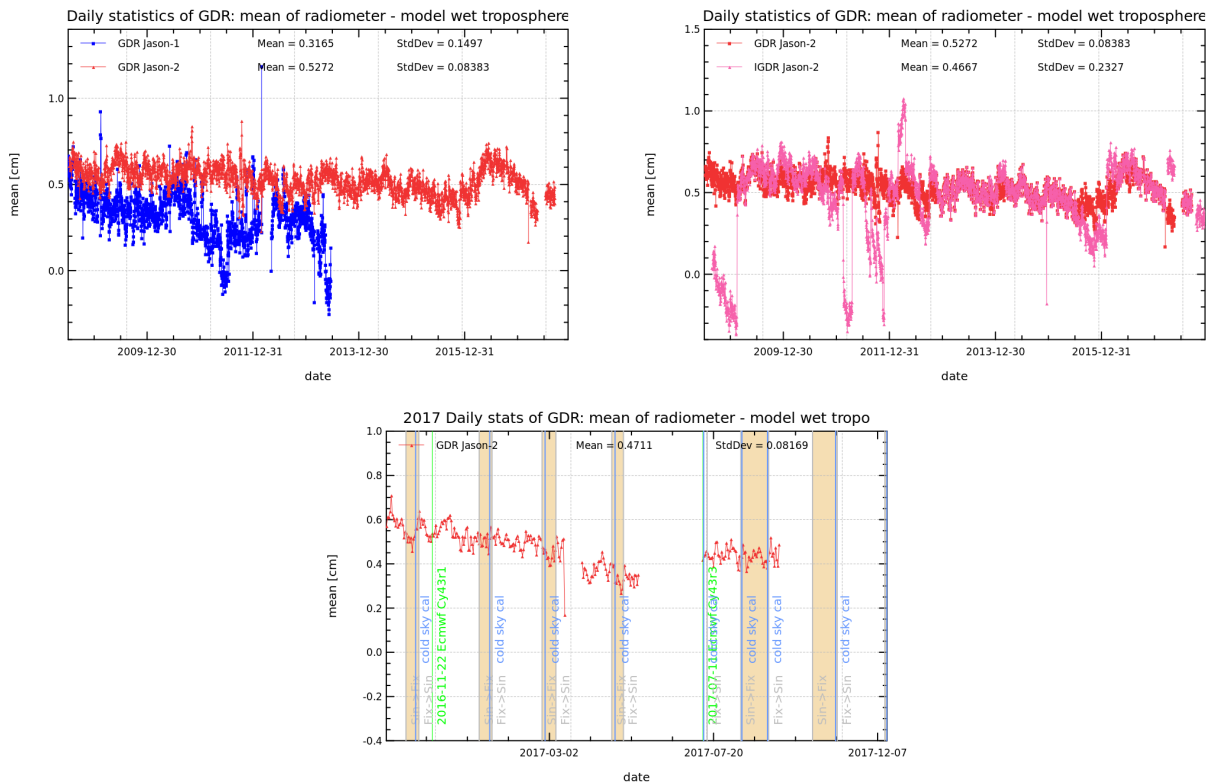


Figure 31 – Left: Daily monitoring of radiometer and ECMWF model wet troposphere correction differences for Jason-1 (blue) and Jason-2 (red). Right: daily monitoring for Jason-2 GDRs (red) and IGDRs (pink). Bottom: Daily monitoring for Jason-2 GDRs (red) for 2016. Vertical gray bands correspond to yaw maneuvers on Jason-2.

#### 4.8. Altimeter wind speed

Detailed comparisons over Jason-2/Jason-1 tandem phase are presented in [9].

Figure 32 shows mean and standard deviation for cycle per cycle altimeter wind speed for several data types of Jason-2. The altimeter wind speed of the different data types is coherent. During 2012 new algorithm is applied to IGDR (for more details see reprocessing report [7]). GDR data are homogeneous thanks to 2012 reprocessing. During the last year, small differences are visible from cycles 321 to 327. A drift is visible on this monitoring. A comparison to model (bottom of figure 32) highlights a drift of about 0.3m/s from 12/2011 to now.

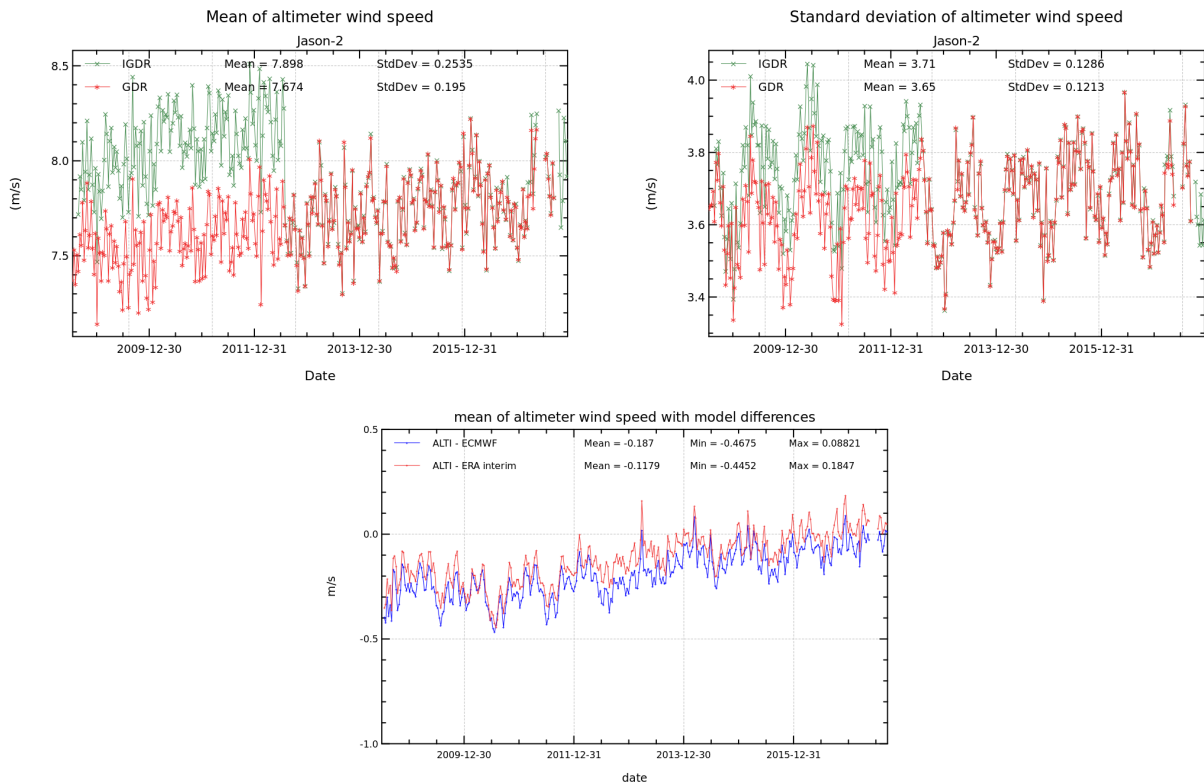


Figure 32 – Cycle per cycle monitoring of mean (**left**) and standard deviation (**right**) of altimeter wind speed for Jason-2 I/GDR. **bottom:** mean difference of altimeter wind speed for Jason-2 GDR minus model (ECMWF and ERA interim)

#### 4.9. Sea state bias

At OSTST 2012 meeting, Tran et al. [92] presented a new SSB model computed using one year of GDR-D data. This model seems better than the SSB model used for the GDR-D product, and as been used for Jason-1 GDR-E reprocessing (computed with GDR-E like Jason-1 data (see [4]). Jason-1 (blue) and Jason-2 GDR (red) sea state bias show a constant and non significant bias due to the way ssb solutions are computed. When using the updated sea state bias proposed by Tran et al. [92] for both missions (Jason-1 GDR-E and Jason-2 Tran2012), differences between Jason-1 and Jason-2 disappear and are about +0.3 cm in average (black and blue curves on left of figure 33). Solutions show no drift or anomaly.

Detailed comparisons over Jason-2/Jason-1 tandem phase are presented in [9].

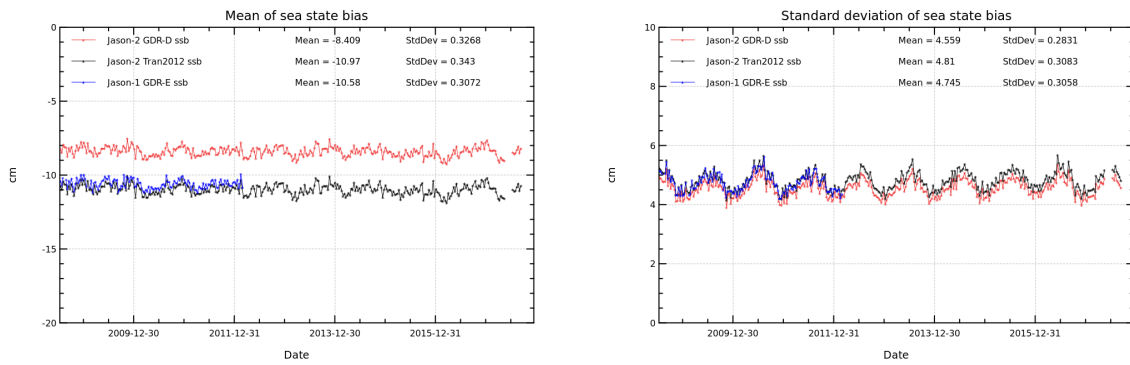


Figure 33 – Cyclic monitoring of mean (left) and standard deviation (right) of Jason-2 and Jason-1 sea state bias, using SSB from Jason-1 GDR-E, Jason-2 GDR-D and updated (2012) SSB for Jason-2.

## 5. SSH crossover analysis

### 5.1. Overview

SSH crossover differences are the main tool to analyze the whole altimetry system performances. They allow us to analyze the SSH consistency between ascending and descending passes. However in order to reduce the impact of oceanic variability, we select crossovers with a maximum time lag of 10 days. Mean and standard deviation of SSH crossover differences are computed from the valid data set to perform maps or a cycle by cycle monitoring over all the altimeter period. In order to monitor the performances over stable surfaces, additional editing is applied to remove shallow waters (bathymetry above -1000m), areas of high ocean variability (variability above 20 cm rms) and high latitudes ( $> |50|deg$ ). SSH performances are then always estimated with equivalent conditions. The main SSH calculation for Jason-2 and Jason-1 are defined below.

$$SSH = Orbit - Altimeter Range - \sum_{i=1}^n Correction_i$$

with  $Jason - 1 / Jason - 2 Orbit = CNES orbit$  for GDR products, and

$$\begin{aligned} \sum_{i=1}^n Correction_i &= \text{Dry troposphere correction} \\ &+ \text{Dynamical atmospheric correction} \\ &+ \text{Radiometer wet troposphere correction} \\ &+ \text{Dual frequency ionospheric correction (filtered)} \\ &+ \text{Non parametric sea state bias correction} \\ &+ \text{Ocean tide correction (including loading tide)} \\ &+ \text{Earth tide height} \\ &+ \text{Pole tide height} \end{aligned}$$

In 2016, Jason-1 GDR were available in version E. In order to allow better comparisons between Jason-1 and Jason-2, some standards of Jason-2 were updated (only when comparisons are done with Jason-1 GDR-E).

*Note that from 7th of May 2012 (Jason-1 cycle 500, which corresponds to end of Jason-2 cycle 141) and until the end of the Jason-1 mission (21st of June 2013, during Jason-2 cycle 183), Jason-1 was on a geodetic ground-track.*

If no precision is done, in case of IGDR results, DUACS updates are applied (ocean tide correction, mean sea surface model, mog2d dynamical atmospheric correction, see [104])

### 5.2. Mean of SSH crossover differences

The cycle by cycle mean of SSH differences is plotted in figure 34 for Jason-2 and Jason-1 (using standards from Jason-1 GDR-E products). The curves are very similar and do not highlight any anomaly. However, a 120 day signal is visible for Jason-1 data (and also, but smaller on Jason-2 updated data).

Mean of SSH differences at crossovers for Jason-2 IGDR products (using MOE orbits, and DUACS updates for some corrections) has noticeable negative values in average (-0.38cm over the last year versus -0.03cm in case of GDR), as can be seen on bottom left of figure 34. In addition, the IGDR (updated with DUACS/CMEMS2018 standards) data monitoring shows a 120 day signal that is reduced in case of GDR (bottom right of figure 34). This difference of behaviour for IGDR and GDR is partly explained by the way the solar radiation pressure is taken into account in orbit solution computation (different for MOE and POE). Thanks to the orbit standard E (an identical modeling of solar radiation pressure is planned for MOE and POE) applied from cycle 254 onwards, the 120 day signal on IGDR is slightly reduced. In addition, even the remaining 120 day signal on GDR is reduced with POE-E, the choice of ocean tide solution used to compute sea surface height impacts the amplitude of the observed 120 days signal (figure 35). This is under investigation. Note that even if FES correction appears to increase the SSH difference between ascending and descending observations, this does not mean that this correction degrades the data quality. A more thorough investigation is detailed in Jason-3 annual report. [11].

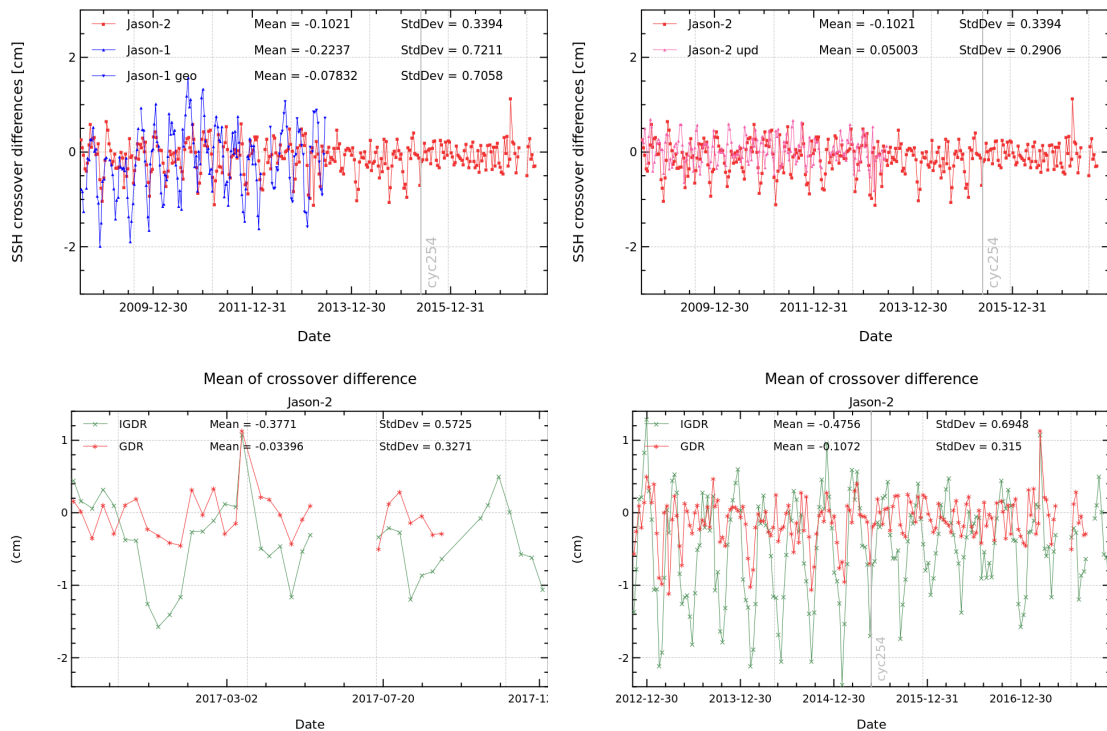


Figure 34 – Top: Monitoring of mean of SSH crossover differences for Jason-2 and Jason-1 using Jason-2 (red), Jason-1 GDR-E (blue), Jason-2 GDR-D Upd with GOT4.10 + POE-E + Tran2012 SSB (pink). Bottom: Monitoring of mean of SSH crossover differences for different data types of Jason-2: IGDR with DUACS updates (green), GDR (red): over 2017 (left) and over 5 years (right).

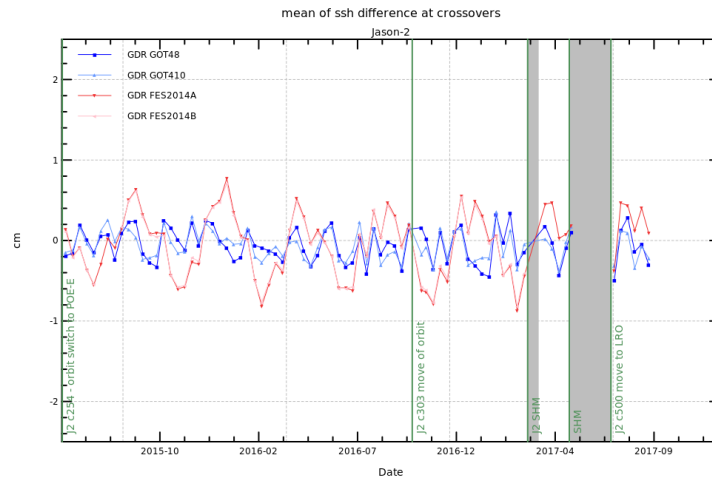


Figure 35 – Mean of SSH crossovers differences for Jason-2 against ocean tide solution used to compute SSH.

The map of mean SSH crossover differences plotted figure 36 was calculated using Jason-2 GDR products, no strong geographically correlated patterns are detected. Nevertheless, there is a slight geographically correlated pattern on the map with GDR-D orbit solution (POE-D until cycle 253 and POE-E from cycle 254 onwards). This pattern disappears using only the final POE-E solution (see details about POE-E in [9], [8] and [15]). This pattern might be related to the 120 day signal, as it disappears in the same time as the 120 day signal is reduced in the periodogram of the final POE-E solution (not shown here).

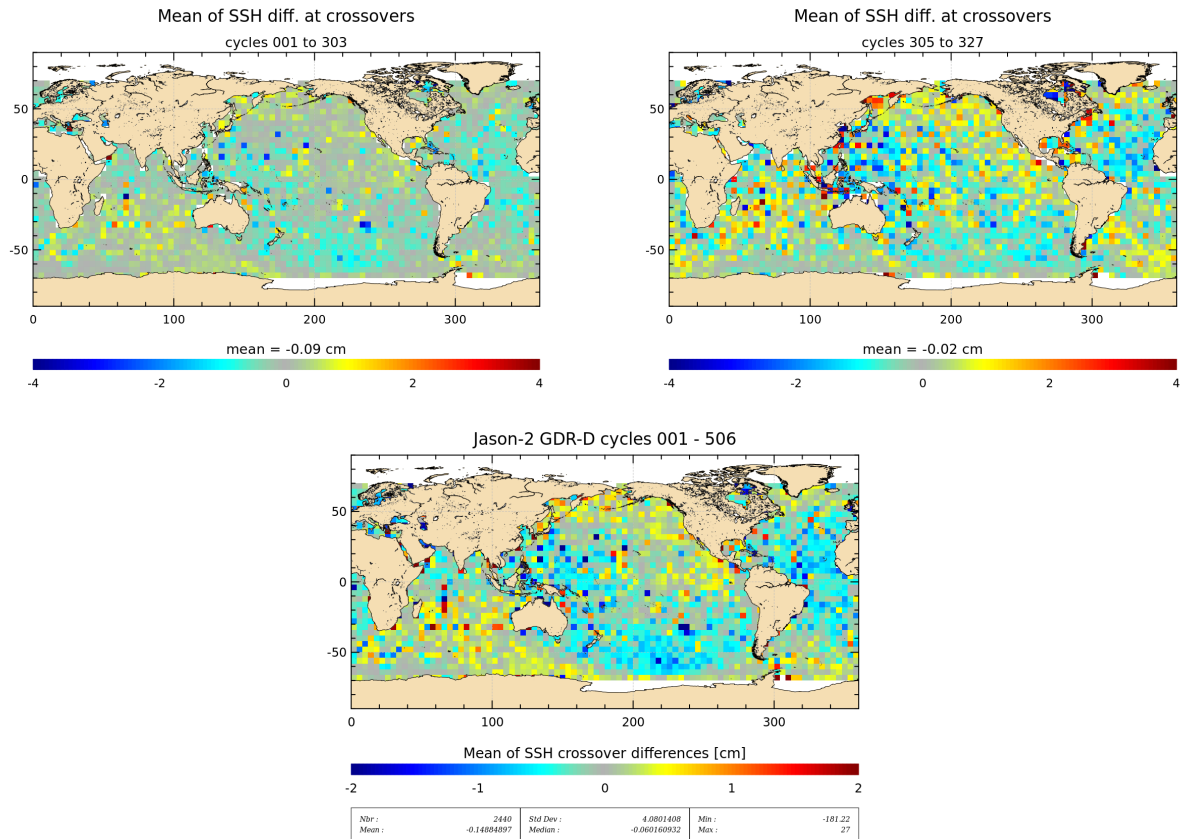


Figure 36 – Bottom: Map of mean of SSH crossovers differences for Jason-2 cycle 1 to 506. note that for cycles 1 to 253, GDR orbit is POE-D. GDR have been available with orbit POE-E since cycle 254. Left: Map of mean of SSH crossovers differences for Jason-2 cycle 1 to 303. Right: Map of mean of SSH crossovers differences for Jason-2 cycle 305 to 327 (less than a year)

### 5.3. Standard deviation of SSH crossover differences

The cycle by cycle standard deviation of SSH crossovers differences are plotted for Jason-2 and Jason-1 in figure 37 after applying geographical criteria (bathymetry, latitude, oceanic variability) as defined previously (chapter 5.1.). Both missions show very good performances, very similar and stable in time. No anomaly is detected. The average figure is 5.0 cm rms for Jason-1, and 4.9 cm rms for Jason-2 data. Keeping in mind that during the Jason-1/TOPEX tandem phase in 2002, the same statistic using Jason-1 GDR-A products was close to 6.15 cm (see [48]). This illustrates the improvements performed in the altimetry ground processing since the Jason-1 launch especially thanks to new retracking algorithms, new geophysical corrections (oceanic tidal, dynamic atmospheric correction, ...) and new orbit calculations. Jason-2 show very good performances.

When comparing the performances of the different Jason-2 data types (IGDR, GDR) over 2017 (right of figure 37), IGDR data have a standard deviation of 4.9 cm over the year (very close to 4.8 cm with GDR) and GDR show the same performance on LRO as on previous orbit.

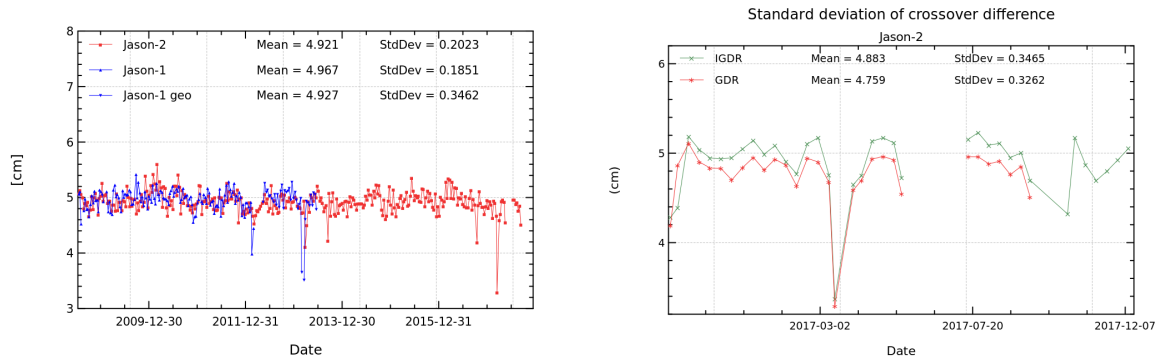


Figure 37 – Cycle by cycle standard deviation of SSH crossover differences for Jason-2 and Jason-1 (left) and Jason-2 GDR versus IGDR (right). Only data with  $abs(latitude) < 50^\circ$ , bathymetry  $< -1000m$  and low oceanic variability were selected.

#### 5.4. Estimation of pseudo time-tag bias

The pseudo time tag bias ( $\alpha$ ) is found by computing at SSH crossovers a regression between SSH and orbital altitude rate ( $\dot{H}$ ), also called satellite radial velocity:  $SSH = \alpha \dot{H}$

This empirical method allows us to estimate the potential real time tag bias but it can also absorb other errors correlated with  $\dot{H}$ . Therefore it is called “pseudo” time tag bias. The monitoring of this coefficient estimated at each cycle is performed for Jason-1 and Jason-2 in figure 38. Both curves are very similar highlighting a 59-day signal with almost no bias (close to -0.01 ms for Jason-1 and -0.02 ms for Jason-2).

Before the Jason-2 reprocessing the GDR-T showed a bias of -0.29 ms. The origin of constant part of the pseudo time tag bias was found by CNES [32] and so corrected in the Jason-2 GDR-D and Jason-1 GDR-E product (see also the Jason-2 [1] and Jason-1 [24] handbooks). The 59 day-signal is reduced for Jason-1 pseudo-datation bias thanks to the use of GOT4.10 ocean tide solution (see [4] and [9]).

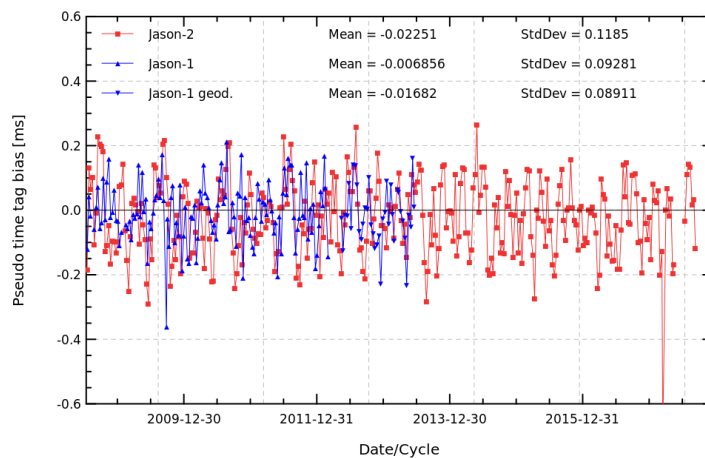


Figure 38 – Monitoring of pseudo time-tag bias estimated cycle by cycle from GDR products for Jason-2 and Jason-1

## 6. Sea Level Anomalies (SLA) Along-track analysis

### 6.1. Overview

The Sea Level Anomalies (SLA) are computed along track from the SSH minus the mean sea surface with the SSH calculated as defined in previous section 5.1. :  $SLA = SSH - MSS$

Note that for better comparison with Jason-1, Jason-2 GDR-D are updated using Jason-1 GDR-E standards (POE-E orbit, Got4.10 ocean tide, MSS\_CNES\_CLS\_2011 (with reference period of 20 years), Tran2012 sea state bias, and recomputed ionosphere correction (using Tran2012 ssb) ).

SLA analysis is an additional indicator to estimate the altimetry system performances. It allows us to study the evolution of SLA mean (detection of jump, abnormal trend or geographical correlated biases), and also the evolution of the SLA variance highlighting the long-term stability of the altimetry system performances. In order to take advantage of the Jason-2/Jason-1 tandem phase (cycles 1 to 20), we performed direct SLA comparisons between both missions during this period. Corrections applied in SSH calculation are theoretically the same for Jason-1 and Jason-2 since both satellites measure the same ocean. Thus, it is possible to not apply them in order to obtain directly information on the altimeter range and the orbit calculation differences. However, as the stability of both ground passes is not exact (the ground track is maintained within a window of  $\pm 1$  km across-track distance from the theoretical ground track), SLA measurements have to be projected and interpolated over the Jason/TOPEX theoretical ground pass after applying the MSS in order to take into account cross-track effects on SSH.

$$\Delta SLA_{J1-J2} = [(Range_{Ku} - Orbite - MSS)_{J1}]_{\bar{T}} - [(Range_{Ku} - Orbite - MSS)_{J2}]_{\bar{T}}$$

This allows us also to select the intersection of both datasets and compare exactly the same data. After Jason-1 ground track change to its interleaved ground track, direct SLA comparisons are no more possible. Thus, global statistics computed cycle by cycle are just basically compared.

### 6.2. Mean of SLA differences between Jason-2 and Jason-1

The cycle by cycle monitoring of mean SLA differences between Jason-1 data and Jason-2 is plotted in figure 39 over all their common period. During the tandem phase, the SSH bias is computed with and without the SSH corrections. During this period, both types of curves are very similar and stable in time with variations close to 1 mm rms, except that they are spaced out by a bias. The global average SSH bias is close to 0.9 cm without corrections, which represents the difference between the two systems. This difference is -0.2 cm using SSH corrections and -0.3 cm when using ECMWF instead of radiometer wet troposphere correction. However, the more crucial point for scientific applications is to insure that there is no drift between both missions, since the global bias can be corrected a fortiori. When Jason-1 was moved to a geodetic ground track, a small jump is visible on Jason-1 minus Jason-2 difference. In addition, a small drift remains after Jason-1 safe hold mode in March 2013 (Jason-2 cycles 171 to 173, black dots at the end of the curve): it seems to be related to radiometer wet troposphere solution as it is not visible using model wet troposphere correction (green dots) (see [4] for more details).

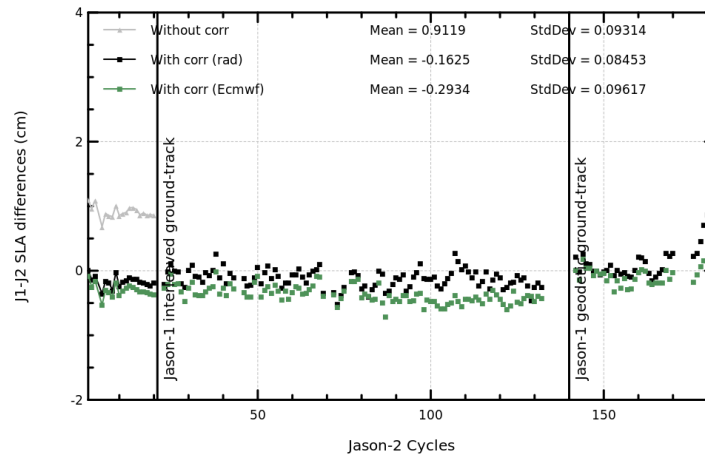


Figure 39 – Cycle by cycle monitoring of SSH bias between Jason-1 and Jason-2 before and after Jason-1 ground-track change (black curve and dots) and SSH bias without applying corrections in SSH calculation for both missions only during the tandem phase (gray curve).

Figure 40 shows the mean differences between Jason-1 and Jason-2 during tandem phase (cycles 1 to 20).

Thanks to the update of sea state bias with the OSTST 2012 solution for both satellites Jason-1 and Jason-2 SLA are quite homogeneous. In order to obtain directly information on the altimeter range and the orbit calculation differences, spatial uncorrected SLA (orbit - range - MSS) differences (only during the Jason-1/Jason-2 tandem phase) between both missions is plotted in right side of figure 40. It shows a weak hemispheric bias lower than 1 cm. These differences are in relationship with orbit calculation differences. Though for both satellites POE-E was used, there are some differences between Jason-1 POE-E and Jason-2 POE-E, for Jason-1 orbit computation the GPS data are no longer available, whereas they are used for the Jason-2 POE computation. Jason-2 POE is therefore based on two orbit determination techniques (Doris and GPS, Laser is used for validation), whereas Jason-1 POE (over the Jason-2 period) is based on two orbit determination techniques (Doris and Laser). When using GSFC std 0905 orbits for both satellites (bottom of figure 40) the hemispheric bias disappears (the same result has been found using GSFC std 1204 orbit solution, but it is not shown here).

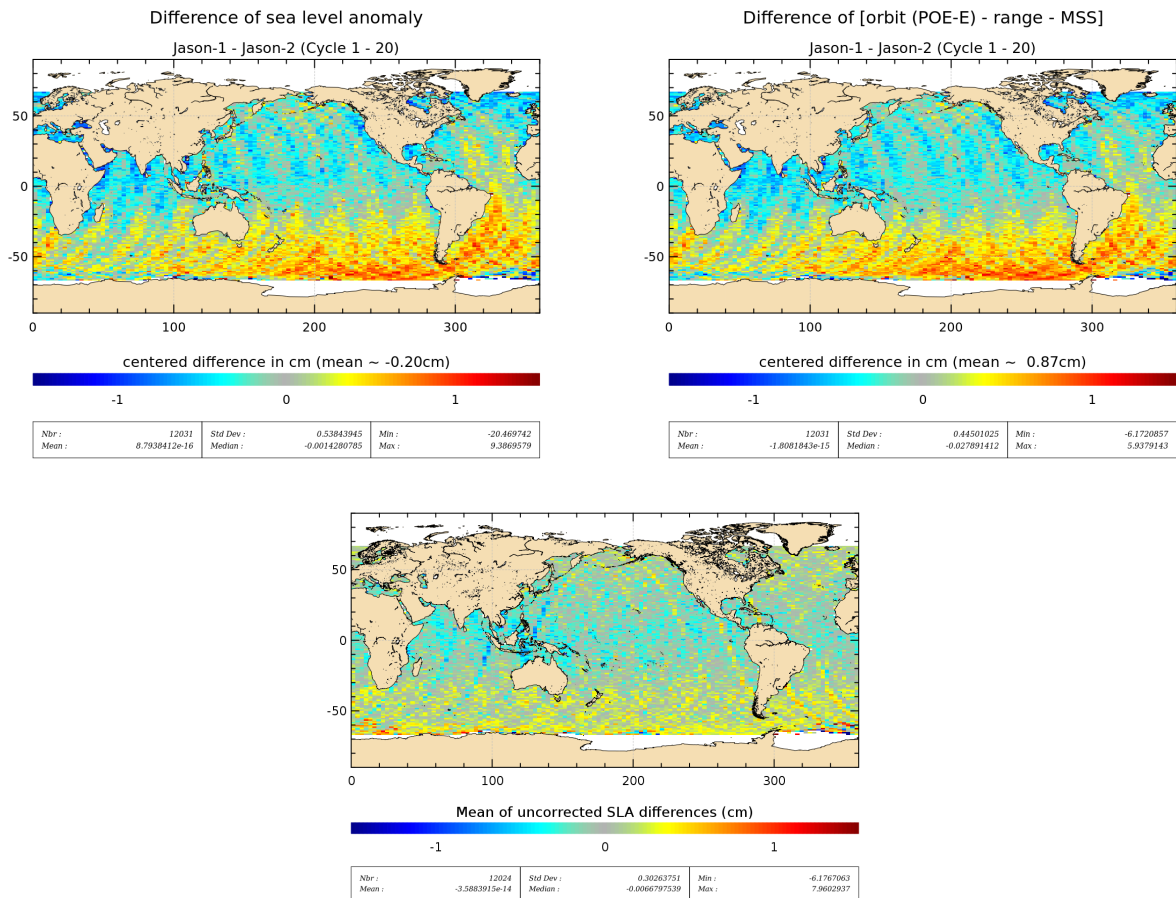


Figure 40 – **Top left:** Maps of SLA (orbit (POE-E) - range - geophysical corrections - MSS 2011 (ref20)) mean differences between Jason-1 and Jason-2 during tandem phase (cycles 1 to 20), using Jason-2 updated GDR-D and Jason-1 GDR-E (the map is centered around the mean of 0.2 cm). **Top right:** without applying geophysical corrections. **Bottom:** using GSFC09 orbits without applying geophysical corrections

### 6.3. Standard deviation of SLA differences between Jason-2 and Jason-1

The monitoring of SLA standard deviation has been computed for both missions (plotted in figure 41). To improve the Sea Surface Height Anomaly (SSHA) data quality in the Jason-2 LRO data products an updated Mean Sea Surface (MSS) model has been adopted. The new MSS model is the latest CNES/CLS MSS 2015 solution [103], which is referenced to the 20-year period spanning 1993-2012 (see 2.3.). The MSS model provided until cycle 327 was the 2011 solution, referenced to the 7-year period spanning 1993-1999 and has a lower quality on LRO ground track: the choice of MSS solution impacts the error that is seen between 50 km and 600 km out of historical ground track (see dedicated to MSS part in [4]). The change of reference period from 7 years to 20 years integrates the evolution of the sea level in terms of trends, but also in terms of interannual signals at small and large scales (e.g. Niño/Niña) in the additional 13 years: changing from a 7 to 20 years reference period leads to better interannual signals and oceanic anomalies (see [83] for more details about the change on reference period). As concerned Jason-1, the blue curve is drawn using the standards that are in the GDR-E products (contain the MSS CNES/CLS 2011 referenced over

20years), whereas GDR-D standards are used to Jason-2 (red curve has been computed using the MSS CNES/CLS 2011 referenced over 7years and purple curve and green curve have been computed using respectively the MSS CNES/CLS 2011 and MSS CNES/CLS 2015 both referenced over 20years).

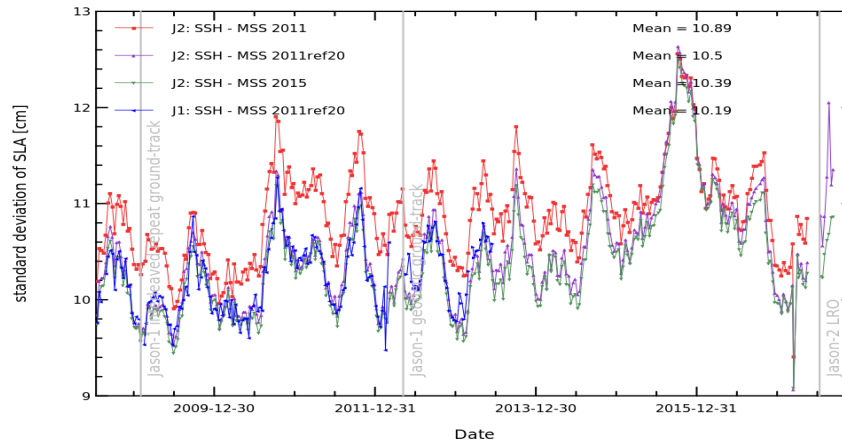
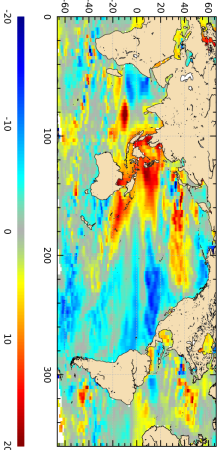
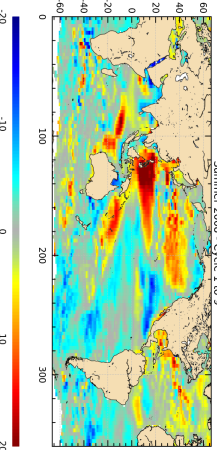
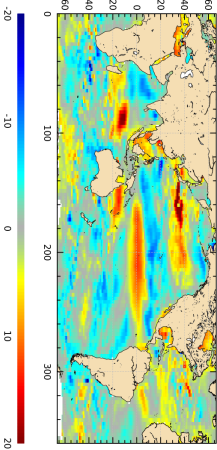
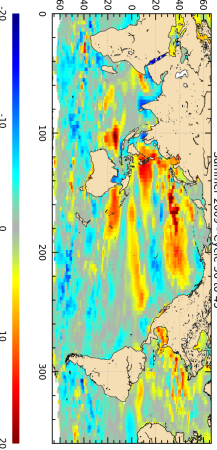
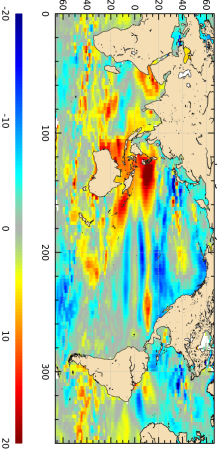
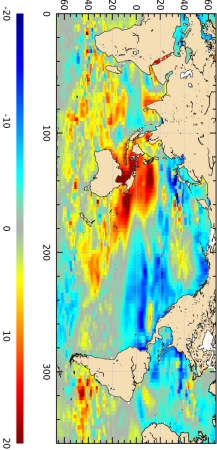
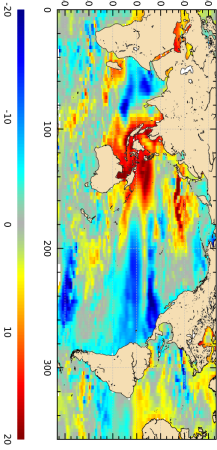
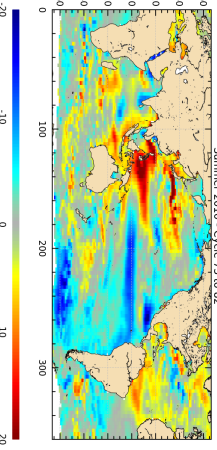
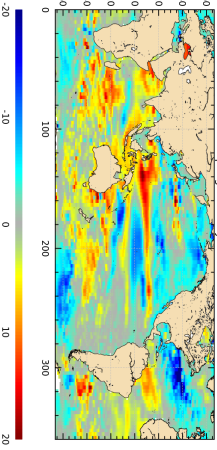
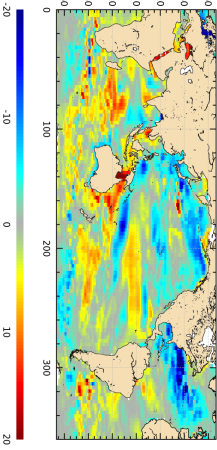
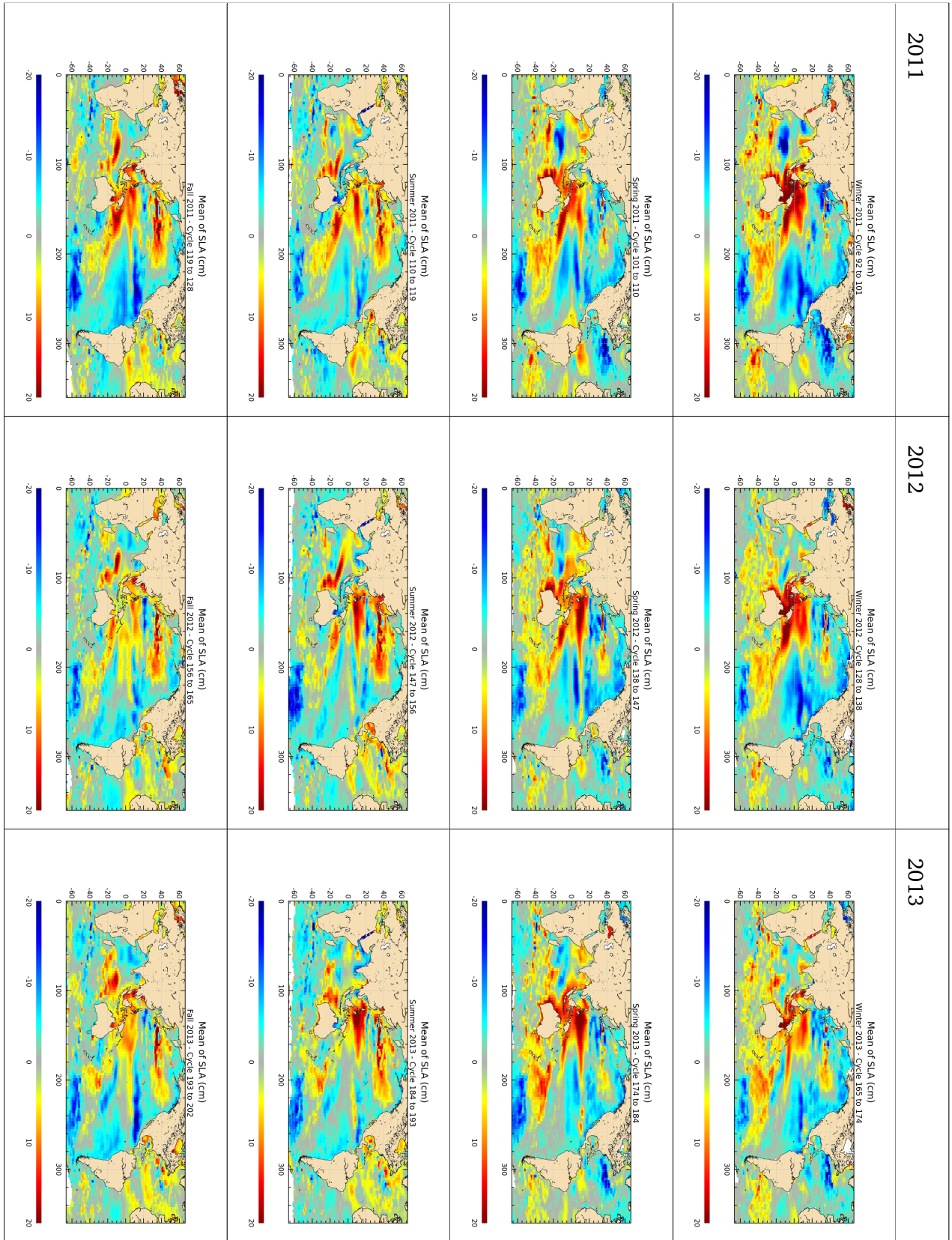


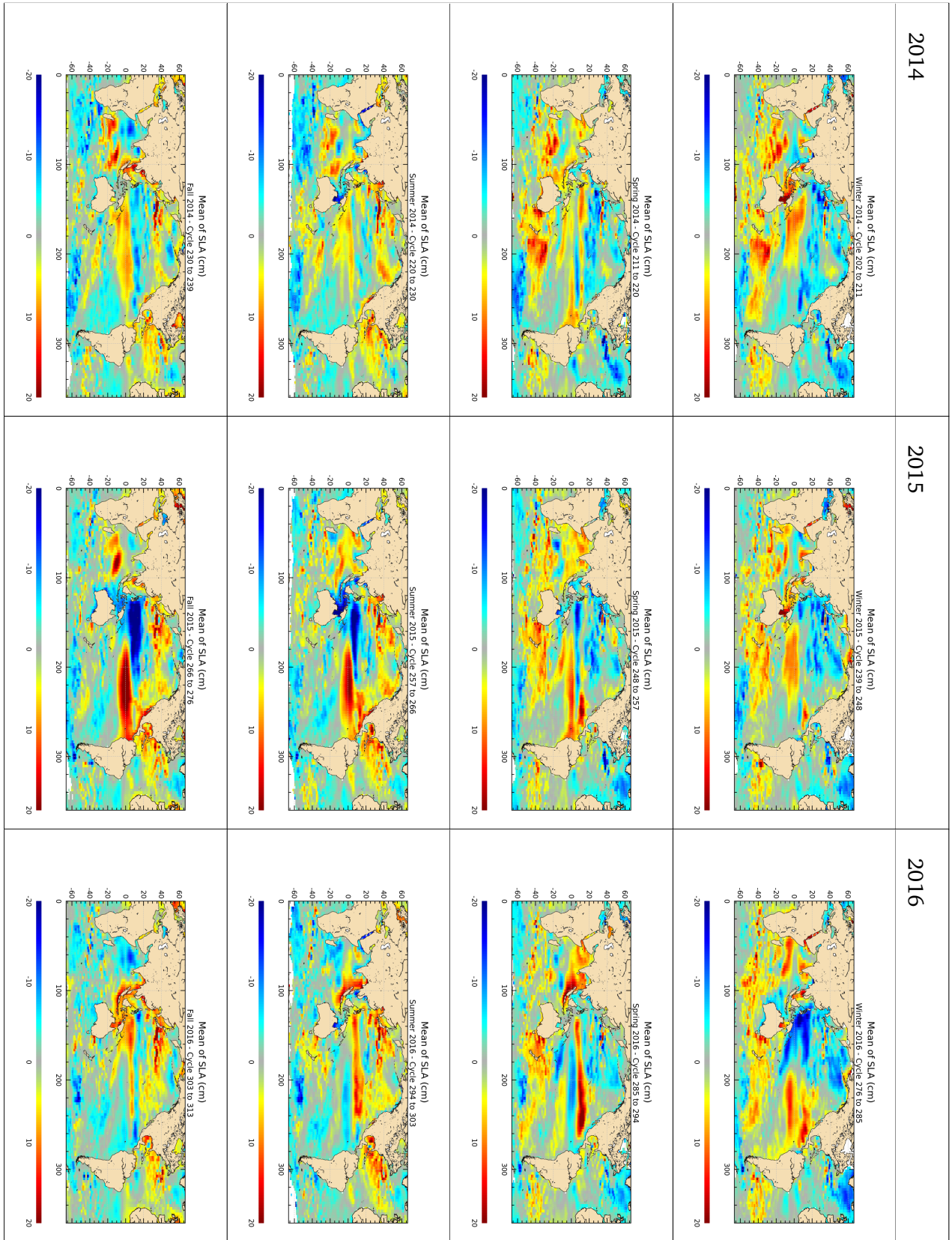
Figure 41 – Cycle by cycle monitoring of SLA standard deviation for Jason-1 and Jason-2 (using different MSS solutions)

#### 6.4. Sea level seasonal variations

From Sea Level Anomalies computed relative to the Mean Sea Surface CNES-CLS 2011, the surface topography seasonal variations have been mapped in table 6 for the overall Jason-2 data set. Major oceanic signals are shown clearly by these maps: it allow us to assess the data quality for oceanographic applications. The most important changes are observed in the equatorial band with the development of El Niño. From mid 2009 to spring 2010 a moderate El Niño event occurred (see [96]). In second half of 2010 a moderate to strong La Niña event developed (see [97]) until spring 2011. During 2015, conditions indicate an El Niño event of strong intensity (see [8]).

Fall	Summer	Spring	Winter	
				2008
				2009
				2010





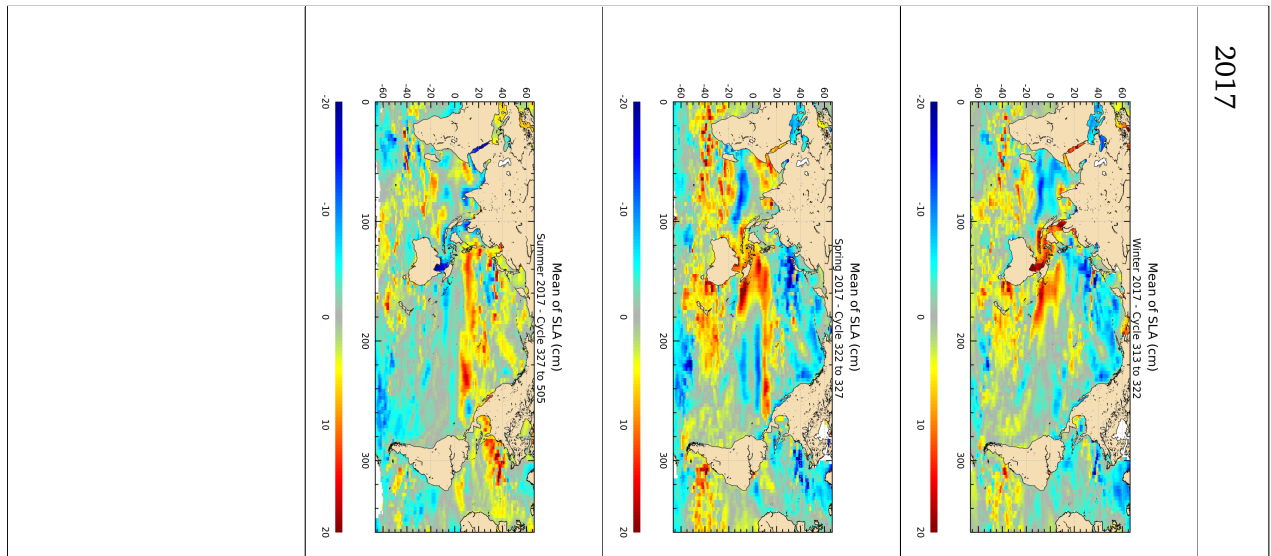


Table 6 – Seasonal variations of Jason SLA (cm) for years 2008 to 2017

## 7. Mean Sea Level (MSL) calculation

A dedicated report on Mean Sea Level activities is available [65].

### 7.1. Overview

---

The global mean level of the oceans is one of the most important indicators of climate change. Precise monitoring of changes in the mean level of the oceans, particularly through the use of altimetry satellites, is vitally important, for understanding not just the climate but also the socioeconomic consequences of any rise in sea level. Thanks to the T/P, Jason-1, Jason-2 and now Jason-3 altimetry missions, the global MSL has been calculated on a continual basis since January 1993 highlighting a trend of 3.3 mm/yr (see <sup>2</sup>).

Jason-2 contributes to the reference GMSL indicator between October 2008 and June 2016. Over this period, its stability is excellent, and no anomalies has been detected. Note that since it has been replaced by Jason-3 data, Jason-2 is no more used to compute the reference serie on historical TOPEX-Poseidon ground track.

The method to compute GMSL time serie and the altimeter standards used are described on [65] and on Aviso website <sup>3</sup>.

### 7.2. Altimeter Mean Sea Level evolution (MSL)

---

#### 7.2.1. Calculation of reference time serie

Regarding the global MSL trend estimated over the Jason-2 period (2008-2015), the trend is 4.42 mm/yr, with an uncertainty of 0.5 mm/yr (within a confidence interval of 90%). Notice, that MSL decreased in 2010/2011 (similar, but much stronger to what was already observed in 2007). According to Boening et al. ([30] and [31]) the global mean sea level drop of 5 mm between beginning 2010 and mid-2011 is due to a decline of ocean mass coinciding with an equivalent increase in terrestrial water storage (primary over Australia, northern South America and Southeast Asia). The authors write, that this temporally shift of water from ocean to land is closely related to the transition from El Niño conditions in 2009/2010 to a strong 2010/2011 La Niña which affected precipitation patterns world wide. As these terrestrial water mass are not all directly linked to the ocean (thanks to rivers for example), they can only return to ocean thanks to evaporation. This process is long, which could explain the rise in GMSL in 2012.

---

<sup>2</sup><http://www.aviso.oceanobs.com/msl>

<sup>3</sup><http://www.aviso.oceanobs.com/en/news/ocean-indicators/mean-sea-level/processing-corrections.html>

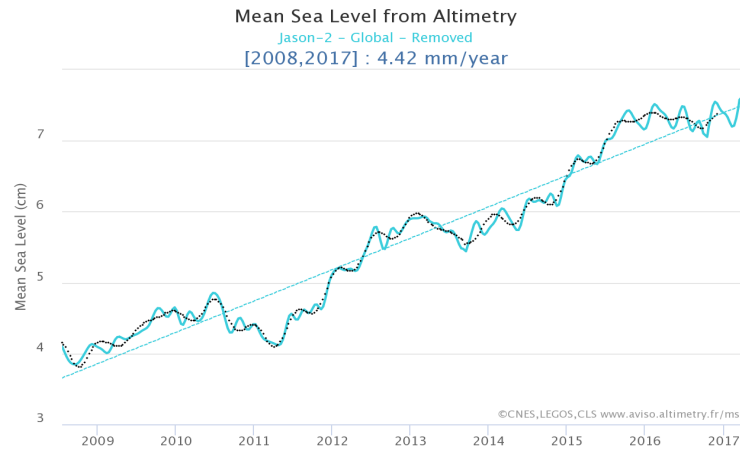


Figure 42 – MSL evolution calculated from Jason-2 data. GIA (-0.3 mm/yr [77]) is applied.

**7.2.2. External data comparisons with tide gauges**

In order to assess the global MSL trend, comparisons to independent in-situ datasets are of great interest. The method below has been developed in the frame of in-situ Calval studies and thoroughly described in annual report [65]. Figure 43 displays the time series of global average differences between the Jason-2 serie used for the GMSL calculation and tide gauges. Uncertainties on the GMSL trend estimates are also reported in the figure. They are explained in detail in [65]. Drifts are presented for GLOSS/CLIVAR network, a small and non-significant negative drift of -0.3 mm/yr is observed on the main Jason-2 period (this means before the orbit change).

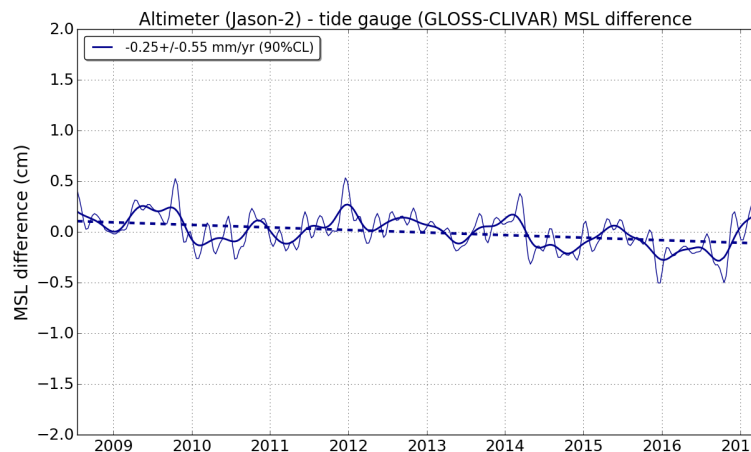


Figure 43 – Jason-2 / tide gauge (GLOSS/CLIVAR network) comparisons. Periodic signals are removed and resulting time series are 2-month (thin line) and 6-month (thick line) low-pass filtered. Dotted line represent a linear regression fit of the time series; slope values are indicated in the legend

**This comparison confirms the excellent stability of the Jason-2 mission with respect to tide gauges.**

### 7.3. Regional mean sea level trend for Jason-2

---

The regional MSL trends over the Jason-2 period (figure 44) show an increase in eastern tropical pacific and a decrease in western tropical pacific. This is probably influenced by the El Niño conditions which occurred in 2015 ([98],[8]). The regional trend uncertainty due to altimetry errors is of the order of 2 to 3 mm/yr depending on the regions (Prandi et al., 2016 in [65]/Annexe)

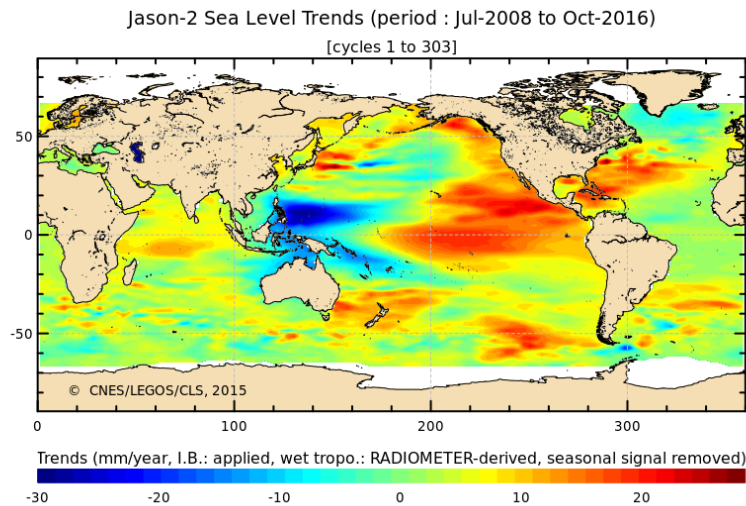


Figure 44 – Maps of regional MSL slopes for Jason-2 cycles 1 to 303, seasonal signal removed.

## 8. Investigations

### 8.1. Safe Hold Modes during 2017

Jason-2 was in SHM from 15 to 30 March 2017 (cycles 321 and 322), from 17/05/2017 (cycle 327) to 11/07/2017 (cycle 500), and from 14/09/2017 (cycle 506) to 13/10/2017 (cycle 509). In each case specific studies are done just after SHM in order to check there is no important degradation on the system performances due to this event.

These several SHM occurred due to gyrometers anomalies. Thanks to many investigations, it is now understood that the gyro temperature was involved in each case. Operational teams are able to evaluate when gyrometers temperature would reach a critical value. The last risk was on 04th December 2017, but Jason-2 did not enter SHM.

### 8.2. Details on new Long Repeat Orbit sub-cycles

The Jason-2 Long Repeat Orbit is partly described in 2.2.

The Jason-2 LRO (Long Repeat Orbit) orbit is approximately 27 km below the historical T/P orbit still used by Jason-3. It has the following sub-cycles (near repeat) and cycle (exact repeat) on table 7. The first two sub-cycles are beneficial for sea-state and mesoscale operational applications respectively: they guarantee a nearly geographically homogeneous sampling for the temporal scales of interest (e.g. for operational model assimilation). The papers [100] and [101] explain how this sub-cycle sequence progressively composes finer-resolution grids through an apparent shift of lower resolution grids.

type	nodal days	days	revolutions	number of pass	size
sub cycle	4	3.97	51	102	
sub cycle	17	16.86	217	434	185km
sub cycle	81	80.31	1034	2068	40km
sub cycle	145	143.77	1851	3702	22km
cycle	371	367.84	4736	9472	8km

Table 7 – Cycle and sub-cycles for the Jason-2 LRO

Sub cycles beginning and end dates for year 2017 are detailed in table 8. Note that due to SHM, 17-days subcycle 005 is entirely missing.

sub cycle type	sub cycle number	begin	end
17 days	1	11-07-2017 10:32:39.505000	28-07-2017 07:02:57.91999
	2	28-07-2017 07:02:57.92000	14-08-2017 03:33:14.517999
	3	14-08-2017 03:33:14.518000	31-08-2017 00:03:31.596999
	4	31-08-2017 00:03:31.597000	16-09-2017 20:33:48.41999
	5	16-09-2017 20:33:48.42000	03-10-2017 17:04:03.770999
	6	03-10-2017 17:04:03.771000	20-10-2017 13:34:20.720999
	7	20-10-2017 13:34:20.721000	06-11-2017 10:04:40.556999
	8	06-11-2017 10:04:40.557000	23-11-2017 06:34:58.413999
	9	23-11-2017 06:34:58.414000	10-12-2017 03:05:16.118999
	10	10-12-2017 03:05:16.119000	26-12-2017 23:35:33.707999
	11	26-12-2017 23:35:33.708000	12-01-2018 20:05:50.896999
80 days	1	11-07-2017 10:32:39.505000	29-09-2017 17:59:59.566999
	2	29-09-2017 17:59:59.567000	19-12-2017 01:27:24.334999
145 days	1	11-07-2017 10:32:39.505000	03-12-2017 10:46:37.574999

Table 8 – 17 days, 80 days and 145 days sub-cycles dates for the Jason-2 LRO

Global sub-cycles coverage is shown from figure 46 to figure 49. On the following maps, IGDR until 2017/12/03 are used. Theoretical points are deduced from MOE orbit files, with an exception: using this method do not allow to draw a theoretical ground track during SHM (MOE orbit files are not produced). In order to visualize missing points due to safe hold mode (14/09/2017 to 13/10/2017), predicted MOE is used. Red points indicate theoretical points location deduced from MOE orbit files, real measurements from July to September (before SHM) are in dark blue and real point from October onwards (after SHM) are in cyan.

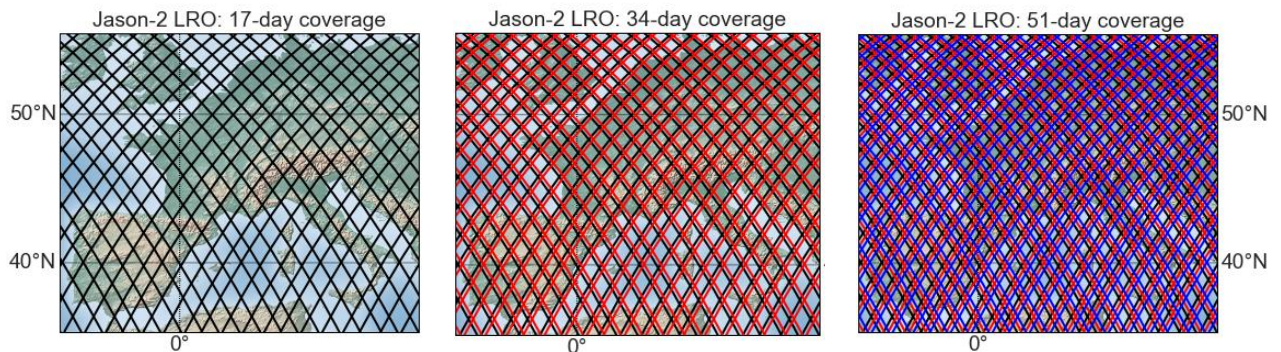


Figure 45 – Jason-2 LRO sampling for 3 subsequent periods of 17 days in black, red and blue (from public release)

Figure 46 shows 17 days subcycles 001 (top) to 004 (bottom) coverage, and figure 47 shows 17 days subcycles 006 (top) to 008 (bottom) coverage. Due to 2017-09-14 SHM, 17-days sub-cycle 005 is entirely missing, and 17-days sub-cycle 004 (figure 46) and 006 (figure 47) are partly missing.

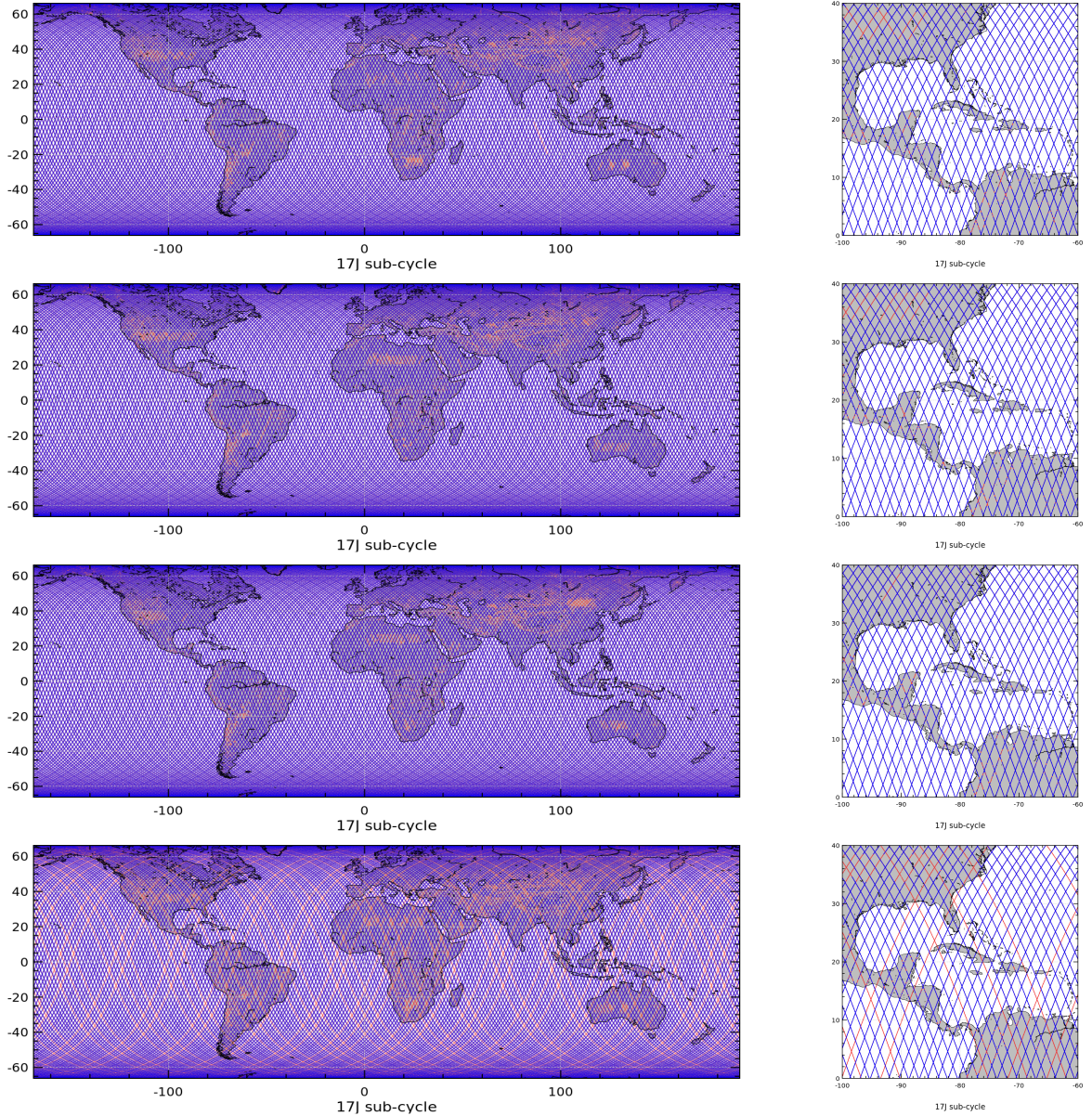


Figure 46

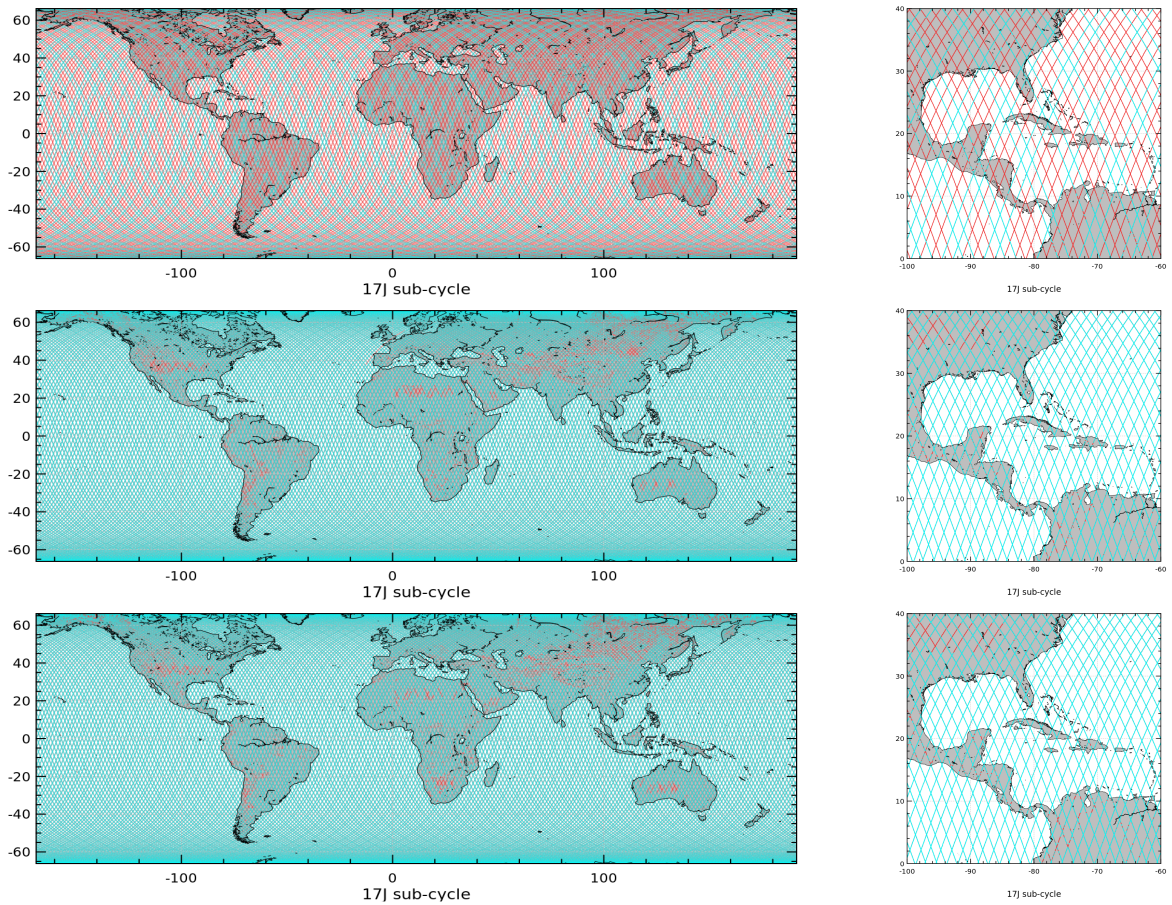


Figure 47 – 17-days subcycle 006 (top) to 008 (bottom) - after SHM (2017-09-14 to 2017-10-13), red: missing theoretical points, cyan: available measurements

Figure 48 shows 80 days subcycles 001 (top) and 002 (bottom) coverage. Except during SHM that occurred over the end of the first 80-days sub cycle and the beginning of the second 80-days subcycle, data coverage is very good.

Figure 49 shows 145-days subcycles 001 coverage (red: missing theoretical points, blue: available measurements before SHM (2017-09-14 to 2017-10-13), cyan available measurements after SHM (2017-09-14 to 2017-10-13)).

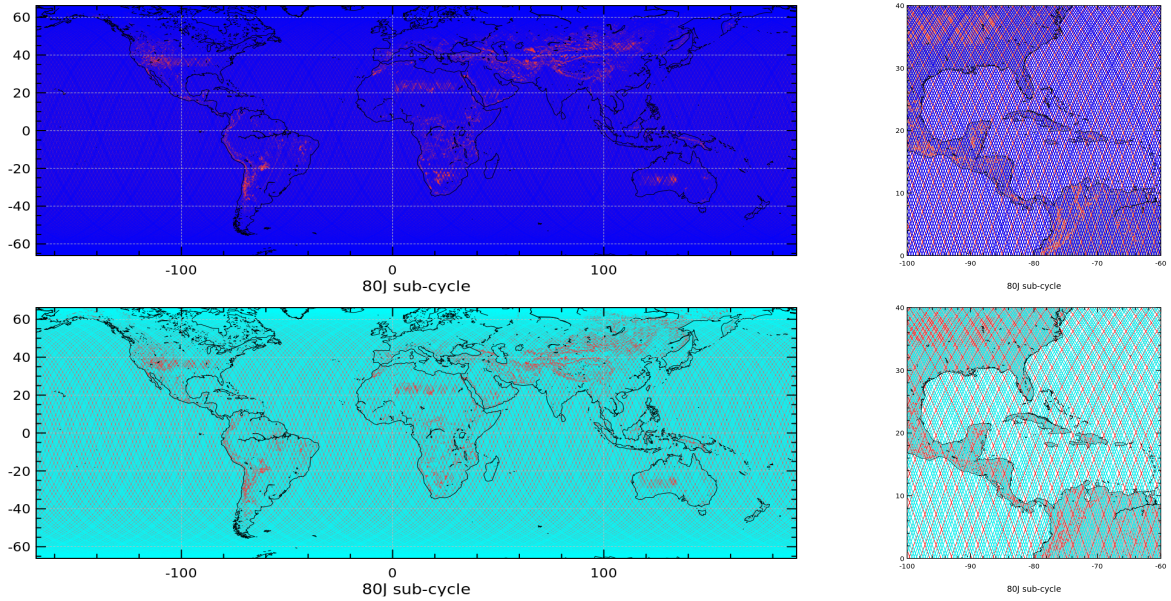


Figure 48 – 80-days subcycle 001 and 002, red: missing theoretical points, blue: available measurements before SHM (2017-09-14 to 2017-10-13), cyan available measurements after SHM (2017-09-14 to 2017-10-13)

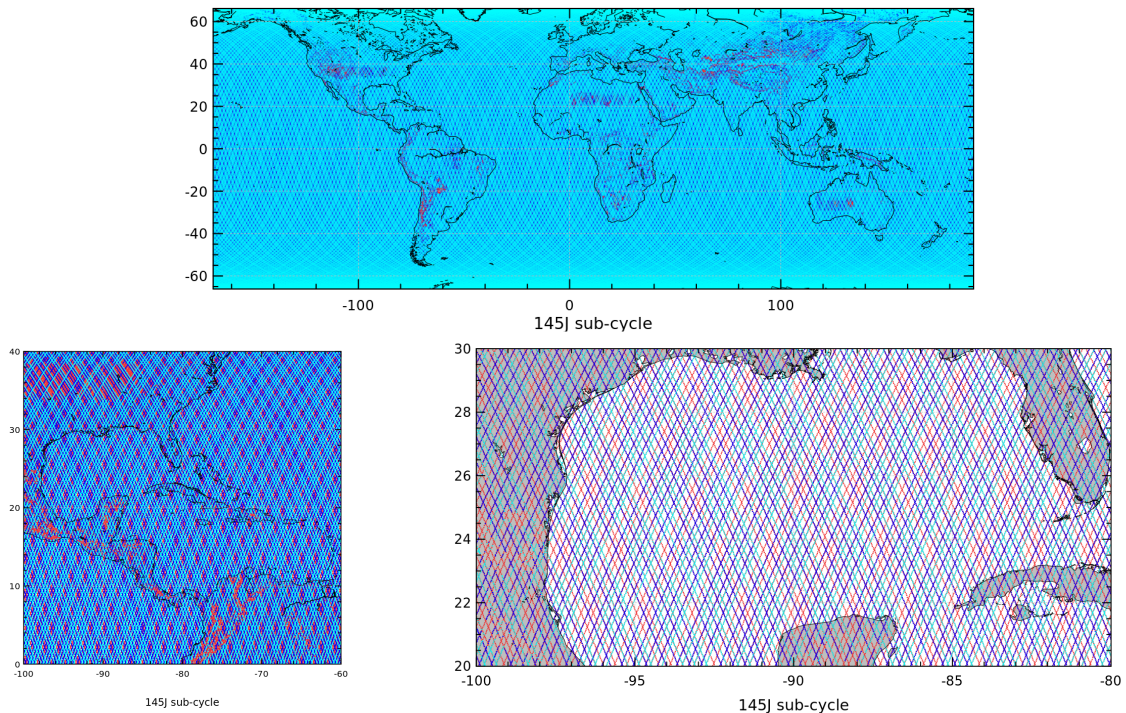


Figure 49 – 145-days subcycle 001, red: missing theoretical points, blue: available measurements before SHM (2017-09-14 to 2017-10-13), cyan available measurements after SHM (2017-09-14 to 2017-10-13)

## 9. Conclusion

Jason-2 is in orbit since 20th of June, 2008. **The more of 9 years of Jason-2 data show excellent quality during Jason-2 flight on historical ground track, on interleaved ground track, and even after move to drifting orbit:**

Scientific studies and operational applications therefore benefit from the combination of altimeter data from several missions. The 2012 reprocessing of the whole mission in GDR-D standard has improved the dataset in comparison to the GDR-T standard for meso-scales, as well as on longer time scales (consistency between ascending and descending passes is improved).

The main points of this performance assessment are summarized below:

- Jason-2 provides an excellent coverage of the ocean, with more than 99% of measurements available over ocean.
- Data quality is excellent, with only 3.3% of edited measurements (after remove of land and ice flagged points).
- SLA statistics show no long term drifts,
- Standard deviation of daily SLA average differences is about 10.4 to 10.9 cm against MSS solution that is used,
- At crossovers Jason-2 shows a standard deviation of 4.9 cm.

All these metrics confirm the excellent data quality of the Jason-2 mission.

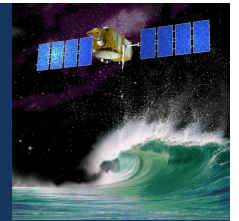
## **10. Appendix: Global Jason-2 Data Quality Assessment on the new Long Repeat Orbit**

# Global Jason-2 Data Quality Assessment on the new Long Repeat Orbit

H. Roinard<sup>1</sup>, E. Cadier<sup>1</sup>, M. Ablain<sup>1</sup>, N. Picot<sup>2</sup>

Contact: [equipe-calval-jason@cls.fr](mailto:equipe-calval-jason@cls.fr)

1. CLS, Toulouse, France
2. CNES, Toulouse, France

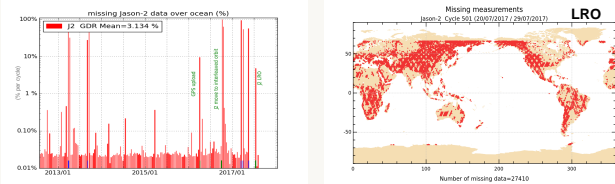


After almost 9 years in orbit as a precise altimeter mission on two different repeat ground tracks, Jason-2 had early this year an interruption of its science mission from 17th May to early July 2017. In the following, it was moved to a long-repeat ground track. Though this orbit is less interesting for the tandem mission with Jason-3 to observe mesoscale ocean signals, the mission can still provide valuable and useful data for several applications. Therefore, the objective of this study is to provide an overview of the global data quality of Jason-2 data on the new orbit. Firstly, the stability of the altimeter and radiometer parameters is carefully monitored and the system performances assessed. This consists in long-term monitoring of the parameters, as well as comparison to Jason-3 data, in order to assess the possible impact of the lower altitude (~27km) on the altimeter data. Furthermore the impact of the new orbit on the sea-level performances is accurately analysed.

## Main performance metrics

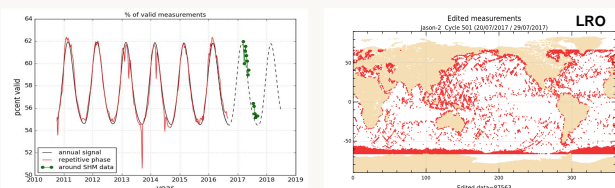
### Data availability

Data availability over ocean is good over the repetitive phase, and seems to continue in that way over Long repeat Orbit



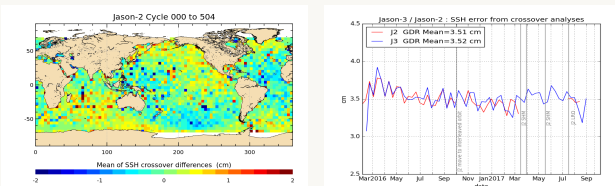
### Rejected data

The number of rejected data is in good agreement before and after move to LRO.



### Crossovers

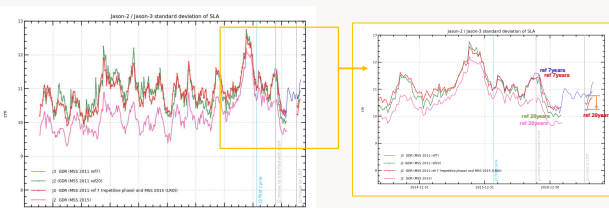
- Sea Level performances: SSH error for Jason-2 is deduced from crossovers analyses using radiometer data (selecting |latitudes| < 50°, bathy < 1000m, oceanic variability < 20 cm) ⇒ SSH error is close to **3.5 cm** for temporal scales < 10 days
  - Mean difference between ascending and descending tracks is near zero (-0.1 cm for GDR, stable since move to LRO),
  - Spatial distribution of mean SSH differences shows geographically correlated patches with differences remaining below 2 cm,
- ⇒ Crossovers analysis demonstrates the good performance of Jason-2



Performance at crossovers: left: map of mean SSH differences (cycle 000 to 504), right: SSH error deduced from SSH crossovers (using radiometer data, with selection on |latitudes| < 50°, bathy < 1000m, oceanic variability < 20 cm)

**CAUTION:** due to an error in ground segment processing, it is advised not to use IGDR data for cycles 505 and 506

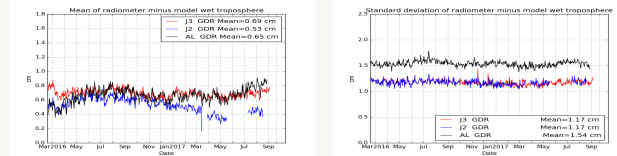
### Standard deviation of mean sea level :



In order to insure a better performance on LRO, Jason-2 products contain the CNES/CLS2015 solution for mean sea level (already delivered in L2P products): this solution improves this performance metric as 20 years of data are used instead of 7years. (see → on figure)

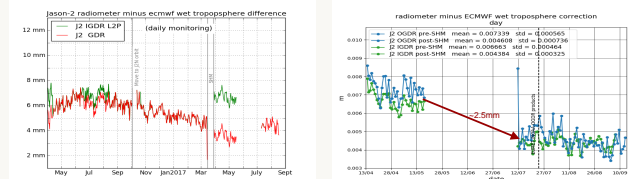
## Radiometer behavior

Compared to other missions, Jason-2 radiometer wet troposphere correction minus ECMWF model difference is drifting over the first quarter of year 2017



Radiometer minus model wet tropospheric correction compared to other missions

Each SHM (in March and in September) introduces a jump of radiometer minus model wet troposphere correction

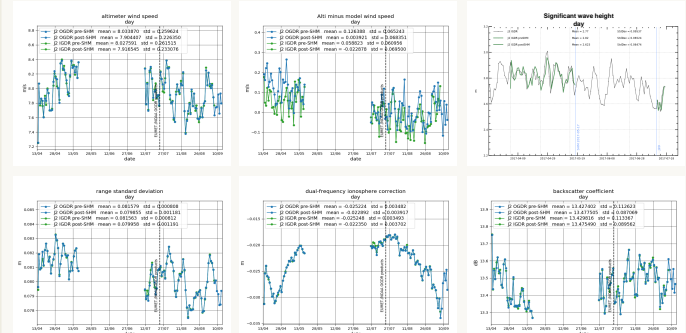


## SHM (17/05 > 11/07) : impact on altimeter parameters



mispointing was slightly increased just after SHM, but only on the first passes: it has been nominal since new instrumental parameters LTM have been applied.

Other parameters behave as expected, taking account the seasonal variations :



The SLA evolution for Jason-2 L2P IGDR (dark green) is in accordance with Jason-3 (blue). GDR data (red) shows a jump at cycle 500, this difference is expected and is due to the use of the new mean sea surface on LRO (from GDR cycle 500 onwards); it is also visible on non updated Jason-2 IGDRs (not shown here).



Note that there is a global bias of -2.4cm from MSS CNES/CLS 2011 [ref7years] to MSS CNES/CLS 2015 [ref20years]

## Conclusions :

- ✓ The Jason-2 mission provides performance of excellent quality on the historical TOPEX/Poseidon and Jason-1 ground track
- ✓ When available, data quality on Long Repeat Orbit is as good as the one observed on the historical ground track (except for IGDR cycles 505 and 506 that are advised not to be used).
- ✓ The use of the last CNES/CLS2015 mss solution on LRO allows a better performance of the mission on its drifting orbit



OSTST Conference  
Oct 23<sup>st</sup> - Oct 27<sup>th</sup>, 2017



## 11. References

### References

- [1] Dumont, J.-P., V. Rosmorduc, N. Picot, S. Desai, H. Bonekamp, J. Figa, J. Lillibridge, R. Sharroo, 2017: OSTM/Jason-2 Products Handbook. CNES: SALP-MU-M-OP-15815-CN. EUMETSAT: EUM/OPS-JAS/MAN/08/0041. JPL: OSTM-29-1237. NOAA/NESDIS: Polar Series/OSTM J400. Available at [http://www.avisooceanobs.com/fileadmin/documents/data/tools/hdbk\\_j2.pdf](http://www.avisooceanobs.com/fileadmin/documents/data/tools/hdbk_j2.pdf)
- [2] Valladeau, G., S. Philipps. Jason-1 validation and cross calibration activities (Annual report 2010).SALP-RP-MA-EA-21903-CLS, CLS.DOS/NT/10-332.
- [3] Roinard H., Philipps S., Ablain M., Valladeau G., and Legeais J.-F., Jason-1 validation and cross calibration activities (Annual report 2013). Reference: CLS.DOS/NT/13-226. Nomenclature: SALP-RP-MA-EA-22269-CLS. Available at [http://www.avisooceanobs.com/fileadmin/documents/calval/validation\\_report/J1/annual\\_report\\_j1\\_2013.pdf](http://www.avisooceanobs.com/fileadmin/documents/calval/validation_report/J1/annual_report_j1_2013.pdf).
- [4] Roinard H., Philipps S.: Jason-1 GDR-E release. Global assessment over ocean. SALP-RP-MA-EA-22426-CLS. Available at [http://www.avisometry.fr/fileadmin/documents/calval/validation\\_report/J1/Jason1\\_ReprocessingReport\\_GDR\\_E.pdf](http://www.avisometry.fr/fileadmin/documents/calval/validation_report/J1/Jason1_ReprocessingReport_GDR_E.pdf)
- [5] Philipps, S., M. Ablain, G. Valladeau, and J.-F. Legeais. Jason-2 validation and cross calibration activities (Annual report 2012). Reference: CLS.DOS/NT/12-223. Nomenclature: SALP-RP-MA-EA-22141-CLS. Available at [http://www.avisooceanobs.com/fileadmin/documents/calval/validation\\_report/J2/annual\\_report\\_j2\\_2012.pdf](http://www.avisooceanobs.com/fileadmin/documents/calval/validation_report/J2/annual_report_j2_2012.pdf).
- [6] Roinard, H., Philipps S., Jason-2 reprocessing impact on ocean data (cycles 001 to 020). Comparison of Jason-2 Gdr-D with Gdr-T, as well as with Jason-1 Gdr-C. SALP-RP-MA-EA-22118-CLS. CLS.DOS/NT/12.138. Available at [ftp://avisoftp.cnes.fr/AVISO/pub/jason-2/documentation/gdr\\_d\\_calval\\_report/JA2\\_GDR\\_D\\_validation\\_report\\_cycles1to20\\_V1\\_1.pdf](ftp://avisoftp.cnes.fr/AVISO/pub/jason-2/documentation/gdr_d_calval_report/JA2_GDR_D_validation_report_cycles1to20_V1_1.pdf)
- [7] Roinard, H., S. Philipps. Jason-2 reprocessing impact on ocean data (cycles 001 to 145). Comparison of Jason-2 Gdr-D with Gdr-T, as well as with Jason-1 Gdr-C and Envisat Gdr v2.1. SALP-RP-MA-EA-22140-CLS. CLS.DOS/NT/12.222.
- [8] Philipps, S., H. Roinard, M. Ablain, G. Valladeau, and J.-F. Legeais. Jason-2 validation and cross calibration activities (Annual report 2015).
- [9] H. Roinard, M. Lievin. Jason-2 validation and cross calibration activities (Annual report 2016). Reference: SALP-RP-MA-EA-23058-CLS. Available at [http://www.avisooceanobs.com/fileadmin/documents/calval/validation\\_report/J2/annual\\_report\\_j2\\_2016.pdf](http://www.avisooceanobs.com/fileadmin/documents/calval/validation_report/J2/annual_report_j2_2016.pdf).
- [10] Lauret O. Jason-3 validation and cross calibration activities (Annual report 2016). SALP-RP-MA-EA-23060-CLS.
- [11] H. Roinard, E. Cadier. Jason-3 validation and cross calibration activities (Annual report 2017). SALP-RP-MA-EA-23187-CLS.

- .....
- [12] M. Guibbaud, A. Ollivier. Envisat RA2/MWR ocean data validation and cross calibration activities (Yearly report 2014). Reference: CLS.DOS/NT/14-253. Nomenclature: SALP-RP-MA-EA-22396-CLS.
- [13] P. Prandi. Saral/AltiKa validation and cross calibration activities (Annual report 2016). Nomenclature: SALP-RP-MA-EA-23073-CLS.
- [14] P. Prandi. Saral/AltiKa validation and cross calibration activities (Annual report 2017). Nomenclature: SALP-RP-MA-EA-23188-CLS.
- [15] A. Ollivier Yearly report 2016 as parts as SALP activities (Annual report 2016).
- [16] Prandi P., Debout V.: Validation of altimeter data by comparison with tide gauges measurements: yearly report 2016 for TOPEX/Poseidon, Jason-1, Jason-2, ERS-2, Envisat and SARAL/AltiKa. SALP-RP-MA-EA-23082-CLS.
- [17] Zawadzski L., Taburet N.: Validation of altimeter data by comparison with in-situ T/S Argo profiles (Annual Report 2016). SALP-RP-MA-EA-22966-CLS.
- [18] Valladeau, G., J.F. Legeais, M. Ablain, S. Guinehut, and N. Picot, 2012: Comparing altimetry with tide gauges and Argo profiling floats for data quality assessment and Mean Sea Level studies. *Marine Geodesy* 2012, DOI: 10.1080/01490419.2012.718226.
- [19] E. Bronner and G. Dibarboure, May 24th, 2012: Technical Note about the Jason-1 Geodetic Mission. *SALP-NT-MA-EA-16267-CNv1.0*. Available at: [http://www.avisioceanobs.com/fileadmin/documents/data/duacs/Technical\\_Note\\_J1\\_Geodetic\\_Mission.pdf](http://www.avisioceanobs.com/fileadmin/documents/data/duacs/Technical_Note_J1_Geodetic_Mission.pdf)
- [20] Ablain, M., A. Cazenave, G. Valladeau, and S. Guinehut. 2009 : A new assessment of the error budget of global mean sea level rate estimated by satellite altimetry over 1993-2008. *Ocean Sci*, **5**, 193-201. Available at <http://www.ocean-sci.net/5/193/2009/os-5-193-2009.pdf>
- [21] Ablain, M., S. Philipps, 2006, Topex/Poseidon 2005 annual validation report, Topex/Poseidon validation activities, 13 years of T/P data (GDR-Ms).
- [22] Ablain, M., S. Philipps, M. Urvoy, N. Tran, and N. Picot (2012) Detection of Long-Term Instabilities on Altimeter Backscattering Coefficient Thanks to Wind Speed Data Comparisons from Altimeters and Models, *Marine Geodesy*, **35:51, 258-275**. Available at <http://www.tandfonline.com/doi/pdf/10.1080/01490419.2012.718675>
- [23] Ablain, M., G. Larnicol, Y. Faugère, A. Cazenave, B. Meyssignac, N. Picot, J. Benveniste, 2012. Error Characterization of altimetry measurements at Climate Scales. Oral presentation at OSTST meeting, Venice, Italy, 27-28 September 2012. Available at: [http://www.avisioceanobs.com/fileadmin/documents/OSTST/2012/oral/02\\_friday\\_28/04\\_errors\\_uncertainties\\_I/03\\_EU1\\_Ablain.pdf](http://www.avisioceanobs.com/fileadmin/documents/OSTST/2012/oral/02_friday_28/04_errors_uncertainties_I/03_EU1_Ablain.pdf)
- [24] AVISO and PODAAC User Handbook. IGDR and GDR Jason-1 Products. Edition 4.1, October 2008. SMM-MU-M5-OP-13184-CN (AVISO), JPL D-21352 (PODAAC). Available at [http://www.avisioceanobs.com/fileadmin/documents/data/tools/hdbk\\_j1\\_gdr.pdf](http://www.avisioceanobs.com/fileadmin/documents/data/tools/hdbk_j1_gdr.pdf).
- [25] Beckley, B. D. , Zelensky, N. P. , Holmes, S. A. , Lemoine, F. G. , Ray, R. D. , Mitchum, G. T. , Desai, S. D. and Brown, S. T. (2010) Assessment of the Jason-2 Extension to the TOPEX/Poseidon, Jason-1 Sea-Surface Height Time Series for Global Mean Sea Level Monitoring, *Marine Geodesy*, **33:1, 447 - 471**. Available at [http://pdfserve.informaworld.com/96442\\_\\_925511460.pdf](http://pdfserve.informaworld.com/96442__925511460.pdf)

- .....
- [26] Bertiger, Willy , Desai, Shailen D. , Dorsey, Angie , Haines, Bruce J. , Harvey, Nate , Kuang, Da. , Sibthorpe, Ant and Weiss, Jan P. (2010) Sub-Centimeter Precision Orbit Determination with GPS for Ocean Altimetry. *Marine Geodesy*, **33:1**, 363 - 378. Available at [http://pdfserve.informaworld.com/858128\\_\\_925510150.pdf](http://pdfserve.informaworld.com/858128__925510150.pdf)
- [27] Bertiger, Willy , Desai, Shailen D. , Haines, Bruce J., R. DeCarvalho, and A. Dorsey (2010) Jason-2/OSTM Precision Orbit Determination with GPS *Oral presentation at OSTST meeting, Lisbon, Portugal*, Available at [http://www.avisooceanobs.com/fileadmin/documents/OSTST/2010/oral/19\\_Tuesday/bertiger.pdf](http://www.avisooceanobs.com/fileadmin/documents/OSTST/2010/oral/19_Tuesday/bertiger.pdf)
- [28] Legeais J-F., P. Prandi, M. Ablain and S. Guinehut: Analyses of altimetry errors using Argo and GRACE data. *Ocean Science Discussion*, doi:10.5194/os-2015-111, in review, 2016.
- [29] Bond, N. A., M. F. Cronin, H. Freeland, and N. Mantua (2015), Causes and impacts of the 2014 warm anomaly in the NE Pacific. *Geophys. Res. Lett.*, 42, 3414–3420. doi: 10.1002/2015GL063306.
- [30] Boening, C., J. K. Willis, F. W. Landerer, R. S. Nerem, and J. Fasullo (2012), The 2011 La Niña: So Strong, the Oceans Fell, *Geophys. Res. Lett.*, doi:10.1029/2012GL053055, in press.
- [31] John T. Fasullo , C. Boening, F. W. Landerer, R. S. Nerem (2013), Australia’s Unique Influence on Global Sea Level in 2010-2011, doi:10.1002/grl.50834, in press.
- [32] Boy, François and Jean-Damien Desjonquieres. 2010. Note technique datation de l’instant de reflexion des échos altimètres pour POSEIDON2 et POSEIDON3 *Reference: TP3-JPOS3-NT-1616-CNES*
- [33] Brown G.S., “The average impulse response of a rough surface and its application”, *IEEE Transactions on Antenna and Propagation*, Vol. AP 25, N1, pp. 67-74, Jan. 1977.
- [34] Brown S., S. Desai, and W. Lu “Initial on-orbit performance assessment of the advanced microwave radiometer and performance of JMR GDR-C”, *Oral presentation at OSTST meeting, Nice, France, 9-12 november 2008*. Available at [http://www.avisooceanobs.com/fileadmin/documents/OSTST/2008/oral/brown\\_calval.pdf](http://www.avisooceanobs.com/fileadmin/documents/OSTST/2008/oral/brown_calval.pdf)
- [35] Brown, S., S. Desai, W. Lu, and A. Sibthorpe. 2009. Performance Assessment of the Advanced Microwave Radiometer after 1 Year in Orbit. *Oral presentation at OSTST meeting, Seattle, USA*. Available at: <http://www.avisooceanobs.com/fileadmin/documents/OSTST/2009/oral/Brown.pdf>
- [36] S. Brown. 2010. A Novel Near-Land Radiometer Wet Path-Delay Retrieval Algorithm: Application to the Jason-2/OSTM Advanced Microwave radiometer. *IEEE TGRS vol. 48 n°4*. Available at [ftp://podaac.jpl.nasa.gov/allData/ostm/preview/L2/AMR/docs/Brown\\_TGARS\\_2010.pdf](ftp://podaac.jpl.nasa.gov/allData/ostm/preview/L2/AMR/docs/Brown_TGARS_2010.pdf)
- [37] Cerri, L. , Berthias, J. P. , Bertiger, W. I. , Haines, B. J. , Lemoine, F. G. , Mercier, F. , Ries, J. C. , Willis, P. , Zelensky, N. P. and Ziebart, M. (2010) Precision Orbit Determination Standards for the Jason Series of Altimeter Missions, *Marine Geodesy*, **33:1**, 379 - 418. Available at [http://pdfserve.informaworld.com/816985\\_\\_925509111.pdf](http://pdfserve.informaworld.com/816985__925509111.pdf)
- [38] Cerri, L., A. Couhert, S. Houry, F. Mercier. 2011. Improving the long-term stability of the GDR orbit solutions. *Oral presentation at OSTST meeting, San Diego, USA*. Available at [http://www.avisooceanobs.com/fileadmin/documents/OSTST/2011/oral/02\\_Thursday/Splinter3POD/05\\_Cerri.pdf](http://www.avisooceanobs.com/fileadmin/documents/OSTST/2011/oral/02_Thursday/Splinter3POD/05_Cerri.pdf).

- .....
- [39] Chambers, D., P., J. Ries, T. Urban, and S. Hayes. 2002. Results of global intercomparison between TOPEX and Jason measurements and models. *Paper presented at the Jason-1 and TOPEX/Poseidon Science Working Team Meeting, Biarritz (France), 10-12 June.*
- [40] Collard, F. (2005). Algorithmes de vent et période moyenne des vagues JASON à base de réseaux de neurons. BO-021-CLS-0407-RF. Boost Technologies.
- [41] Commien, L., S. Philipps, M. Ablain and N. Picot. 2009. SSALTO CALVAL Performance assessment Jason-1 GDR “C”/GDR “b”. *Poster presented at OSTST meeting, Seattle, USA.* Available at: <http://www.avisooceanobs.com/fileadmin/documents/OSTST/2009/poster/commien.pdf>
- [42] Couhert, A., L. Cerri, F. Mercier, S. Houry. 2010. Status of Jason-1 and Jason-2 GDR orbits. *Talk presented at OSTST meeting, Lisbon, Portugal.* Available at: <http://www.avisooceanobs.com/fileadmin/documents/OSTST/2010/oral/couhert.pdf>
- [43] DeCarvalho, R., S. Brown, B. Haines and S. Desai. 2009. Global cross calibration and validation of the Jason-1 and Jason-2/OSTM data products. *Oral presentation at OSTST meeting, Seattle, USA.* Available at: <http://www.avisooceanobs.com/fileadmin/documents/OSTST/2009/oral/deCarvalho.pdf>
- [44] Desjonqueres, J.-D., G. Carayon, J.-L. Courriere, and N. Steunou “POSEIDON-2 In-Flight results”, *Oral presentation at OSTST meeting, Nice, France, 9-12 november 2008.* Available at <http://www.avisooceanobs.com/fileadmin/documents/OSTST/2008/oral/desjonqueres.pdf>
- [45] Desjonquères, J. D. , Carayon, G. , Steunou, N. and Lambin, J. (2010) Poseidon-3 Radar Altimeter: New Modes and In-Flight Performances, *Marine Geodesy*, **33:1**, 53 - 79. Available at [http://pdfserve.informaworld.com/542982\\_\\_925503482.pdf](http://pdfserve.informaworld.com/542982__925503482.pdf)
- [46] Dettmering, Denise and Bosch, Wolfgang (2010) Global Calibration of Jason-2 by Multi-Mission Crossover Analysis, *Marine Geodesy*, **33:1**, 150 - 161. Available at [http://pdfserve.informaworld.com/315039\\_\\_925510361.pdf](http://pdfserve.informaworld.com/315039__925510361.pdf)
- [47] - Dibarboure, G., F. Boy, J. D. Desjonqueres, S. Labroue, Y. Lasne, N. Picot, J. C. Poisson, and P. Thibaut, 2014: Investigating short-wavelength correlated errors on low-resolution mode altimetry. *J. Atmos. Oceanic Technol.*, **31**, 1337–1362, doi:10.1175/JTECH-D-13-00081.1
- [48] Dorandeu.,J., M. Ablain, Y. Faugère, F. Mertz, 2004 : Jason-1 global statistical evaluation and performance assessment. Calibration and cross-calibration results. *Marine Geodesy* **27: 345-372.**
- [49] - Dufau, C., M. Orszynowicz,G. Dibarboure, R. Morrow, and P.-Y. Le Traon (2016), Mesoscale resolution capability of altimetry:Present and future, *J. Geophys. Res.Oceans*, **121**, doi:10.1002/2015JC010904.
- [50] Faugère, Y. et al. 2009. The SLOOP project: preparing the next generation of altimetry products for open ocean. *Poster presented at OSTST meeting, Seattle, USA.* Available at: <http://www.avisooceanobs.com/fileadmin/documents/OSTST/2009/poster/Faugere2.pdf>
- [51] Faugère, Y. et al. 2010. CROSS-CALIBRATION between ENVISAT and JASON-1/2. *Oral presentation at OSTST meeting, Lisbon, Portugal.* Available at: [http://www.avisooceanobs.com/fileadmin/documents/OSTST/2010/oral/19\\_Tuesday/Tuesday\\_afternoon/faugere.pdf](http://www.avisooceanobs.com/fileadmin/documents/OSTST/2010/oral/19_Tuesday/Tuesday_afternoon/faugere.pdf)

- .....
- [52] Jason-2 Version "T" Geophysical Data Records : Public Release, August 2009. Available at : [http://www.avisioceanobs.com/fileadmin/documents/data/products/Jason-2\\_GDR\\_T\\_disclaimer.pdf](http://www.avisioceanobs.com/fileadmin/documents/data/products/Jason-2_GDR_T_disclaimer.pdf)
- [53] Renaudie C., S. Philipps, 2014: Comparison of the latest GSFC SLR/DORIS std1204 orbits with current orbits for TP,J1 and J2. CLS Ramonville St Agne.
- [54] Gourrion, J., Vandemark, D., Bailey, S., Chapron, B., Gommenginger, G.P., Challenor, P.G. and Srokosz, M.A., 2002: A two-parameter wind speed algorithm for Ku-band altimeters, *Journal of Atmospheric and Oceanic Technology*. **19(12)** 2030-2048.
- [55] [http://grgs.obs-mip.fr/grace/variable-models-grace-lageos/mean\\_fields](http://grgs.obs-mip.fr/grace/variable-models-grace-lageos/mean_fields)
- [56] Hernandez, F. and P. Schaeffer, 2000: Altimetric Mean Sea Surfaces and Gravity Anomaly maps inter-comparisons. AVI-NT-011-5242-CLS, 48 pp. CLS Ramonville St Agne.
- [57] Huffman, G. and D.T.Bolvin, 2009: TRMM and Other Data Precipitation Data Set Documentation. Available at [ftp://precip.gsfc.nasa.gov/pub/trmmdocs/3B42\\_3B43\\_doc.pdf](ftp://precip.gsfc.nasa.gov/pub/trmmdocs/3B42_3B43_doc.pdf)
- [58] Imel, D.A. 1994. Evaluation of the TOPEX/POSEIDON dual-frequency ionospheric correction. *J. Geophys. Res.*, **99**, 24,895-24,906.
- [59] Jalabert,E., A.Couhert, J. Moyard, F. Mercier, S. Houry, S. Rios-Bergantinos. 2015. JASON-2, SARAL AND CRYOSAT-2 STATUS. *Talk presented at OSTST meeting, Reston, USA, 20-23 October 2015.*[http://meetings.avisioaltimetry.fr/fileadmin/user\\_upload/tx\\_ausyclsseminar/files/OSTST2015/POD-01-Jalabert.pdf](http://meetings.avisioaltimetry.fr/fileadmin/user_upload/tx_ausyclsseminar/files/OSTST2015/POD-01-Jalabert.pdf)
- [60] Lemoine, F.G., Zelensky N.P., Chinn, D.S., et al. (2010), Towards development of a consistent orbit series for TOPEX, Jason-1, and Jason-2 Adv. Space Res., 46(12), 1513–1540, doi: 10.1016/j.asr.2010.05.007 (updated).
- [61] Lemoine, F., N.P. Zelensky, S. Melachroinos, D.S. Chinn, B.D. Beckley, D.D. Rowlands, and S.B. Luthcke. 2011. GSFC OSTM (Jason-2), Jason-1 & TOPEX POD Update. *Oral presentation at OSTST meeting, San Diego, USA.* Available at [http://www.avisioceanobs.com/fileadmin/documents/OSTST/2011/oral/02\\_Thursday/SplinterPOD/03Lemoine\\_etal\\_SWT2011\\_v01.pdf](http://www.avisioceanobs.com/fileadmin/documents/OSTST/2011/oral/02_Thursday/SplinterPOD/03Lemoine_etal_SWT2011_v01.pdf).
- [62] Lemoine F., N.P. Zelensky, D.S. Chinn, B.D. Beckley, D.E. Pavlis, J. Wimert, O. Bordyugov. 2014 : New GSC POD Standards for TOPEX/Poseidon, Jason-1, Jason-2 (OSTM). *Oral presentation at OSTST meeting, Konstanz, Germany.* Available at <http://www.avisioaltimetry.fr/fr/coin-utilisateur/equipes-scientifiques/sci-teams.html>.
- [63] Le Traon, P.-Y., J. Stum, J. Dorandeu, P. Gaspar, and P. Vincent, 1994: Global statistical analysis of TOPEX and POSEIDON data. *J. Geophys. Res.*,**99**, 24619-24631.
- [64] MSEs (CNES, NASA, NOAA, EUMETSAT). 2011. GDR Status. *Oral presentation (by N. Picot) at OSTST meeting, San Diego, USA.* Available at [http://www.avisioceanobs.com/fileadmin/documents/OSTST/2011/oral/03\\_Friday/Plenary/GDRProducts/02PicotGDR\\_status\\_2011.pdf](http://www.avisioceanobs.com/fileadmin/documents/OSTST/2011/oral/03_Friday/Plenary/GDRProducts/02PicotGDR_status_2011.pdf).
- [65] M. Ablain. SALP annual report (2017) of Mean Sea Level Activities (SALP-RP-MA-EA-23189-CLS)
- [66] Aviso one-satellite-based Mean Sea Level reprocessing, [http://www.avisioaltimetry.fr/fileadmin/documents/data/products/indic/msl/MSL\\_reprocessing\\_201402.pdf](http://www.avisioaltimetry.fr/fileadmin/documents/data/products/indic/msl/MSL_reprocessing_201402.pdf).

- .....
- [67] Moyard J., E. Jalabert, A. Couhert, S. Rios-Bergantinos, F. Mercier, S.Houry. 2014 : Jason-2 POD status. *Oral presentation at OSTST meeting, Konstanz, Germany*. Available at <http://www.aviso.altimetry.fr/fr/coin-utilisateur/equipes-scientifiques/sci-teams.html>.
- [68] Roinard,H., S.Philipps, O.Lauret, M.Ablain, E.Bronner, N.Picot. Jason-1 GDR-E reprocessing.*Talk presented at OSTST meeting, Reston, USA, 20-23 October 2015*. [http://meetings.aviso.altimetry.fr/fileadmin/user\\_upload/tx\\_ausyclsseminar/files/Poster\\_OSTST15\\_JASON-1\\_GDR-E\\_Reprocessing.pdf](http://meetings.aviso.altimetry.fr/fileadmin/user_upload/tx_ausyclsseminar/files/Poster_OSTST15_JASON-1_GDR-E_Reprocessing.pdf).
- [69] Obligis, E., L. Eymard, M. Ablain, B. Picard, J.F. Legeais, Y. Faugere and N. Picot, 2010. The wet tropospheric correction for altimetry missions: A mean sea level issue.*Oral presentation at OSTST meeting, Lisbon, Portugal*. Available at [http://www.aviso.oceanobs.com/fileadmin/documents/OSTST/2010/oral/19\\_Tuesday/OBLIGIS.pdf](http://www.aviso.oceanobs.com/fileadmin/documents/OSTST/2010/oral/19_Tuesday/OBLIGIS.pdf).
- [70] Ollivier A., Faugere Y., Granier N., 2008: Envisat RA-2/MWR ocean data validation and cross-calibration activities. Yearly report. Technical Note CLS.DOS/NT/09.10, Contract N° SALP-RP-MA-EA-21633-CLS [http://www.aviso.oceanobs.com/fileadmin/documents/calval/validation\\_report/EN/annual\\_report\\_en\\_2008.pdf](http://www.aviso.oceanobs.com/fileadmin/documents/calval/validation_report/EN/annual_report_en_2008.pdf)
- [71] Ollivier A., Faugere Y., P. Thibaut, G. Dibarboure, and J.-C. Poisson, 2008: Investigation on the high frequency content of Jason-1 and Jason-2. CLS.DOS/NT/09-027
- [72] Ollivier A., M. Guibbaud, Faugere Y. Envisat RA2/MWR ocean data validation and cross-calibration activities. Yearly report 2011. SALP-RP-MA-EA-22062-CLS, CLS.DOS/NT/12-021.
- [73] Ollivier A., A. Couhert, V. Pignot, C. Renaudie, S. Phillips, N. Picot, 2014 : Assessment of orbit quality through the SSH calculation towards GDR-E standards. *Oral presentation at OSTST meeting, Constance, Germany*. Available at <http://www.aviso.altimetry.fr/fr/coin-utilisateur/equipes-scientifiques/sci-teams.html>
- [74] Ollivier A., S. Philipps, M. Ablain, A. Edwell, L. Cerri, N. Picot, 2013 : Assessment of Orbit Quality through the Sea Surface Height calculation, New insight in resolving long term and inter-annual signal for climate studies. *Oral presentation at OSTST meeting, Boulder, USA*. Available at <http://www.aviso.altimetry.fr/fr/coin-utilisateur/equipes-scientifiques/sci-teams.html>
- [75] Ollivier A., Dibarboure G., Picard B., Ablain M., OSTST2014, Konstanz - Germany, "Spectral analysis of altimetric signal and errors Towards a spectral error budget of Nadir Altimetric missions" [http://meetings.aviso.altimetry.fr/fileadmin/user\\_upload/tx\\_ausyclsseminar/files/30Ball0900-2\\_Pres\\_OSTST2014\\_J2\\_ErrorBugdet\\_Spectra\\_Ollivier.pdf](http://meetings.aviso.altimetry.fr/fileadmin/user_upload/tx_ausyclsseminar/files/30Ball0900-2_Pres_OSTST2014_J2_ErrorBugdet_Spectra_Ollivier.pdf)
- [76] Otten M., C. Flohrer, T. Springer, and W. Enderle. 2011. Generating precise and homogeneous orbits for Jason-1 and Jason-2. *Oral presentation at OSTST meeting, San Diego, USA*. Available at [http://www.aviso.oceanobs.com/fileadmin/documents/OSTST/2011/oral/03\\_Friday/Splinter6POD/01\\_Otten.pdf](http://www.aviso.oceanobs.com/fileadmin/documents/OSTST/2011/oral/03_Friday/Splinter6POD/01_Otten.pdf).
- [77] Peltier, 2004, Global Glacial Isostasy And The Surface of The Ice-Age Earth: The ICE-5G (VM2) Model and GRACE. *Annual Review of Earth and Planetary Sciences*, May 2004, **Vol. 32**, **Pages 111-149**, doi: 10.1146/annurev.earth.32.082503.144359

- .....
- [78] Philipps, S., M. Ablain, J. Dorandeu, P. Thibaut, N. Picot and J. Lambin. 2006. SSALTO CALVAL Performance assessment Jason-1 GDR 'B'/GDR 'A'. *Poster presented at OSTST meeting, Hobart, Australia*. Available at: <http://www.avisooceanobs.com/fileadmin/documents/OSTST/2006/ablain1.pdf>
- [79] Picot, N., P. Thibaut, N. Tran, S. Philipps, J.C. Poisson, T. Moreau, and E. Bronner. 2010. New Jason-2 GDR-C standards. *Oral presentation at OSTST meeting, Lisbon, Portugal*. Available at [http://www.avisooceanobs.com/fileadmin/documents/OSTST/2010/oral/PThibaut\\_Jason2.pdf](http://www.avisooceanobs.com/fileadmin/documents/OSTST/2010/oral/PThibaut_Jason2.pdf).
- [80] Picot, N., P. Thibaut, N. Tran, S. Philipps, J.C. Poisson, E. Bronner, C. Garcia and many others. 2011. Jason-2 GDR-D standards. *Oral presentation at OSTST meeting, San Diego, USA*. Available at [http://www.avisooceanobs.com/fileadmin/documents/OSTST/2011/oral/02\\_Thursday/Splinter5IP/05NPicot\\_et\\_al\\_OSTST\\_2011\\_J2-GDRD-Standards.pdf](http://www.avisooceanobs.com/fileadmin/documents/OSTST/2011/oral/02_Thursday/Splinter5IP/05NPicot_et_al_OSTST_2011_J2-GDRD-Standards.pdf).
- [81] Schaeffer, P., A. Ollivier, Y. Faugere, E. Bronner, and N. Picot. The new CNES CLS 2010 Mean Sea Surface. *Oral presentation at OSTST meeting, Lisbon, Portugal, 18-20 october 2010*. Available at [http://www.avisooceanobs.com/fileadmin/documents/OSTST/2010/oral/19\\_Tuesday/Schaeffer.pdf](http://www.avisooceanobs.com/fileadmin/documents/OSTST/2010/oral/19_Tuesday/Schaeffer.pdf).
- [82] Schaeffer, P., Y. Faugere, J.-F. Legeais, A. Ollivier, T. Guinle, and N. Picot (2012). The CNES\_CLS11 Global Mean Sea Surface Computed from 16 Years of Satellite Altimeter Data. *Marine Geodesy* **35: sup1, 3-19**. Available at <http://www.tandfonline.com/doi/abs/10.1080/01490419.2012.718231>
- [83] DUACS/Aviso team 'A new version of SSALTO/Duacs products available in April 2014' <http://www.avisooceanobs.com/fileadmin/documents/data/duacs/Duacs2014.pdf>
- [84] Scharroo, R., J. Lillibridge, and W.H.F. Smith, 2004: Cross-calibration and long-term monitoring of the Microwave Radiometers of ERS, Topex, GFO, Jason-1 and Envisat. *Marine Geodesy*, 97.
- [85] Solar Radio Flux (10.7cm) (daily solar data). Available at [http://www.swpc.noaa.gov/ftpmenu/indices/old\\_indices.html](http://www.swpc.noaa.gov/ftpmenu/indices/old_indices.html)
- [86] Thibaut, P. O.Z. Zanifé, J.P. Dumont, J. Dorandeu, N. Picot, and P. Vincent, 2002. Data editing: The MQE criterion. *Paper presented at the Jason-1 and TOPEX/Poseidon Science Working Team Meeting, New-Orleans (USA), 21-23 October*.
- [87] Thibaut, P., J.-C. Poisson, A. Ollivier, S. Philipps, and M. Ablain: "Jason-2 waveforms, tracking and retracking analysis", *Oral presentation at OSTST meeting, Nice, France, 9-12 november 2008*. Available at <http://www.avisooceanobs.com/fileadmin/documents/OSTST/2008/oral/thibaut.pdf>
- [88] Moreau, T., P. Thibaut, 2009. Etude dépointage Poseidon-3: optimisation de l'angle d'ouverture d'antenne. CLS-DOS-NT-09-028. 15 pp, CLS Ramonville St. Agne.
- [89] P. Thibaut. Bilan des activités d'expertise altimétriques menées en 2009 : Lot 2D. SALP-RP-MA-EA-21808-CLS, CLS-DOS-NT-10-029.
- [90] Tran, N. , Labroue, S. , Philipps, S. , Bronner, E. and Picot, N. (2010) Overview and Update of the Sea State Bias Corrections for the Jason-2, Jason-1 and TOPEX Missions, *Marine Geodesy*, **33:1, 348 - 362**. Available at [http://pdfserve.informaworld.com/804727\\_925502357.pdf](http://pdfserve.informaworld.com/804727_925502357.pdf)

- .....
- [91] Tran, N., P. Thibaut, J.-C. Poisson, S. Philipps, E. Bronner, and N. Picot. Jason-1, Jason-2 and TOPEX Sea State Bias. Overview and Updates. *Oral presentation at OSTST meeting, Lisbon, Portugal, 18-20 october 2010*. Available at <http://www.avisooceanobs.com/fileadmin/documents/OSTST/2010/oral/TRAN.pdf>
- [92] N. Tran, S. Philipps, J.-C. Poisson, S. Urien, E. Bronner, and N. Picot. Impact of GDR\_D standards on SSB corrections. *Oral presentation at OSTST meeting, Venice, Italy, 27-28 September 2012*. Available at [http://www.avisooceanobs.com/fileadmin/documents/OSTST/2012/oral/02\\_friday\\_28/01\\_instr\\_processing\\_I/01\\_IP1\\_Tran.pdf](http://www.avisooceanobs.com/fileadmin/documents/OSTST/2012/oral/02_friday_28/01_instr_processing_I/01_IP1_Tran.pdf).
- [93] Zlotnicky, V. 1994. Correlated environmental corrections in TOPEX/POSEIDON, with a note on ionospheric accuracy. *J. Geophys. Res.*, **99**, 24,907-24,914
- [94] Edward D. Zaron , Robert deCarvalho, 2016. Identification and Reduction of Retracker-Related Noise in Altimeter-Derived Sea Surface Height Measurements. *Journal of Atmospheric and Oceanic Technology*, p201-210, doi:10.1175/JTECH-D-15-0164.1
- [95] Zawaszki, L., M. Ablain, A. Cazenave, B. Meyssignac. 2014. Confidence envelop of the Global MSL time-series deduced from Jason-1 and Jason-2 altimetric missions. *Poster presentation at OSTST meeting, Constance, Germany, 28-31 October 2014*, Available at [http://meetings.avisooceanobs.com/fileadmin/user\\_upload/tx\\_ausyclsseminar/files/Poster\\_OSTST14\\_GMSLUncertainty.pdf](http://meetings.avisooceanobs.com/fileadmin/user_upload/tx_ausyclsseminar/files/Poster_OSTST14_GMSLUncertainty.pdf)
- [96] World Meteorological Organization, 2010: El Nino/ La Nina Update (30 March 2010). Available at [http://www.wmo.ch/pages/prog/wcp/wcasp/documents/El\\_Nino\\_Mar10\\_Eng.pdf](http://www.wmo.ch/pages/prog/wcp/wcasp/documents/El_Nino_Mar10_Eng.pdf).
- [97] World Meteorological Organization, 2011: El Nino/ La Nina Update (25 January 2011). Available at [http://www.wmo.ch/pages/prog/wcp/wcasp/documents/El-Nino\\_Jan11\\_Eng.pdf](http://www.wmo.ch/pages/prog/wcp/wcasp/documents/El-Nino_Jan11_Eng.pdf).
- [98] World Meteorological Organization, 2015: El Nino/ La Nina Update (16 November 2015). Available at [http://www.wmo.int/pages/prog/wcp/wcasp/documents/WMO\\_ENSO\\_Nov15\\_Eng.pdf](http://www.wmo.int/pages/prog/wcp/wcasp/documents/WMO_ENSO_Nov15_Eng.pdf)
- [99] Correction Troposphérique Humide pour le radiomètre Jason-3 : approche neuronale. CLS-J3PROTO-15-0002. Projet CNES PEACHI-J3
- [100] JA1-GM <http://dx.doi.org/10.1080/01490419.2012.717854>
- [101] JA2-EOL <http://dx.doi.org/10.1175/JTECH-D-16-0015.1>
- [102] OSTST2016 - Jason-1/2/3 and SARAL GDR Status [https://meetings.avisooceanobs.com/fileadmin/user\\_upload/tx\\_ausyclsseminar/files/CLOS\\_15\\_GDR\\_status\\_2016\\_11h45.pdf](https://meetings.avisooceanobs.com/fileadmin/user_upload/tx_ausyclsseminar/files/CLOS_15_GDR_status_2016_11h45.pdf)
- [103] Mean Sea Surface CNES/CLS model <https://www.avisooceanobs.com/en/data/products/auxiliary-products/mss.html>
- [104] <https://www.avisooceanobs.com/en/data/product-information/updates-and-reprocessing/ssaltoduacs-product-changes-and-updates.html>